8-28-2014

Development of Novel Tools for Radial Glia Lineage Tracing and Modeling Central Nervous System Tumor

Fuyi Chen
University of Connecticut - Storrs, fuyi.chen@uconn.edu

Development of Novel Tools for Radial Glia Lineage Tracing and Modeling Central Nervous System Tumors

Fuyi Chen, PhD

University of Connecticut, 2014

In this dissertation, I first established a novel non viral *piggyBac* transposon mediated transgenesis approach delivered by *in utero* electroporation for radial glia lineage tracing. Furthermore, I developed a novel central nervous system tumor model in rat using *piggyBac* IUE. By directing expression of oncogenic HRasV12/AKT in radial glia, astrocytes and oligodendrocytes, glioblastoma multiforme and anaplastic oligoastrocytoma were induced. Also addition of neurogenic bHLH transcription factors Neurogenin 2 and Neural differentiation 1 to GBM inducing HRasV12/AKT, malignant pediatric atyical teratoid rhabdoid tumor like tumor was induced. These results shad lights on the sources of tumor heterogeneity and indicate that oncogenic event occurring in disparate cell types and/or molecular context can lead to different tumor formation. Last, I explored the application of RNA guided genome engineering tool CRISPR/Cas9 in studying necortical development and model human neural developmental disorder as well as glioblastoma multiforme using CRISPR/Cas9 system. *In utero* electroporation of CRISPR/Cas9 constructs targeting PTEN, successfully knocked out PTEN expression in neurons. PTEN negative neurons showed hypertrophy and decreased resting membrane potential, increased sEPSCs and mEPSCs. Combinations of gRNAs targeting PTEN, NF1 and P53 induced glioblastoma multiforme. These new tools shall be proven to be powerful to study neocortical development and central nervous system tumors.

Development of Novel Tools for Radial Glia Lineage Tracing and Modeling Central Nervous System Tumors

Fuyi Chen

B.S., Laiyang Agricultural College, 2004

M.S., Xiamen University, 2008

A Dissertation

Submitted in Partial Fulfillment of the

Requirements for the Degree of Doctor of Philosophy

at the

University of Connecticut

2014

APPROVAL PAGE

Doctor of Philosophy Dissertation

Development of Novel Tools for Radial Glia Lineage Tracing and Modeling Central Nervous System Tumor

Presented by

Fuyi Chen, B.S., M.S.

Major Advisor

_____

Joseph J. LoTurco

Associate Advisor

_____

Akiko Nishiyama

Associate Advisor

_____

David J. Goldhamer

Associate Advisor

_____

Anastasios V. Tzingounis

University of Connecticut

2014

Acknowledgement

I would like to express my deepest gratitude to my major adviser, Dr. Joseph LoTurco for his enormous help, advices and guidance during my graduate study. I would also like to thank the members of my thesis committee, Dr. Akiko Nishiyama, Dr. David Goldhamer and Dr. Anastasios Tzingounis for their valuable suggestions. In addition, I would like to express my thanks to current and past LoTurco lab members, Dr. Anne Booker, Dr, Brady Maher, Dr. Radamila Fillopovic ,Dr. Yu Wang, Dr, Faez Sidiqqi, Dr. Xiuyun Yin, Komal Patel, Aarti Tarkar, Matthew Girgenti, Alicia Che, Saranya Santhosh Kumar, Chris Fiondella, Scott Finnace and Roma Goz for their help and suggestions. I would also like to thank the tri-lab lab members for their valuable and insightful critiques. I also owe my thanks to PBB vivarium, for their help with the animal work. I also to express my appreciation to Dr. Xinnian Chen, Dr. Donnasue Graesser, Penny Dobbins, Ann Hamlin and all the TAs for making the teaching a happy experience. Lastly and most importantly, I would like to express my deepest gratitude to all my family, my wife Ping, my lovely son Jeffrey, my sister and my parents for their unconditional love and support. This dissertation is forever dedicated to them.

TABLE OF CONTENTS

Chapter 1 Introduction

Central nervous system tumor and tumor heterogeneity

Primary malignant central nervous system (CNS) tumors represent about 2% of all cancers but account for a disproportionate rate of morbidity and mortality (Buckner et al., 2007). The incidence rate of all primary malignant and non-malignant brain and CNS tumors is 20.6 cases per 100,000 (7.3 per 100,000 for malignant tumors and 13.3 per 100,000 for non–malignant tumors). The rate is higher in females (22.3 per 100,000) than males (18.8 per 100,000). An estimated 24,620 new cases of primary malignant (13,630 in males and 10,990 in females) and 45,100 new cases of non–malignant brain and CNS tumors are expected to be diagnosed in the United States in 2013. An estimated 13,700 deaths will be attributed to primary malignant brain and CNS tumors in the United States in 2012 (http://www.cbtrus.org/factsheet/factsheet.html).

It has been long appreciated that cancers including CNS tumors have extensive cellular and genetic diversity. Such high heterogeneity complicates cancer diagnosis, treatment and prognosis. The molecular and cellular mechanisms underpinning these heterogeneities remain central questions in cancer biology. Extensive genetic and phenotypic diversity exist not only between tumors (inter-tumor heterogeneity) but also within individual tumors (intra-tumor heterogeneity) (Burrell et al., 2013). Inter-tumor heterogeneity occurs between tumors arising from same organ, leading to classification of different tumor subtypes. Intra-tumor heterogeneity occurs within individual tumors in which tumor cells often differ in features such as size, morphology, and

membrane composition as well as behaviors such as proliferation rate, cell-cell interaction, metastatic proclivity, and sensitivity to chemotherapy (Heppner, 1984).

Cancer stem cells and clonal evolution models have been established to explain intra-tumor heterogeneity (Campbell and Polyak, 2007). The cancer stem cell model states that a small population of tumor cells serves as the cancer stem cells and drives tumor initiation, progression and recurrence. The clonal evolution model states that cancer cells over time acquire various combinations of mutations within a tumor and that genetic drift and stepwise natural selection for the fittest, most aggressive cells drive tumor progression(Polyak, 2007, 2011). Two models have been proposed to explain inter-tumor heterogeneity, the genetic mutation model and the cell of origin model(Visvader, 2011). In genetic mutation model, oncogenic mutations primarily determine tumor phenotype. Different genetic and/or epigenetic mutations cause different tumor formation. In the cell of origin model, the cell types that serve as the cell of origin determine tumor phenotype. Different tumor types are arising from distinct cells types(Visvader, 2011). Understanding the cause of tumor heterogeneity will greatly help to develop more effective targeted therapy and new treatment regimen.

Development of Neocortex

Normal tissue development follows pre-determined developmental program from stem cells to committed progenitors, which then will generate differentiated cells that constitute the bulk of the tissue or organ(Visvader, 2011). Many human diseases including cancers are caused by perturbation of this development program. Understanding developmental hierarchy in normal

tissue is essential to understand the etiology of tumors, to pinpoint the sources of tumor heterogeneity. The normal lineage developmental order serves a frame work to probe potential therapy targets for disease treatment. Brain tumors constitute large proportion of the CNS tumors thus in this section the current model for neocortical development is being reviewed.

Early during neocortical development, pseudostratified neuroepithelium of ectodermal origin lining the lateral ventricular walls of mammals function as neural stem cells (NSCs). Neuroepithelial cells undergo symmetric division to expand the stem cell pool. When neurogenesis begins, neuroepithelial cells start to transform into radial glia cells which serve as common progenitors for many cell types in CNS. Radial glia maintain both neuroepithelial features such as expression of neuroepithelial marker Nestin (Hartfuss et al., 2001) and apical-basal polarity (Chenn et al., 1998) as well as astroglia properties such as astrocytes specific glutamate transporter (GLAST), glial fibrillary acidic protein (GFAP) (Choi and Lapham, 1978; Levitt and Rakic, 1980), vimentin and brain lipid binding protein (BLBP) (Campbell and Gotz, 2002).

During cortical neurogenesis, radial glia undergo asymmetric division and generate neurons either directly or indirectly through intermediate progenitors (IPCs) (Haubensak et al., 2004; Noctor et al., 2004; Noctor et al., 2007).Neuronal IPCs (nIPCs), sometimes referred to as basal progenitors, populate a region above the ventricular zone (VZ) called subventricular zone (SVZ), which is thought as the major site of neurogenesis (Haubensak et al., 2004; Miyata et al., 2004; Noctor et al., 2004; Noctor et al., 2007; Zecevic et al., 2005). nIPCs either undergo symmetric division to generate two daughter neurons or divide symmetrically to produce two additional IPCs (Haubensak et al., 2004; Kriegstein and Alvarez-Buylla, 2009; Miyata et al., 2004; Noctor et al., 2004; Noctor et al., 2007).

Later during cortical development, most radial glia cells lose their apical contact with ventricular surface and migrate toward to cortical plate through somal translocation. During somal translocation, radial glia gradually change morphology from bipolar to unipolar and eventually take astrocytic morphology with multi polar processes (Choi and Lapham, 1978; Noctor et al., 2008; Schmechel and Rakic, 1979; Voigt, 1989). Some astrocytes might go through astrocytic IPC stage and divide locally before terminal differentiation (Ichikawa et al., 1983; Kriegstein and Alvarez-Buylla, 2009; Mares and Bruckner, 1978). At the end of embryonic development, a subpopulation of radial glia retains apical contact. Some of these neonatal radial glia convert into ependymal cells. The others convert into adult SVZ astrocytes (type B cells) that function as adult neural stem cells and generate olfactory bulb interneurons(Kriegstein and Alvarez-Buylla, 2009; Merkle et al., 2007; Merkle et al., 2004). Oligodendrocytes are also generated from radial glia during embryonic cortical development (Gorski et al., 2002; Kessaris et al., 2006). A population of oligodendrocyte progenitor cells (OPCs) is generated by type B cells in SVZ (Aguirre et al., 2007; Levison and Goldman, 1993; Menn et al., 2006; Merkle et al., 2004).

Existing methods for labeling and manipulating neural progenitor lineage

Retroviral vectors have been widely used for tracing radial glia lineage. For example, early radial glia lineage tracing experiments using retroviral vectors provided early *in vivo* evidence that radial glia are the common progenitors for neurons and astroglia(Gray and Sanes, 1992; Kamei et al., 1998; Walsh and Cepko, 1988, 1993). Combinations of retroviral radial glia labeling and time lapse imaging provide definitive *in vivo* evidence that radial glia give rise to neurons and astrocytes(Noctor et al., 2001; Noctor et al., 2002; Tamamaki et al., 2001).Because

of the cargo limit, it is difficult to achieve simultaneous labeling and manipulation of lineage using retrovirus.

The RCAS-*tva* system has also been widely used to trace neural progenitor lineage. It uses the avian RCAS (replication-competent avian sarcoma-leukosis virus long terminal repeat with splice acceptor)/tumor virus A (TVA). The RCAS virus only transduce cells that express the cognate avian retroviral receptor TVA (Orsulic, 2002). For example, Menn etal (Menn et al., 2006) used the RACS –tva system to label the lineage of SVZ type B cells and found that both myelinating and nonmyelinating oligodendrocytes originated from SVZ type B cells.

Radial glia fate labeling experiments have also been performed using transgenic mice with developmentally regulated promoter driving Cre/loxp recombination (Anthony and Heintz, 2008; Anthony et al., 2004; Murdoch and Roskams, 2008). For example, Anthony and colleagues have used transgenic mouse in which Cre recombinase was driven by BLBP promoter to fate label the Blbp+ radial glia and demonstrated that radial glia serve as the neural progenitors(Anthony et al., 2004). Another study also performed by Anthony et al directly compared the lineage of Blbp+, Glast+ and hGFAP+ radial glia subpopulations and found Blbp+Glast+hGFAP- radial glia were neurogenic and Blbp+Glast+hGFAP+ were gliogenic in ventral telencephalon(Anthony and Heintz, 2008).

Another elegant genetic lineage labeling approach named Mosaic Analysis With Double Marker (MADM) allows for simultaneous labeling and gene knockout in clones of somatic cells or isolated single cells in vivo(Liu et al.; Zong et al., 2005). In MADM, Cre-mediated interchromosomal recombination results in the generation of complete coding sequence of

fluorescent reporter genes and cells generated from same progenitor are labeled with same color. Even though effective, it is costly to generate and maintain transgenic mouse lines.

Table 1 Comparison of existing methods for neural progenitor lineage tracing

Methods	Merits	Limitations
Retrovirus	Time-control, Permanent	Differential infectivity of cells, Potential integration site effects, Cargo limit
RACS-tva system	Permanent	Dependent on gene/promoter expression Require transgenic animals Labor and cost intensive Species dependent
Tissue-specific recombinase	Noninvasive Permanent	Dependent on gene/promoter expression Require transgenic animals Labor and cost intensive Species dependent
MADM	Noninvasive Multicolor, Permanent, Sparse labeling	Require transgenic animals Labor and cost intensive Species dependent
Electroporation of DNA transposon	Simultaneously labeling and manipulation Time control Cheaper and faster Not species dependent	Invasive Accessibility to cells

Recently, DNA transposons have also been reported to trace and manipulate progenitor lineage. For example, Lu *et al* (Lu et al., 2009) used *piggyBac* transposon to label and manipulate progenitor lineage in chicken spinal cord. Yoshida *et al* (Yoshida et al., 2010) used the *Tol2* transposon in mouse to label and manipulate the radial glia lineage. The relative ease of implementation and experimental flexibility of DNA transposon system will make it a valuable tool for tracking and manipulating neural progenitor lineage.

Animal models for CNS tumors

Orthotopic Xenograft mouse models, genetically engineered mouse models (GEM) and somatic-cell engineered mouse models (SEM) are the main glioma animal models and the prevailing model is the SEM.

Xenograft mouse models are generated by orthotopically implanting human glioma cell lines or human tumor cells into immune-compromised mouse. Although they are widely used for preclinical testing, histologically, xenograft tumors don't recapitulate human tumors and the tumor -host immunoresponse is inhibited (Candolfi et al., 2007; Jones and Holland, 2011). For tumors that genetically engineered mouse models still don't exist for some tumors such as atypical teratoid rhabdoid tumor, group 3 and 4 medullablastoma (Swartling et al., 2013), xenograft mouse models provide an alternative approach.

Genetically engineered mouse (GEM) models are generated by introducing genetic abnormalities found in human to mice through either germ-line modification or somatic modification. Most frequently used genetic abnormalities used in CNS tumor models include: mutated or constitutively active tyrosine kinase receptors (RTKs), mutated components in downstream RTKs pathway, loss of function of tumor suppressors or in combinations with each other (Swartling et al., 2013). Expression of constitutively active EGFR *VIII* together with loss of function tumors suppressors such as Ink4a/Arf (Persson et al., 2010; Weiss et al., 2003) as well as PTEN (Bachoo et al., 2002; Ding et al., 2003; Zhu et al., 2009) in astrocytes induced oligodendroglioma and glioblastoma. Another widely used growth factor is platelet-derived growth factor receptor beta (PDGFRB), expression of PDGFRB alone or in combination with loss of tumor suppressor in different cell types have resulted in oligodendroglioma, glioblastoma

formation (Calzolari et al., 2008; Dai et al., 2001; Hede et al., 2009; Lindberg et al., 2009; Shih et al., 2004; Uhrbom et al., 1998; Uhrbom et al., 2000). Germ line or somatic cell deletions of tumor suppressors have been exploited intensively to model low and high grade glioma (Alcantara Llaguno et al., 2009; Jacques et al., 2010; Kwon et al., 2008; Wang et al., 2009; Wei et al., 2006; Xiao et al., 2002; Zhu et al., 2005). Many studies have been reported using mutant Ras protein, including HRas, VRas and NRas to induce CNS tumors (Abel et al., 2009; Ding et al., 2003; Holland et al., 2000; Shannon et al., 2005; Uhrbom et al., 2002; Wei et al., 2006).

Somatic genetic engineering by recombinant virus allows control of gene expression in particular organs, cell types and at specific developmental stages. There are several systems that have been reported. A previous study reported the induction of brain tumor by PDGFR-B using the replication competent MMLV (Moloney Murine Leukemia Virus) (Uhrbom, et al 1998). MMLV can infect all cell types but the tumor cell-of-origin is not determinable in this experiment. Another widely used system is the RACS-TVA system (Holland, et al 1998; Holland, et al 2000; Uhrbom, et al 2002 ; Hambardzumyan, et al 2009; Holmen, et al 2005).Recently GFAP-tva (tva expresses in astrocytes) and Nestin-tva (tva expresses in neural stem cells) mouse lines are available (Holland, 2000). Adenovirus (Wei, et al 2006; Charest, et al 2006) and lentivirus (Marumoto, et al 2009) are also used to induce glioma in mouse. More recently Wiesner reported (Wiesner, et al 2009) that the Sleeping Beauty transposon can be used as a non-viral delivery tool to induce glioma.

Table 2 Features of existing CNS tumor models

Animal models	Features
Orthotopic Xenograft	Tumor histology doesn't resemble human tumors Fast
Genetic Engineered Mouse Model (GEM)	Tumor histology resembles human GBM. Can't distinguish primary mutation and secondary mutation. Species dependent. Laborious
Somatic Engineered Mouse Model (SEM) - Viral vector	Controlled gene expression in particular organs, cell types and at specific developmental stages. Clonal origin and migration pattern is difficult to track. Not suitable for multigene delivery.
Somatic Engineered Mouse Model (SEM) – *Sleeping Beauty* transposon	Similar to viral vector. Multigene delivery

Tools for somatic cell transgenesis and genome editing

Most of human disease including cancers are caused by somatic mutations (Poduri et al.). Thus tools for somatic cell transgenesis are exceedingly important for understanding etiology of somatic disease. Transposon system and recently discovered CRISPR/Cas9 system have been adapted as somatic cell transgenesis tool. For better understanding of both systems, the history and background of transposon and CRISPR/Cas are briefly reviewed below.

Transposon system

Transposons, sometimes referred to as transposable elements, also known as "jumping genes", are DNA sequences that move from one location in the genome to another. They were first identified in maize by Barbara McClintock. Originally, they were thought to be "junk" in the genome. Nowadays it is more and more clear that they have important functions in disease development (Miki et al., 1992), driving the evolution of genome as (Koga et al., 2006) well as increase genetic diversity (Beck et al.). There are mainly two classes of transposons: RNA transposon and DNA transposon. In the following section I will talk about the features of DNA transposons that make it a valuable tool for genetic studies; the currently widely used *Tol2*, *Sleeping Beauty* and *piggyBac* transposon as well as their related transposon plasmid system.

DNA transposons

DNA transposons transpose through cut and paste mechanism: the transposon encoded transposase excises the transposon from its original location and integrates it into elsewhere in the genosme (Ivics et al., 1997; Plasterk, 1996). In order to transpose, transposons should consist two essential components: an enzyme, namely tranposase, that work in *trans* to excise tranposon from original location and reintegrate it elsewhere in the genome and DNA sequences that work in *cis*, are recognized and mobilized by transposase. These sequences are usually found in the terminal repeats of transposon and are required for transposition in the presence of a complementary transposase(Ivics et al., 1997). Transposons can be classified as autonomous and nonautonomous transposons. Autonomous transposons encode active transposase, and are capable of transposition on their own. The non autonomous transposons do not express active transposase but retain DNA sequences that are necessary for transposition. This feature makes transposon system a valuable tool for integrating DNA sequences into chromosomes (Ivics et al.,

1997). Many DNA transposons have been utilized as powerful genetic tools such as the *P* elements in *Drosophila* (Cooley et al., 1988) and the *Tc1* element in *Caenorhabditis elegans* (Plasterk, 1996). *Tol2*, *Sleeping Beauty* and *piggyBa*c transposon are recently discovered or resurrected and have been shown to be powerful tools for cellular transgenesis.

Tol2 transposon

Tol2 transposon was identified from the genome of medaka fish (Oryzias latipes) (Koga et al., 1996) and is the only autonomously active transposon in hTA transposon family (Kawakami et al., 1998; Koga et al., 1996). Structurally, it is about 4.7kb in length and contains a 649 amino acids transposase protein. *Tol2* randomly transpose within the genome and upon transposition an 8bp duplication is created (Kawakami et al., 2000). 200bp and 150bp minimal sequence which contains 12bp inverted terminal repeats have been discovered embedding in the left and right ends of *Tol2* transposon (Urasaki et al., 2006). Any foreign DNA fragments that are cloned between these sequences can integrate in to host genome in the presence of Tol2 tranposase. It has been shown that *Tol2* vectors can carry 11kb cargo without affecting the transposition efficiency (Urasaki et al., 2006). *Tol2* transposon system has been successfully applied in many model organisms including zebra fish, chicken and mouse (Kawakami, 2007).

Sleeping Beauty Transposon

Even though DNA transposons have been isolated in many species including fish, Xenopus and human (Ivics et al., 1996; Koga et al., 1996; Oosumi et al., 1995) , almost no autonomous transposon has been isolated from vertebrate, except the *Tol2* transposon mentioned above. These transposons are not functional due to mutations in transposase coding sequence caused by a process named "vertical inactivation" (Ivics et al., 1997; Lohe et al., 1995). Many efforts have been made to reconstruct active DNA transposon from non functional inactive transposons by

engineering the coding sequence of transposase. In 1997, Ivics et al used accumulated phylogenetic data to reconstruct a transposase gene of Tc1 like transposon from salmonid subfamily. This transposon system was wakened from a long evolutionary sleep; thus they named the resulted active transposase *Sleeping Beauty* (Ivics et al., 1997).

Since its resurrection, the features of *Sleeping Beauty* transposon (SB) have been explored. Structurally SB is 1.6kb in length and consists of SB transposase coding region along with two approximately 230bp long inverted repeats containing the minimal sequences for transposition. Similar to Tol2, the SB transposase gene can be physically separated from the inverted repeats and replaced with other DNA sequence (Izsvak and Ivics, 2004). The cargo limit for SB is around 10kb (Izsvak et al., 2000). Like other transposons in Tc1/mariner family, SB preferentially integrate into TA dinucleotide that is duplicated during insertion (Ivics et al., 1997; Plasterk, 1996). A 3 bp "footprint" is left in the genome when SB is excised (Luo et al., 1998). SB also exhibits a phenomenon called "overproduction inhibition" which means once SB transposase exceeds the optimal concentration, increase in the amount of transposase will decrease transposition activity(Belur et al., 2003; Lohe and Hartl, 1996). SB has been widely used in insertional mutagenesis (Carlson and Largaespada, 2005; Dupuy, 2010), generating transgenic animals (Ivics and Izsvak, 2005)and gene therapy(Izsvak and Ivics, 2004). Albeit powerful, there are several aspects, for instance, low cargo capacity and low transposase activity, need to be improved Many progresses have been made in improving SB including increasing SB transposase activity by construction hyperactive SB transposase (Mates et al., 2009; Zayed et al., 2004) as well as increasing the cargo capacity(de Silva et al., 2010). Garrison et al reported the postintegrative gene silencing within *Sleeping Beauty* transposon system (Garrison et al., 2007).

It has been reported that cHS4 can prevent SB delivered transgene cassette from silencing (Dalsgaard et al., 2009; Sharma et al., 2012).

PiggyBac transposon

PiggyBac (PB) transposon, formerly named as IFP2, was first isolated from the genome of a cabbage looper moth *Trichoplusia ni* (Fraser, et al 1995). Structurally, it is 2472 bp in length and has a 2.1 kb open reading frame, encoding 549 amino acids 68kD transposase PBase (Elick et al., 1996). The *piggyBac* transposon has been engineered into a binary system that consists of two plasmids: the helper plasmid, providing the enzyme, *piggyBac* transposase (PBase), which catalyzes transposition and a donor plasmid, providing the recognition sequence, the transgene for insertion and the terminal repeats (TR) of the transposase. DNA fragments or genes of interest that are flanked by the two TRs in the donor plasmid are inserted into the host genome. *PiggyBac* preferentially integrate into the TTAA sites of the genome (Cary et al., 1989). No "footprint" is left in the genome after *piggyBac* excision. *PiggyBac* has large cargo capacity and can accommodate as much as 14 kb and 18kb of DNA with *epiggyBac* (Lacoste, et al 2009) without compromising transposition efficiency. The number of transposition events can be regulated by controlling the concentration of donor and helper plasmids. Overproduction inhibition and postintegration silencing has not been reported using *piggyBac* system yet. It has been widely used in insertional mutagenesis, iPS cell induction and lineage tracing studies (Yusa, et al 2009; Lu, et al 2009; Rad, et al 2010).

Table 3 Comparison of Tol2, Sleeping Beauty and *piggyBac* transposon

Transposon	Integration site	Cargo capacity	Footprint	Overproducti on inhibition
Tol2	random	11kb	8bp	no
Sleeping Beauty	TA	12kb	3bp	yes
piggyBac	TTAA	18kb	no	no

Targeted Genome engineering using CRISPR/Cas9

Genome engineering using homologous recombination (Capecchi, 1989) revolutionized biological research. It is capable of providing conclusive causal relationship between genotype and phenotype. However, several factors such as the low efficiency of homologous recombination, the time consuming and labor intensive strategies hamper its applications. As alternative, series of programmable nuclease based genome engineering technologies have been developed. These technologies utilize sequence specific DNA binding domain fused to a nonspecific DNA cleavage module (Carroll, 2011; Urnov et al., 2010). These chimeric nucleases can introduce double strand break (DSB) at target DNA sites. Efficient and precise genetic modifications are then introduced at the DSB sites through DNA repair mechanism including error prone non homologous end joining pathway (NHEJ) and homologous directed repair pathway (HDR)(Wyman and Kanaar, 2006). Easy production of customized programmable DNA binding domains makes this approach versatile and can be used to target virtually any genomic location. Four classes of customizable DNA binding proteins: meganucleases(Smith et al., 2006), zinc finger proteins (ZFP) (Miller et al., 2007; Urnov et al., 2005), transcription activator like effectors (TALEs) (Miller et al., 2011; Moscou and Bogdanove, 2009) and type II clustered

regularly interspaced short palindromic repeats (CRISPR) associated endnonuclease Cas9 (Cong et al., 2013; Mali et al., 2013) have been engineered to achieve effective genome engineering. Due to lack of clear correlation between meganulcease protein residues and their target DNA specificity, meganucleases have not been widely used as genome engineering platform (Hsu et al., 2014). Compared to CRISPR/Cas9, zinc finger domains and TALE arrays exhibit context-dependent binding preference (Juillerat et al., 2014; Maeder et al., 2008) and the construction of customized DNA binding domain are labor intensive and costly. Unlike meganucleases, ZF and TALE proteins recognize DNA sequences through protein-DNA interaction; Cas9 is recruited to specific DNA sequences by20 nucleotides short guide RNA (gRNAs). The versatility of CRISPR system is greatly facilitated by the easy construction of gRNA. CRISPR system has been become a platform technology for targeted genome engineering and modification.

Endogenous CRISPR/Cas9 system function as bacterial acquired immune system against invading foreign DNA such as phage DNA through RNA guided DNA cleavage (Wiedenheft et al., 2012). Three types endogenous CRISPR system have been indentified and the type II CRISPR system has been engineered for genome editing for its relatively simple structure. Once infected, bacteria will convert foreign DNA into short segments (spacers) and incorporate them in CRISPR loci. These short spacers will get transcribed and processed into short CRISPR RNA (crRNA) via RNase III and Cas9. The crRNA then hybridize with non coding trans-activating crRNAs (tracer RNA) and the crRNA-tracerRNA hybrid then recruit Cas9 to the target site and pathogenic foreign DNA is cleaved by Cas9(Gaj et al., 2013). In order for efficient cleavage by Cas9, a 3 nucleotide protospacer adjacent motif (PAM) sequence must be present immediately downstream the target sites (Jinek et al., 2012). Two pioneer studies in 2013 demonstrated that co-delivery of plasmids encoding Cas9, crRNA and tracerRNA successfully modified human

genome (Cong et al., 2013; Mali et al., 2013). In only a year, CRISPR/Cas9 system has been applied to many applications beyond genome engineering including large scale gene screen (Shalem et al., 2014; Wang et al., 2014), activate or repress gene expression (Cheng et al., 2013; Gilbert et al., 2013; Qi et al., 2013), visualize specific genomic regions of interest (Chen et al., 2013), just to name a few. As Rodolphe Barrangou (the scientist who first demonstrated CRISPR function as acquired immune system in bacteria) said, "The only limitation today is people's ability to think of creative ways to harness CRISPR"(Pennisi, 2013).

Conclusion

Despite the fact that we know a lot more about cancer than 50 years ago, we still only know a small fraction of it. Cancers still are the leading cause of death and the mortality for cancers hasn't changed little in the past 50 years. This is partly because cancer is not a disease; it is hundreds if not thousands of diseases. Each different types of cancer might have different cell of origin, different genetic mutation or both. New tools thus are badly needed to parse out the contribution of cell of origin and genetic mutation to tumor initiation and progression. The ideal tools would require convenient tracking of normal development lineage and manipulate the cells in the lineage with genomic mutations found in human patients. Transposon and CRISPR/Cas9 system will complement existing methods for lineage labeling and somatic transgenesis.

References

Abel, T.W., Clark, C., Bierie, B., Chytil, A., Aakre, M., Gorska, A., and Moses, H.L. (2009). GFAP-Cre-mediated activation of oncogenic K-ras results in expansion of the subventricular zone and infiltrating glioma. Mol Cancer Res *7*, 645-653.

Aguirre, A., Dupree, J.L., Mangin, J.M., and Gallo, V. (2007). A functional role for EGFR signaling in myelination and remyelination. Nat Neurosci *10*, 990-1002.

Alcantara Llaguno, S., Chen, J., Kwon, C.H., Jackson, E.L., Li, Y., Burns, D.K., Alvarez-Buylla, A., and Parada, L.F. (2009). Malignant astrocytomas originate from neural stem/progenitor cells in a somatic tumor suppressor mouse model. Cancer Cell *15*, 45-56.

Anthony, T.E., and Heintz, N. (2008). Genetic lineage tracing defines distinct neurogenic and gliogenic stages of ventral telencephalic radial glial development. Neural Dev *3*, 30.

Anthony, T.E., Klein, C., Fishell, G., and Heintz, N. (2004). Radial glia serve as neuronal progenitors in all regions of the central nervous system. Neuron *41*, 881-890.

Bachoo, R.M., Maher, E.A., Ligon, K.L., Sharpless, N.E., Chan, S.S., You, M.J., Tang, Y., DeFrances, J., Stover, E., Weissleder, R.*, et al.* (2002). Epidermal growth factor receptor and Ink4a/Arf: convergent mechanisms governing terminal differentiation and transformation along the neural stem cell to astrocyte axis. Cancer Cell *1*, 269-277.

Beck, C.R., Collier, P., Macfarlane, C., Malig, M., Kidd, J.M., Eichler, E.E., Badge, R.M., and Moran, J.V. (2010). LINE-1 retrotransposition activity in human genomes. Cell *141*, 1159-1170.

Belur, L.R., Frandsen, J.L., Dupuy, A.J., Ingbar, D.H., Largaespada, D.A., Hackett, P.B., and Scott McIvor, R. (2003). Gene insertion and long-term expression in lung mediated by the Sleeping Beauty transposon system. Mol Ther *8*, 501-507.

Buckner, J.C., Brown, P.D., O'Neill, B.P., Meyer, F.B., Wetmore, C.J., and Uhm, J.H. (2007). Central nervous system tumors. Mayo Clin Proc *82*, 1271-1286.

Burrell, R.A., McGranahan, N., Bartek, J., and Swanton, C. (2013). The causes and consequences of genetic heterogeneity in cancer evolution. Nature *501*, 338-345.

Calzolari, F., Appolloni, I., Tutucci, E., Caviglia, S., Terrile, M., Corte, G., and Malatesta, P. (2008). Tumor progression and oncogene addiction in a PDGF-B-induced model of gliomagenesis. Neoplasia *10*, 1373-1382, following 1382.

Campbell, K., and Gotz, M. (2002). Radial glia: multi-purpose cells for vertebrate brain development. Trends Neurosci *25*, 235-238.

Campbell, L.L., and Polyak, K. (2007). Breast tumor heterogeneity: cancer stem cells or clonal evolution? Cell Cycle *6*, 2332-2338.

Candolfi, M., Curtin, J.F., Nichols, W.S., Muhammad, A.G., King, G.D., Pluhar, G.E., McNiel, E.A., Ohlfest, J.R., Freese, A.B., Moore, P.F.*, et al.* (2007). Intracranial glioblastoma models in preclinical neuro-oncology: neuropathological characterization and tumor progression. J Neurooncol *85*, 133-148.

Capecchi, M.R. (1989). Altering the genome by homologous recombination. Science *244*, 1288-1292.

Carlson, C.M., and Largaespada, D.A. (2005). Insertional mutagenesis in mice: new perspectives and tools. Nat Rev Genet *6*, 568-580.

Carroll, D. (2011). Genome engineering with zinc-finger nucleases. Genetics *188*, 773-782.

Cary, L.C., Goebel, M., Corsaro, B.G., Wang, H.G., Rosen, E., and Fraser, M.J. (1989). Transposon mutagenesis of baculoviruses: analysis of Trichoplusia ni transposon IFP2 insertions within the FP-locus of nuclear polyhedrosis viruses. Virology *172*, 156-169.

Chen, B., Gilbert, L.A., Cimini, B.A., Schnitzbauer, J., Zhang, W., Li, G.W., Park, J., Blackburn, E.H., Weissman, J.S., Qi, L.S.*, et al.* (2013). Dynamic imaging of genomic loci in living human cells by an optimized CRISPR/Cas system. Cell *155*, 1479-1491.

Cheng, A.W., Wang, H., Yang, H., Shi, L., Katz, Y., Theunissen, T.W., Rangarajan, S., Shivalila, C.S., Dadon, D.B., and Jaenisch, R. (2013). Multiplexed activation of endogenous genes by CRISPR-on, an RNA-guided transcriptional activator system. Cell Res *23*, 1163-1171.

Chenn, A., Zhang, Y.A., Chang, B.T., and McConnell, S.K. (1998). Intrinsic polarity of mammalian neuroepithelial cells. Mol Cell Neurosci *11*, 183-193.

Choi, B.H., and Lapham, L.W. (1978). Radial glia in the human fetal cerebrum: a combined Golgi, immunofluorescent and electron microscopic study. Brain Res *148*, 295-311.

Cong, L., Ran, F.A., Cox, D., Lin, S., Barretto, R., Habib, N., Hsu, P.D., Wu, X., Jiang, W., Marraffini, L.A*., et al.* (2013). Multiplex genome engineering using CRISPR/Cas systems. Science *339*, 819-823.

Cooley, L., Kelley, R., and Spradling, A. (1988). Insertional mutagenesis of the Drosophila genome with single P elements. Science *239*, 1121-1128.

Dai, C., Celestino, J.C., Okada, Y., Louis, D.N., Fuller, G.N., and Holland, E.C. (2001). PDGF autocrine stimulation dedifferentiates cultured astrocytes and induces oligodendrogliomas and oligoastrocytomas from neural progenitors and astrocytes in vivo. Genes Dev *15*, 1913-1925.

Dalsgaard, T., Moldt, B., Sharma, N., Wolf, G., Schmitz, A., Pedersen, F.S., and Mikkelsen, J.G. (2009). Shielding of sleeping beauty DNA transposon-delivered transgene cassettes by heterologous insulators in early embryonal cells. Mol Ther *17*, 121-130.

de Silva, S., Mastrangelo, M.A., Lotta, L.T., Jr., Burris, C.A., Izsvak, Z., Ivics, Z., and Bowers, W.J. (2010). Herpes simplex virus/Sleeping Beauty vector-based embryonic gene transfer using the HSB5 mutant: loss of apparent transposition hyperactivity in vivo. Human gene therapy *21*, 1603-1613.

Ding, H., Shannon, P., Lau, N., Wu, X., Roncari, L., Baldwin, R.L., Takebayashi, H., Nagy, A., Gutmann, D.H., and Guha, A. (2003). Oligodendrogliomas result from the expression of an activated mutant epidermal growth factor receptor in a RAS transgenic mouse astrocytoma model. Cancer Res *63*, 1106-1113.

Dupuy, A.J. (2010). Transposon-based screens for cancer gene discovery in mouse models. Seminars in cancer biology *20*, 261-268.

Elick, T.A., Bauser, C.A., and Fraser, M.J. (1996). Excision of the piggyBac transposable element in vitro is a precise event that is enhanced by the expression of its encoded transposase. Genetica *98*, 33-41.

Gaj, T., Gersbach, C.A., and Barbas, C.F., 3rd (2013). ZFN, TALEN, and CRISPR/Cas-based methods for genome engineering. Trends Biotechnol *31*, 397-405.

Garrison, B.S., Yant, S.R., Mikkelsen, J.G., and Kay, M.A. (2007). Postintegrative gene silencing within the Sleeping Beauty transposition system. Mol Cell Biol *27*, 8824-8833.

Gilbert, L.A., Larson, M.H., Morsut, L., Liu, Z., Brar, G.A., Torres, S.E., Stern-Ginossar, N., Brandman, O., Whitehead, E.H., Doudna, J.A*., et al.* (2013). CRISPR-mediated modular RNA-guided regulation of transcription in eukaryotes. Cell *154*, 442-451.

Gorski, J.A., Talley, T., Qiu, M., Puelles, L., Rubenstein, J.L., and Jones, K.R. (2002). Cortical excitatory neurons and glia, but not GABAergic neurons, are produced in the Emx1-expressing lineage. J Neurosci *22*, 6309-6314.

Gray, G.E., and Sanes, J.R. (1992). Lineage of radial glia in the chicken optic tectum. Development *114*, 271-283.

Hartfuss, E., Galli, R., Heins, N., and Gotz, M. (2001). Characterization of CNS precursor subtypes and radial glia. Dev Biol *229*, 15-30.

Haubensak, W., Attardo, A., Denk, W., and Huttner, W.B. (2004). Neurons arise in the basal neuroepithelium of the early mammalian telencephalon: a major site of neurogenesis. Proc Natl Acad Sci U S A *101*, 3196-3201.

Hede, S.M., Hansson, I., Afink, G.B., Eriksson, A., Nazarenko, I., Andrae, J., Genove, G., Westermark, B., and Nister, M. (2009). GFAP promoter driven transgenic expression of PDGFB in the mouse brain leads to glioblastoma in a Trp53 null background. Glia *57*, 1143-1153.

Heppner, G.H. (1984). Tumor heterogeneity. Cancer Res *44*, 2259-2265.

Holland, E.C., Celestino, J., Dai, C., Schaefer, L., Sawaya, R.E., and Fuller, G.N. (2000). Combined activation of Ras and Akt in neural progenitors induces glioblastoma formation in mice. Nat Genet *25*, 55-57.

Hsu, P.D., Lander, E.S., and Zhang, F. (2014). Development and applications of CRISPR-Cas9 for genome engineering. Cell *157*, 1262-1278.

Ichikawa, M., Shiga, T., and Hirata, Y. (1983). Spatial and temporal pattern of postnatal proliferation of glial cells in the parietal cortex of the rat. Brain Res *285*, 181-187.

Ivics, Z., Hackett, P.B., Plasterk, R.H., and Izsvak, Z. (1997). Molecular reconstruction of Sleeping Beauty, a Tc1-like transposon from fish, and its transposition in human cells. Cell *91*, 501-510.

Ivics, Z., and Izsvak, Z. (2005). A whole lotta jumpin' goin' on: new transposon tools for vertebrate functional genomics. Trends in genetics : TIG *21*, 8-11.

Ivics, Z., Izsvak, Z., Minter, A., and Hackett, P.B. (1996). Identification of functional domains and evolution of Tc1-like transposable elements. Proc Natl Acad Sci U S A *93*, 5008-5013.

Izsvak, Z., and Ivics, Z. (2004). Sleeping beauty transposition: biology and applications for molecular therapy. Mol Ther *9*, 147-156.

Izsvak, Z., Ivics, Z., and Plasterk, R.H. (2000). Sleeping Beauty, a wide host-range transposon vector for genetic transformation in vertebrates. Journal of molecular biology *302*, 93-102.

Jacques, T.S., Swales, A., Brzozowski, M.J., Henriquez, N.V., Linehan, J.M., Mirzadeh, Z., C, O.M., Naumann, H., Alvarez-Buylla, A., and Brandner, S. (2010). Combinations of genetic mutations in the adult neural stem cell compartment determine brain tumour phenotypes. Embo J *29*, 222-235.

Jinek, M., Chylinski, K., Fonfara, I., Hauer, M., Doudna, J.A., and Charpentier, E. (2012). A programmable dual-RNA-guided DNA endonuclease in adaptive bacterial immunity. Science *337*, 816-821.

Jones, T.S., and Holland, E.C. (2011). Animal models for glioma drug discovery. Expert Opin Drug Discov *6*, 1271-1283.

Juillerat, A., Beurdeley, M., Valton, J., Thomas, S., Dubois, G., Zaslavskiy, M., Mikolajczak, J., Bietz, F., Silva, G.H., Duclert, A*., et al.* (2014). Exploring the transcription activator-like effectors scaffold versatility to expand the toolbox of designer nucleases. BMC molecular biology *15*, 13.

Kamei, Y., Inagaki, N., Nishizawa, M., Tsutsumi, O., Taketani, Y., and Inagaki, M. (1998). Visualization of mitotic radial glial lineage cells in the developing rat brain by Cdc2 kinase-phosphorylated vimentin. Glia *23*, 191-199.

Kawakami, K. (2007). Tol2: a versatile gene transfer vector in vertebrates. Genome biology *8 Suppl 1*, S7.

Kawakami, K., Koga, A., Hori, H., and Shima, A. (1998). Excision of the tol2 transposable element of the medaka fish, Oryzias latipes, in zebrafish, Danio rerio. Gene *225*, 17-22.

Kawakami, K., Shima, A., and Kawakami, N. (2000). Identification of a functional transposase of the Tol2 element, an Ac-like element from the Japanese medaka fish, and its transposition in the zebrafish germ lineage. Proc Natl Acad Sci U S A *97*, 11403-11408.

Kessaris, N., Fogarty, M., Iannarelli, P., Grist, M., Wegner, M., and Richardson, W.D. (2006). Competing waves of oligodendrocytes in the forebrain and postnatal elimination of an embryonic lineage. Nat Neurosci *9*, 173-179.

Koga, A., Iida, A., Hori, H., Shimada, A., and Shima, A. (2006). Vertebrate DNA transposon as a natural mutator: the medaka fish Tol2 element contributes to genetic variation without recognizable traces. Mol Biol Evol *23*, 1414-1419.

Koga, A., Suzuki, M., Inagaki, H., Bessho, Y., and Hori, H. (1996). Transposable element in fish. Nature *383*, 30.

Kriegstein, A., and Alvarez-Buylla, A. (2009). The glial nature of embryonic and adult neural stem cells. Annu Rev Neurosci *32*, 149-184.

Kwon, C.H., Zhao, D., Chen, J., Alcantara, S., Li, Y., Burns, D.K., Mason, R.P., Lee, E.Y., Wu, H., and Parada, L.F. (2008). Pten haploinsufficiency accelerates formation of high-grade astrocytomas. Cancer Res *68*, 3286-3294.

Levison, S.W., and Goldman, J.E. (1993). Both oligodendrocytes and astrocytes develop from progenitors in the subventricular zone of postnatal rat forebrain. Neuron *10*, 201-212.

Levitt, P., and Rakic, P. (1980). Immunoperoxidase localization of glial fibrillary acidic protein in radial glial cells and astrocytes of the developing rhesus monkey brain. J Comp Neurol *193*, 815-840.

Lindberg, N., Kastemar, M., Olofsson, T., Smits, A., and Uhrbom, L. (2009). Oligodendrocyte progenitor cells can act as cell of origin for experimental glioma. Oncogene *28*, 2266-2275.

Liu, C., Sage, J.C., Miller, M.R., Verhaak, R.G., Hippenmeyer, S., Vogel, H., Foreman, O., Bronson, R.T., Nishiyama, A., Luo, L.*, et al.* (2011). Mosaic analysis with double markers reveals tumor cell of origin in glioma. Cell *146*, 209-221.

Lohe, A.R., and Hartl, D.L. (1996). Autoregulation of mariner transposase activity by overproduction and dominant-negative complementation. Mol Biol Evol *13*, 549-555.

Lohe, A.R., Moriyama, E.N., Lidholm, D.A., and Hartl, D.L. (1995). Horizontal transmission, vertical inactivation, and stochastic loss of mariner-like transposable elements. Mol Biol Evol *12*, 62-72.

Lu, Y., Lin, C., and Wang, X. (2009). PiggyBac transgenic strategies in the developing chicken spinal cord. Nucleic Acids Res *37*, e141.

Luo, G., Ivics, Z., Izsvak, Z., and Bradley, A. (1998). Chromosomal transposition of a Tc1/mariner-like element in mouse embryonic stem cells. Proc Natl Acad Sci U S A *95*, 10769-10773.

Maeder, M.L., Thibodeau-Beganny, S., Osiak, A., Wright, D.A., Anthony, R.M., Eichtinger, M., Jiang, T., Foley, J.E., Winfrey, R.J., Townsend, J.A.*, et al.* (2008). Rapid "open-source" engineering of customized zinc-finger nucleases for highly efficient gene modification. Molecular cell *31*, 294-301.

Mali, P., Yang, L., Esvelt, K.M., Aach, J., Guell, M., DiCarlo, J.E., Norville, J.E., and Church, G.M. (2013). RNA-guided human genome engineering via Cas9. Science *339*, 823-826.

Mares, V., and Bruckner, G. (1978). Postnatal formation of non-neuronal cells in the rat occipital cerebrum: an autoradiographic study of the time and space pattern of cell division. J Comp Neurol *177*, 519-528.

Mates, L., Chuah, M.K., Belay, E., Jerchow, B., Manoj, N., Acosta-Sanchez, A., Grzela, D.P., Schmitt, A., Becker, K., Matrai, J.*, et al.* (2009). Molecular evolution of a novel hyperactive Sleeping Beauty transposase enables robust stable gene transfer in vertebrates. Nat Genet *41*, 753-761.

Menn, B., Garcia-Verdugo, J.M., Yaschine, C., Gonzalez-Perez, O., Rowitch, D., and Alvarez-Buylla, A. (2006). Origin of oligodendrocytes in the subventricular zone of the adult brain. J Neurosci *26*, 7907-7918.

Merkle, F.T., Mirzadeh, Z., and Alvarez-Buylla, A. (2007). Mosaic organization of neural stem cells in the adult brain. Science *317*, 381-384.

Merkle, F.T., Tramontin, A.D., Garcia-Verdugo, J.M., and Alvarez-Buylla, A. (2004). Radial glia give rise to adult neural stem cells in the subventricular zone. Proc Natl Acad Sci U S A *101*, 17528-17532.

Miki, Y., Nishisho, I., Horii, A., Miyoshi, Y., Utsunomiya, J., Kinzler, K.W., Vogelstein, B., and Nakamura, Y. (1992). Disruption of the APC gene by a retrotransposal insertion of L1 sequence in a colon cancer. Cancer Res *52*, 643-645.

Miller, J.C., Holmes, M.C., Wang, J., Guschin, D.Y., Lee, Y.L., Rupniewski, I., Beausejour, C.M., Waite, A.J., Wang, N.S., Kim, K.A.*, et al.* (2007). An improved zinc-finger nuclease architecture for highly specific genome editing. Nat Biotechnol *25*, 778-785.

Miller, J.C., Tan, S., Qiao, G., Barlow, K.A., Wang, J., Xia, D.F., Meng, X., Paschon, D.E., Leung, E., Hinkley, S.J.*, et al.* (2011). A TALE nuclease architecture for efficient genome editing. Nat Biotechnol *29*, 143-148.

Miyata, T., Kawaguchi, A., Saito, K., Kawano, M., Muto, T., and Ogawa, M. (2004). Asymmetric production of surface-dividing and non-surface-dividing cortical progenitor cells. Development *131*, 3133-3145.

Moscou, M.J., and Bogdanove, A.J. (2009). A simple cipher governs DNA recognition by TAL effectors. Science *326*, 1501.

Murdoch, B., and Roskams, A.J. (2008). A novel embryonic nestin-expressing radial glia-like progenitor gives rise to zonally restricted olfactory and vomeronasal neurons. J Neurosci *28*, 4271-4282.

Noctor, S.C., Flint, A.C., Weissman, T.A., Dammerman, R.S., and Kriegstein, A.R. (2001). Neurons derived from radial glial cells establish radial units in neocortex. Nature *409*, 714-720.

Noctor, S.C., Flint, A.C., Weissman, T.A., Wong, W.S., Clinton, B.K., and Kriegstein, A.R. (2002). Dividing precursor cells of the embryonic cortical ventricular zone have morphological and molecular characteristics of radial glia. J Neurosci *22*, 3161-3173.

Noctor, S.C., Martinez-Cerdeno, V., Ivic, L., and Kriegstein, A.R. (2004). Cortical neurons arise in symmetric and asymmetric division zones and migrate through specific phases. Nat Neurosci *7*, 136-144.

Noctor, S.C., Martinez-Cerdeno, V., and Kriegstein, A.R. (2007). Contribution of intermediate progenitor cells to cortical histogenesis. Arch Neurol *64*, 639-642.

Noctor, S.C., Martinez-Cerdeno, V., and Kriegstein, A.R. (2008). Distinct behaviors of neural stem and progenitor cells underlie cortical neurogenesis. J Comp Neurol *508*, 28-44.

Oosumi, T., Belknap, W.R., and Garlick, B. (1995). Mariner transposons in humans. Nature *378*, 672.

Orsulic, S. (2002). An RCAS-TVA-based approach to designer mouse models. Mamm Genome *13*, 543-547.

Pennisi, E. (2013). The CRISPR craze. Science *341*, 833-836.

Persson, A.I., Petritsch, C., Swartling, F.J., Itsara, M., Sim, F.J., Auvergne, R., Goldenberg, D.D., Vandenberg, S.R., Nguyen, K.N., Yakovenko, S.*, et al.* (2010). Non-stem cell origin for oligodendroglioma. Cancer Cell *18*, 669-682.

Plasterk, R.H. (1996). The Tc1/mariner transposon family. Current topics in microbiology and immunology *204*, 125-143.

Poduri, A., Evrony, G.D., Cai, X., and Walsh, C.A. Somatic mutation, genomic variation, and neurological disease. Science *341*, 1237758.

Polyak, K. (2007). Breast cancer: origins and evolution. J Clin Invest *117*, 3155-3163.

Polyak, K. (2011). Heterogeneity in breast cancer. J Clin Invest *121*, 3786-3788.

Qi, L.S., Larson, M.H., Gilbert, L.A., Doudna, J.A., Weissman, J.S., Arkin, A.P., and Lim, W.A. (2013). Repurposing CRISPR as an RNA-guided platform for sequence-specific control of gene expression. Cell *152*, 1173-1183.

Schmechel, D.E., and Rakic, P. (1979). A Golgi study of radial glial cells in developing monkey telencephalon: morphogenesis and transformation into astrocytes. Anat Embryol (Berl) *156*, 115-152.

Shalem, O., Sanjana, N.E., Hartenian, E., Shi, X., Scott, D.A., Mikkelsen, T.S., Heckl, D., Ebert, B.L., Root, D.E., Doench, J.G*., et al.* (2014). Genome-scale CRISPR-Cas9 knockout screening in human cells. Science *343*, 84-87.

Shannon, P., Sabha, N., Lau, N., Kamnasaran, D., Gutmann, D.H., and Guha, A. (2005). Pathological and molecular progression of astrocytomas in a GFAP:12 V-Ha-Ras mouse astrocytoma model. Am J Pathol *167*, 859-867.

Sharma, N., Hollensen, A.K., Bak, R.O., Staunstrup, N.H., Schroder, L.D., and Mikkelsen, J.G. (2012). The impact of cHS4 insulators on DNA transposon vector mobilization and silencing in retinal pigment epithelium cells. PLoS One *7*, e48421.

Shih, A.H., Dai, C., Hu, X., Rosenblum, M.K., Koutcher, J.A., and Holland, E.C. (2004). Dose-dependent effects of platelet-derived growth factor-B on glial tumorigenesis. Cancer Res *64*, 4783-4789.

Smith, J., Grizot, S., Arnould, S., Duclert, A., Epinat, J.C., Chames, P., Prieto, J., Redondo, P., Blanco, F.J., Bravo, J*., et al.* (2006). A combinatorial approach to create artificial homing endonucleases cleaving chosen sequences. Nucleic Acids Res *34*, e149.

Swartling, F.J., Hede, S.M., and Weiss, W.A. (2013). What underlies the diversity of brain tumors? Cancer Metastasis Rev *32*, 5-24.

Tamamaki, N., Nakamura, K., Okamoto, K., and Kaneko, T. (2001). Radial glia is a progenitor of neocortical neurons in the developing cerebral cortex. Neurosci Res *41*, 51-60.

Uhrbom, L., Dai, C., Celestino, J.C., Rosenblum, M.K., Fuller, G.N., and Holland, E.C. (2002). Ink4a-Arf loss cooperates with KRas activation in astrocytes and neural progenitors to generate glioblastomas of various morphologies depending on activated Akt. Cancer Res *62*, 5551-5558.

Uhrbom, L., Hesselager, G., Nister, M., and Westermark, B. (1998). Induction of brain tumors in mice using a recombinant platelet-derived growth factor B-chain retrovirus. Cancer Res *58*, 5275-5279.

Uhrbom, L., Hesselager, G., Ostman, A., Nister, M., and Westermark, B. (2000). Dependence of autocrine growth factor stimulation in platelet-derived growth factor-B-induced mouse brain tumor cells. Int J Cancer *85*, 398-406.

Urasaki, A., Morvan, G., and Kawakami, K. (2006). Functional dissection of the Tol2 transposable element identified the minimal cis-sequence and a highly repetitive sequence in the subterminal region essential for transposition. Genetics *174*, 639-649.

Urnov, F.D., Miller, J.C., Lee, Y.L., Beausejour, C.M., Rock, J.M., Augustus, S., Jamieson, A.C., Porteus, M.H., Gregory, P.D., and Holmes, M.C. (2005). Highly efficient endogenous human gene correction using designed zinc-finger nucleases. Nature *435*, 646-651.

Urnov, F.D., Rebar, E.J., Holmes, M.C., Zhang, H.S., and Gregory, P.D. (2010). Genome editing with engineered zinc finger nucleases. Nat Rev Genet *11*, 636-646.

Visvader, J.E. (2011). Cells of origin in cancer. Nature *469*, 314-322.

Voigt, T. (1989). Development of glial cells in the cerebral wall of ferrets: direct tracing of their transformation from radial glia into astrocytes. J Comp Neurol *289*, 74-88.

Walsh, C., and Cepko, C.L. (1988). Clonally related cortical cells show several migration patterns. Science *241*, 1342-1345.

Walsh, C., and Cepko, C.L. (1993). Clonal dispersion in proliferative layers of developing cerebral cortex. Nature *362*, 632-635.

Wang, T., Wei, J.J., Sabatini, D.M., and Lander, E.S. (2014). Genetic screens in human cells using the CRISPR-Cas9 system. Science *343*, 80-84.

Wang, Y., Yang, J., Zheng, H., Tomasek, G.J., Zhang, P., McKeever, P.E., Lee, E.Y., and Zhu, Y. (2009). Expression of mutant p53 proteins implicates a lineage relationship between neural stem cells and malignant astrocytic glioma in a murine model. Cancer Cell *15*, 514-526.

Wei, Q., Clarke, L., Scheidenhelm, D.K., Qian, B., Tong, A., Sabha, N., Karim, Z., Bock, N.A., Reti, R., Swoboda, R.*, et al.* (2006). High-grade glioma formation results from postnatal pten loss or mutant epidermal growth factor receptor expression in a transgenic mouse glioma model. Cancer Res *66*, 7429-7437.

Weiss, W.A., Burns, M.J., Hackett, C., Aldape, K., Hill, J.R., Kuriyama, H., Kuriyama, N., Milshteyn, N., Roberts, T., Wendland, M.F.*, et al.* (2003). Genetic determinants of malignancy in a mouse model for oligodendroglioma. Cancer Res *63*, 1589-1595.

Wiedenheft, B., Sternberg, S.H., and Doudna, J.A. (2012). RNA-guided genetic silencing systems in bacteria and archaea. Nature *482*, 331-338.

Wyman, C., and Kanaar, R. (2006). DNA double-strand break repair: all's well that ends well. Annual review of genetics *40*, 363-383.

Xiao, A., Wu, H., Pandolfi, P.P., Louis, D.N., and Van Dyke, T. (2002). Astrocyte inactivation of the pRb pathway predisposes mice to malignant astrocytoma development that is accelerated by PTEN mutation. Cancer Cell *1*, 157-168.

Yoshida, A., Yamaguchi, Y., Nonomura, K., Kawakami, K., Takahashi, Y., and Miura, M. (2010). Simultaneous expression of different transgenes in neurons and glia by combining in utero electroporation with the Tol2 transposon-mediated gene transfer system. Genes Cells *15*, 501-512.

Zayed, H., Izsvak, Z., Walisko, O., and Ivics, Z. (2004). Development of hyperactive sleeping beauty transposon vectors by mutational analysis. Mol Ther *9*, 292-304.

Zecevic, N., Chen, Y., and Filipovic, R. (2005). Contributions of cortical subventricular zone to the development of the human cerebral cortex. J Comp Neurol *491*, 109-122.

Zhu, H., Acquaviva, J., Ramachandran, P., Boskovitz, A., Woolfenden, S., Pfannl, R., Bronson, R.T., Chen, J.W., Weissleder, R., Housman, D.E*., et al.* (2009). Oncogenic EGFR signaling cooperates with loss of tumor suppressor gene functions in gliomagenesis. Proc Natl Acad Sci U S A *106*, 2712-2716.

Zhu, Y., Guignard, F., Zhao, D., Liu, L., Burns, D.K., Mason, R.P., Messing, A., and Parada, L.F. (2005). Early inactivation of p53 tumor suppressor gene cooperating with NF1 loss induces malignant astrocytoma. Cancer Cell *8*, 119-130.

Zong, H., Espinosa, J.S., Su, H.H., Muzumdar, M.D., and Luo, L. (2005). Mosaic analysis with double markers in mice. Cell *121*, 479-492.

Chapter 2 A method for stable transgenesis of radial glia lineage in rat neocortex by *piggyBac* mediated transposition

(This chapter is published in Journal of Neurosciecen Methods as Fuyi Chen, Joseph LoTurco (2012): A method for stable transgenesis of radial glia lineage in rat neocortex by piggyBac mediated transposition. Journal of Neuroscience Methods, 207 (2): 172-180.)

Abstract

Methods that combine lineage tracing with cellular transgenesis are needed in order to determine mechanisms that specify neural cell types. Currently available methods include viral infection and Cre-mediated recombination. *In utero* electroporation (IUE) has been used in multiple species to deliver multiple transgenes simultaneously into neural progenitors. In standard IUE, most plasmids remain episomal, are lost during cell division, and so transgenes are not expressed in the complete neural lineage. Here we combined IUE with a binary *piggyBac* transposon system (PB-IUE), and show that unlike conventional IUE, a single embryonic transfection of neocortical radial glia with a *piggyBac* transposon system results in stable transgene expression in the neural lineage of radial glia: cortical neurons, astrocytes, oligodendrocytes, and olfactory bulb interneurons. We also developed a modular toolkit of donor and helper plasmids with different promoters that allows for *sh*RNA, bicistronic expression, and trangenesis in subsets of progenitors. As a demonstration of the utility of the toolkit we show that transgenesis of epidermal growth factor receptor (EGFR) expands the number of astrocytes and oligodendrocyrtes generated from progenitors. The relative ease of implementation and experimental flexibility should make the *piggyBac* IUE method a valuable new tool for tracking and manipulating neural lineages.

Introduction

In utero electroporation (IUE) is an efficient method for delivering multiple plasmid DNAs into CNS progenitors *in vivo* (Saito and Nakatsuji, 2001; Tabata and Nakajima, 2001). While an effective method for delivering multiple plasmids with high efficiency into the same progenitor, it suffers from a disadvantage relative to retrovirus or transgenic reporter lines in that it does not result in labeling of an entire lineage. IUE has become widely used in studies of neuronal migration in developing neocortex, and is ideal for labeling pyramidal neurons of defined regions and layers of neocortex (Bai et al., 2003; Manent et al., 2009). In order to label a particular cell type with IUE, the time and location of transfection is varied based on the birthdate and site of generation of that cell type desired to be labeled (LoTurco et al., 2009). Birthdating by IUE is likely caused by plasmid loss and inactivation upon cell division, because viruses applied at the same time label an entire lineage that includes neurons and glia (LoTurco et al., 2009).

A possible non-viral solution to the loss or inactivation of episomal plasmid in IUE is the use of DNA transposon systems such as the *piggyBac* transposon to drive genomic integration of transgenes. Such systems have been used successfully for efficient and stable transgene delivery in multiple cell types (Ding et al., 2005; Wilson et al., 2007; Woltjen et al., 2009; Yoshida et al.). The typical transposon system involves a transgene from a "donor" plasmid and a "helper" plasmid that expresses a transposase. The donor plasmid must contain terminal repeats flanking the transgene of interest for transposition into the genome to occur (Cadinanos and Bradley, 2007). If the helper plasmid does not contain the terminal repeats necessary for DNA transposition, then as with any episomal plasmid, expression of the transposase is lost, and without further transposase expression transgenes are stably integrated into the genome.

Currently there are two well established transposon systems adapted for use in mammalian cells: *Sleeping Beauty* (SB) and *piggyBac* (PB) (VandenDriessche et al., 2009). *PiggyBac* was originally isolated from the genome of the cabbage looper moth *Trichoplusia ni* (Cary et al., 1989; Elick et al., 1996; Fraser et al., 1995). Compared to *Sleeping Beauty*, *piggyBac* has a more precise "cut and paste" mechanism (Fraser et al., 1996; Yusa et al., 2009), higher transposition efficiency (Wu et al., 2006) and larger cargo capacity (Ding et al., 2005; Lacoste et al., 2009). *PiggyBac* has been used to generate iPS cells (Lacoste et al., 2009; Woltjen et al., 2009; Yusa et al., 2009), in gene therapy models (Wilson et al., 2007), and for neuronal development studies in Drosophila (Schuldiner et al., 2008) and chicken (Lu et al., 2009).

Here we report a novel application of *piggyBac* mediated transgenesis in neocortical progenitors in rat by *in utero* electroporation (PB-IUE). This method, unlike standard IUE, can be used to successfully label the complete lineage of neural progenitors: neurons, astrocytes, oligodendrocytes and olfactory bulb interneurons. We additionally developed a *piggyBac* plasmid toolkit that allows for *sh*RNA, bicistronic expression and trangenesis in subsets of neural progenitors. The relative ease of implementation and inherent flexibility of a plasmid-based system should make this method valuable to many interested in marking and manipulating neural lineages in the CNS for rats and other species for which Cre reporter lines are not available.

Results

PiggyBac labels cortical lineage of neural progenitors

We investigated whether *piggyBac* mediated trangenesis can label the progeny of neural progenitors and whether transgenes are stably maintained in progeny. In order to test this, we electroporated the *piggyBac* donor plasmid pPBCAG-eGFP, along with the helper plasmid pCAG-PBase, into developing rat brain at embryonic day 13 (E13) or embryonic day 15 (E15), using episomal pCAG-mRFP as transfection control (Fig.2-1A). The *piggyBac* transposon system is a binary system with a helper plasmid (pCAG-PBase) providing *piggyBac* transposase (PBase), and the donor plasmid (pPBCAG-eGFP) providing the CAG-eGFP transgene between the 5' and 3' terminal repeats (TRs) of the donor plasmid.

In brains electroporated at E13, RFP labeled neurons were restricted to deep layers while GFP labeled cells were found in all layers (Fig. 2-1B). As shown in Fig. 2-1D, deep layer neurons were double labeled with GFP and RFP while the upper layer neurons were only positive for GFP. GFP positive cells in both grey and white matter were GFAP and S100B positive indicating that astrocytes, generated late during cortical development (Kriegstein and Alvarez-Buylla, 2009), can also be labeled by *piggyBac* IUE (Fig. 2-1E-F). When performed with pPBCAG-eGFP alone at E13, IUE labeled deep layer neurons but not upper layer neurons or astrocytes (data not shown). The absence of upper layer neurons and astrocytes in both episomal pCAG-mRFP (Fig. 2-1B) and pPBCAG-eGFP when transfected without the PBase expressing plasmid indicates that episomal plasmid is not maintained through multiple progenitor cell divisions.

In brains electroporated at E15, at the time when upper layer neurons are generated (Langevin et al., 2007), neurons were double labeled with GFP and RFP while astrocytes were only positive for GFP (Fig. 2-1C). We also found that there were more astrocytes labeled by E15 electroporation than by E13 electroporation. At P21, E13 PB-IUE resulted in 79.8 ± 3.3% neurons and 20.2 ± 3.3% astrocytes (Fig. 2-1G), while at E15 there were 26.6 ± 2.7% neurons, 73.4 ± 2.7% astrocytes (one way ANOVA, $p<0.0001$). In summary, unlike conventional IUE with episomal plasmid which only labels birthdated progeny, single embryonic transfections with the *piggyBac* system results in labeling of all cell types in the lineage of embryonic neocortical progenitor cells.

Figure 2-1 *PiggyBac* labels radial glia lineages

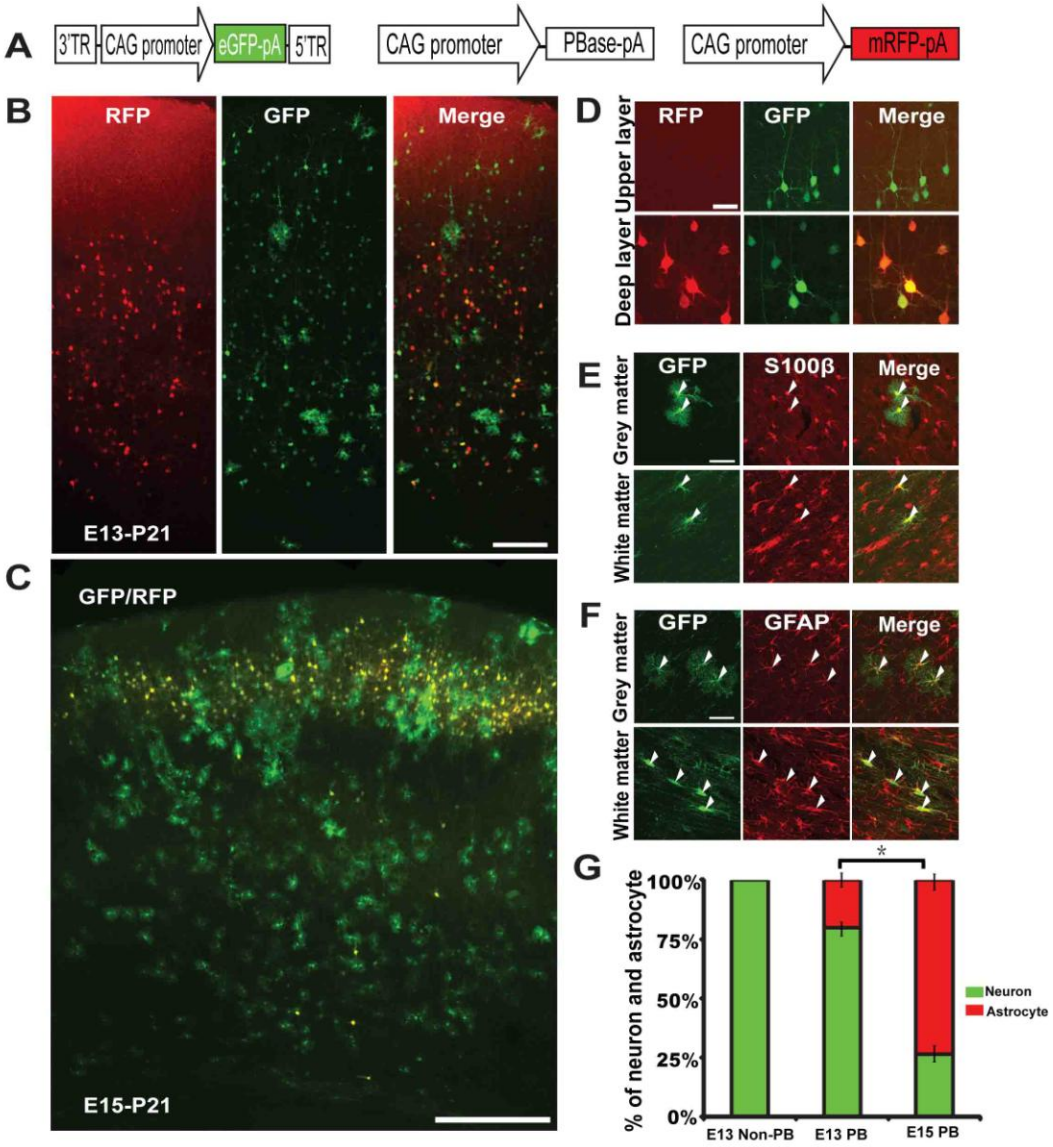

(A), Schematic representation of plasmids used. (B), Images of brains electroporated at E13. (C), Image of brains electroporated at E15. (D), Upper layer neurons were labeled with GFP but not RFP. Deep layer neurons were double labeled with GFP and RFP. (E), GFP labeled cells that were positive for S100B in both white matter and gray matter. (F), GFP labeled cells that were GFAP positive in both white matter and gray matter. (G), Quantifications of astrocyte to neuron

ratio in brains electroporated at E13 and E15. Asterisk indicates significant difference (one way ANOVA, P< 0.001). Scale bar: 200 μm in B, 50 μm in C, 20 μm in D and E, 500 μm in F.

PiggyBac labels olfactory bulb interneurons and oligodendrocytes

To further demonstrate lineage labeling of neural progenitors by the *piggyBac* system, we assessed the presence of other cell types not typically labeled by standard IUE. We found GFP+ but RFP- labeled granule cells and periglomerular cells in the olfactory bulb (Fig. 2-2A). GFP positive cells were positive for the neuroblast marker DCX and these cells were found in rostral migratory stream (RMS) (Fig. 2-2B). In the SVZ of P21 brains, we found GFP positive cells positive for both GFAP (Fig. 2-2C) and Ki67 (Fig. 2-2D). Taken together, these results show that *piggyBac* IUE applied embryonically labels stable staining of SVZ neuroblasts, migrating RMS cells, and olfactory bulb interneurons.

The next question we asked was whether *piggyBac* IUE could label oligodendrocytes. GFP positive cells showed oligodendrocyte (Fig. 2-2F) morphology and were positive for the oligogendrocyte marker CC1 in both grey matter and white matter. Cells co-expressing GFP and the oligodendrocyte precursor marker NG2 were also found in both white and grey matter (Fig.2-2E), supporting the hypothesis that radial glia are a source of at least some oligodendrocyte precursors (Malatesta et al., 2003; Trotter et al., ; Ventura and Goldman, 2007).

Next we applied *piggyBac IUE* in hippocampus. When we electroporated hippocampus at E15 with the *piggyBac* donor (pPBCAG-eGFP) and helper (pCAG-PBase) plasmids, GFP positive cells were found in CA1, CA2, CA3 and dentate gyrus. As shown in Fig. 2-2G, GFP positive neurons, astrocytes (GFAP positive), oligodendrocytes (CC1 positive) and oliogodendrocyte precursors (NG2 positive) were present in hippocampus. In contrast, in brains electroporated

with pPBCAG-eGFP alone, without the PBases expression plasmid, neurons but not astrocytes or oligodendroyctes were labeled by GFP (data not shown). Taken together, our data show that *piggyBac* IUE can be used to label the lineage of progenitors present at the surface of the ventricular zone in the neocortex, olfactory bulb and hippocampus.

Figure 2-2 *PiggyBac* labels olfactory interneurons and oligodendrocytes

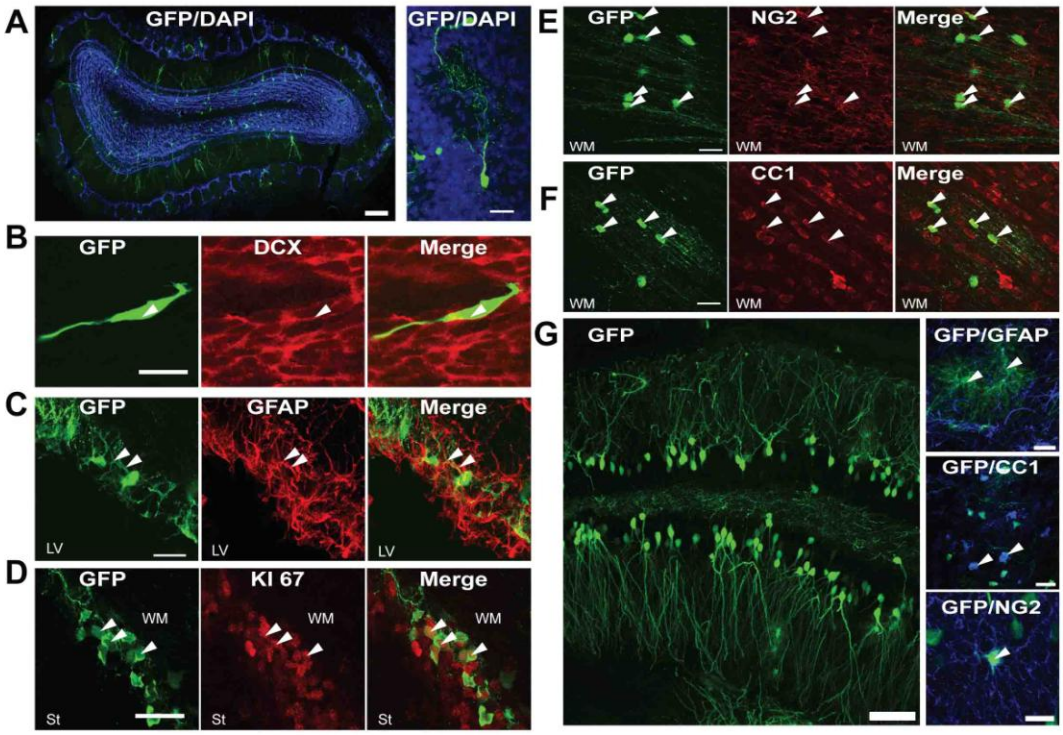

(A), Left panel, Image of P21 olfactory bulb stained with DAPI. GFP positive cells can be seen. Right panel, confocal image of GFP labeled cells in glomeruli. (B), Confocal images of DCX positive cells labeled with GFP in RMS. (C), GFAP positive cells in SVZ double labeled for GFP. (D), Ki67 positive cells in SVZ positive for GFP. (E), NG2 positive cells labeled with GFP in white matter. (F), CC1 positive cells labeled with GFP in white matter. (G), Left, images of hippocampus electroporated at E15. Right, GFAP positive, CC1 positive, and NG2 positive cells

labeled with GFP in hippocampus. Scale bar: A: 100 μm in left panel and 10 μm in right panel. 20 μm in B- G: 50 μm in left panel and 20 μm in right panel.

A modular plasmid toolkit for *piggyBac* IUE

The inherent experimental flexibility of a plasmid system led us to develop additional plasmids that can be used in combination for gain- and loss- of function studies. In addition, we developed plasmids with different promoters in order to selectively target progenitors and progeny of different types (Fig. 2-3). First, we produced an *shRNA piggyBac* donor plasmid (pPBmU6pro) which contains the U6 promoter to drive expression of *shRNAs* for RNA*i* experiments. Second, we made and tested a bicistronic eGFP-t2a-mRFP donor plasmid (pPBCAG-eGFPt2amRFP). This T2A donor plasmid can be used to express two proteins from the same transcript, and so by replacing the mRFP cassette with a gene of interest this plasmid can be useful in experiments where a "within tissue" control is desirable. For example, clones in which eGFP signal is present (i.e. containing the transgene for a gene of interest) can be compared to clones that are missing an eGFP signal but labeled by other fluorescent proteins. Finally, the binary nature of the *piggyBac* system makes possible independent control of the promoters in helper and donor plasmids. We have made a series of helper and donor plasmids with different promoters that can be used alone or in combination. These include the helper plasmids pGLAST-PBase, pGFAP-PBase, pTα1-PBase and pNestin-PBase and donor plasmids pPBGFAP-eGFP, pPBDCX-eGFP, pPBMBP-eGFP and pPBCAMKII-eGFP. Conceptually, these can be mixed in different combinations of donor and helper to integrate transgenes in subpopulations of progenitors (selected by the promoter in the helper plasmid), and have the transgene expressed in subsets of progeny (selected by the promoter in the donor plasmid). For

example, by combining pGLAST-PBase with pPBGFAP-eGFP it is possible to label the astrocytes generated from GLAST positive progenitors.

Figure 2-3 *PiggyBac* toolkit

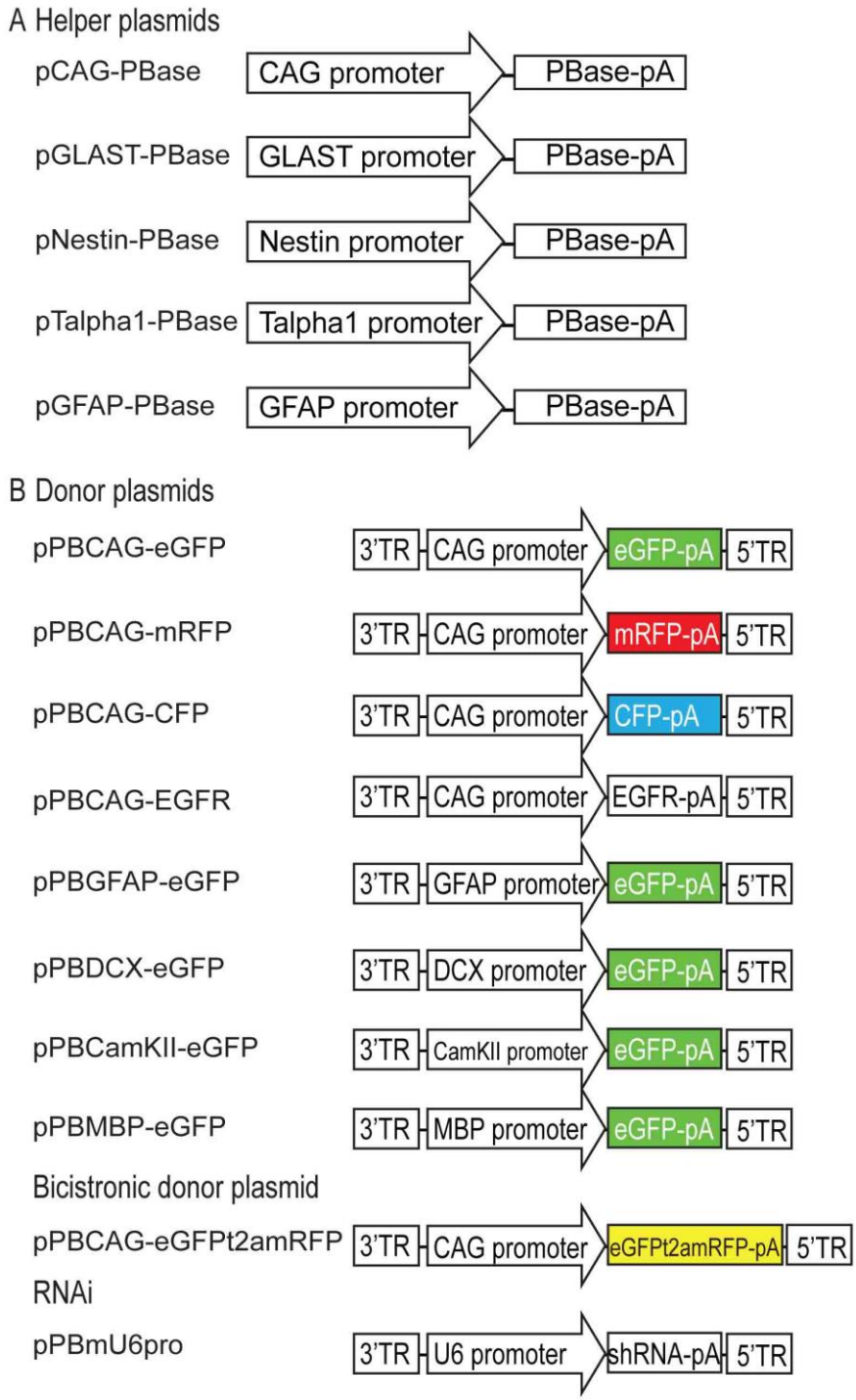

(A), Schematic summaries of *piggyBac* helper plasmids with five different promoters available to drive expression of PBase. (B), Schematics of the collection of *piggyBac* donor plasmids, including multi color *piggyBac* donor plasmid, donor plasmid driven by cell type specific promoters, bicistronic donor plasmid and donor plasmid for expression of *sh*RNAs by the U6 promoter.

EGFR transgenesis expands astrocyte clones in cortex

To demonstrate the utility of the multi plasmid *piggyBac* system in gain-of-function experiments, we transfected a *piggyBac* system mixture of plasmids containing fluorescent proteins. Transfection of three fluorescent trangenes (pPBCAG-eGFP, pPBCAG-mRFP and pPBCAG-CFP) resulted in approximately 70% of cells expressing all three fluorescent proteins, albeit at varied levels, 20% expressing 2 and 10% expressing one fluorescent protein. This relatively high co-expression rate indicated that gain-of-function experiments could be achieved in combination with two-color labeling by simply adding additional donor plasmids to the transfection mixture. For these IUE experiments we used the GLAST promoter to direct expression of transposase in radial glia at E15. In a test of this gain-of-function application we introduced a donor plasmid, pPBCAG-EGFR, which encodes epidermal growth factor receptor (EGFR). EGFR expression has been previously shown to increase the proliferation of astrocyte progenitors, and we hypothesized that increased proliferation of astrocytes or astrocyte progenitors would result in more cells in same color astrocyte groups. As shown in Fig.2-4 A-D the expression of EGFR increased the density of astrocytes in cortex and striatum. Within neocortex, EGFR trangenesis expanded same color astrocyte groups and this gave rise to large patches of single color groupings of astrocytes. This expansion was further demonstrated by a significant increase in the distribution of distances between same color cells within 250 x 250

μm regions (Fig. 2-4E). The EGFR related expansion of same color distances is consistent with previous studies showing an increase in proliferation of astrocytes following EGFR overexpression (Ayuso-Sacido et al., ; Burrows et al., 1997; Sun et al., 2005), and extends these results to show that clonal expansion can result in an increase in the spatial domains occupied by clonally related astrocytes. Moreover, the result supports the idea that same color groups of astrocytes are clonally related and demonstrates the gain-of-function application.

Figure 2-4 EGFR transgenesis induces spatial expansion of same colored astrocyte groups

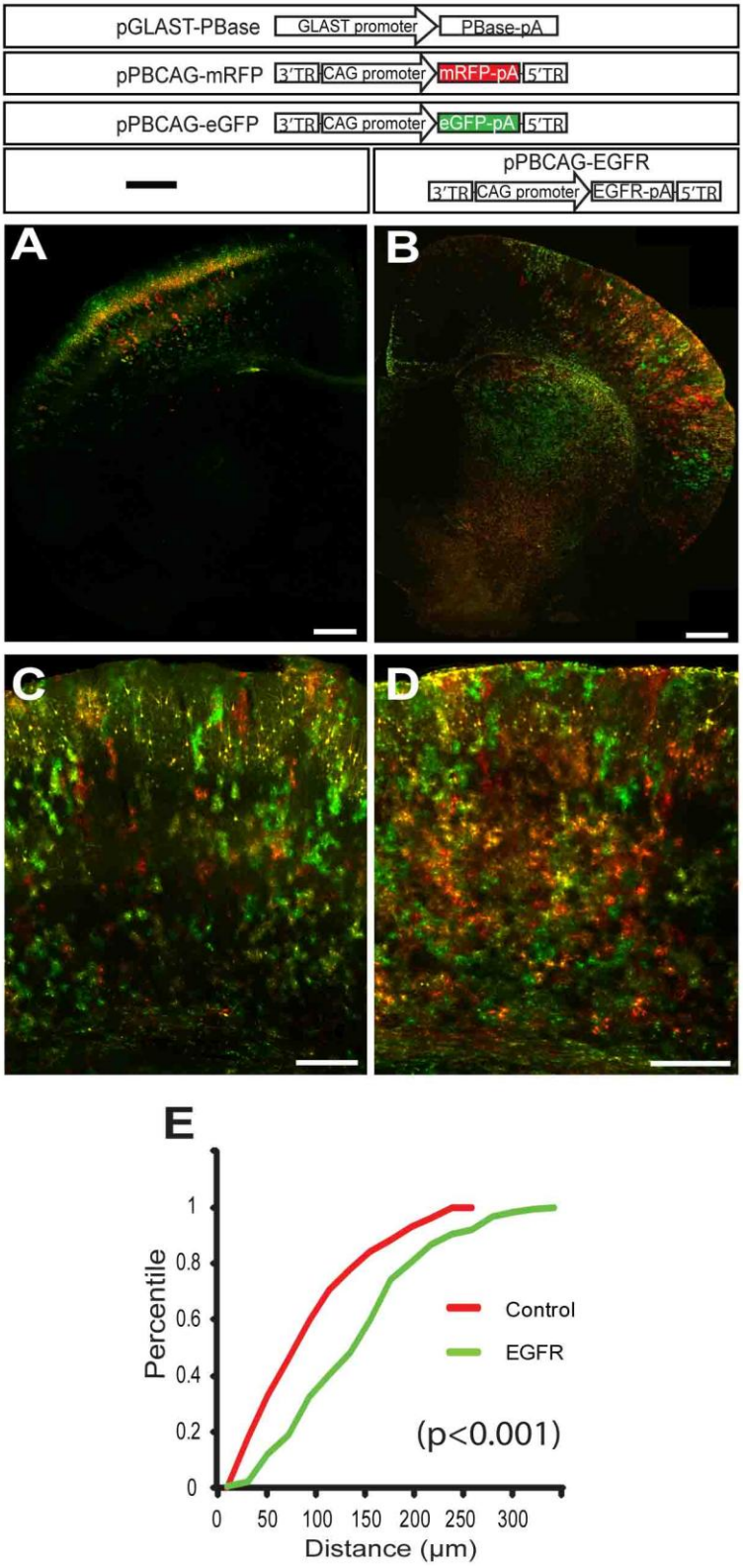

(A), Images from a control transfected hemisphere at P27 transfected with the multicolor plasmid system without the addition of an EGFR donor plasmid. (B), Example of a hemisphere at P27 transfected with EGFR donor plasmid and the multicolor plasmid system. High magnification of control transfected cortex is shown in (C) and EGFR transfected cortex is shown in (D). (E), Cumulative probability histogram showing the distribution of same colored cell distances in 250x250 m areas of cortex with (green line) and without (red line) transfection of EGFR donor plasmid. (Kolmogorov-Smirnov; $P<0.0001$). Scale bar: 500 μm in A and B, 100 μm in C and D.

Patterned clonal astrocyte expansion following EGFR transgenesis

In areas outside of dorsal-lateral neocortex, EGFR transgenesis showed unique patterns of multicolor labeling that were not apparent in transfections without EGFR. Large color-defined patches of astrocytes appeared following EGFR transgenesis (Fig. 2-5A) in the forebrain medial wall and the striatum. Without EGFR transgenesis only scattered cells in striatum were labeled (Fig. 2-4A), but as shown in Fig.2-4B and Fig.2-5B, after EGFR transgenesis extremely large single color groups of astrocytes were found spread throughout striatum. EGFR trangenesis also expanded oligodendrocytes of single color within the anterior commissure and corpus callosum (data not shown). The number of interneurons labeled in the olfactory bulb was also increased following EGFR transgenesis. Unlike astrocytes, granule cell numbers in the olfactory bulb were expanded without any apparent clustering of color-defined groups suggesting that expansion of granule cell numbers did not result in expansion of spatially restricted clonal related neurons (Fig. 2-5C). Astrocytes in the olfactory bulb, similar to astrocytes elsewhere, showed expansion of single color groups (Fig. 2-5D).

Figure 2-5 EGFR induced patterns of clonal expansion in forebrain

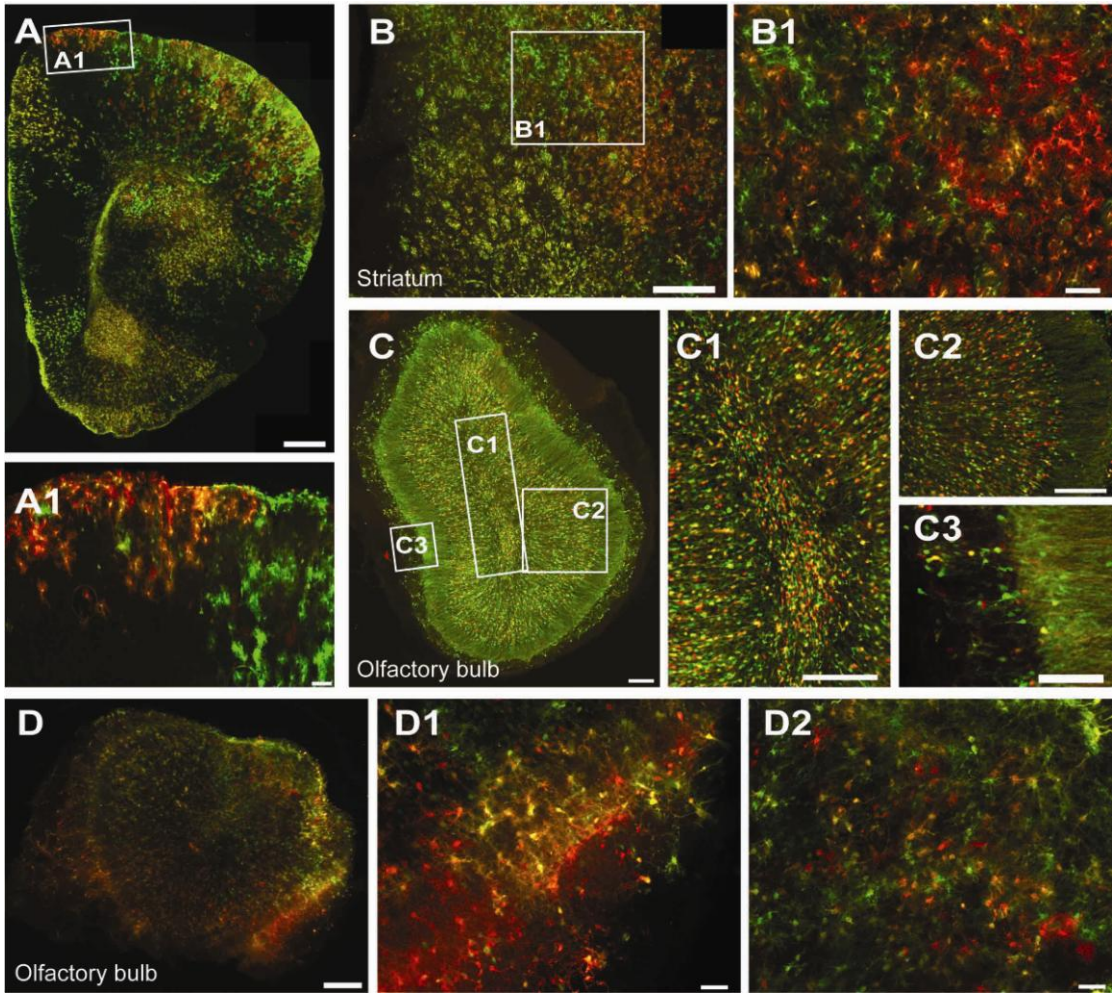

(A), Image of an anterior section from a P27 rat brain with EGFR trangenesis. Large astrocyte groupings were observed as shown in A1. Stripes of astrocytes of same color are also noticeable. (B), Striatum with EGFR transgenesis. Large same color astrocyte groupings were apparent with some color mixing within the larger groups. B1 shows an example of large red astrocyte grouping mixing with other astrocytes. (C), Images of olfactory bulb with EGFR transgenesis. Expansion of the number of olfactory interneurons and clonal mixing were observed. Higher magnification of the olfactory ventricle, granule layer and periglomerular layer are shown in C1, C2 and C3. (D), Images of olfactory bulb with same color astrocyte clusters in the EGFR

transgenesis condition. Examples of astocytes in olfactory bulb are shown in D1 and D2. Scale bar: 100 μm in A-D, 20 μm in A1, B1, C1, C2 and C3, 50 μm in D1 and D2.

Discussion

In utero electroporation (IUE) is a relatively efficient method for delivering plasmid DNA into CNS progenitors *in vivo* (Saito and Nakatsuji, 2001; Tabata and Nakajima, 2001). The approach has become widely used in studies of neuronal migration in developing neocortex, and is ideal for labeling pyramidal neurons of defined regions and layers of neocortex (Bai et al., 2003; Manent et al., 2009). While an effective method, it suffered from a disadvantage, relative to retrovirus, when applied to neocortex in that it did not reliably label the entire lineage of radial glia. Here we reported that the combination of *in utero* electroporation and *piggyBac* mediated transposition (PB-IUE) successfully labels the lineage of radial glia. The method extends the application of IUE to a unique lineage labeling approach in which the "birthdated" progenies are labeled by two transgenes and subsequent progenies are labeled only by transgenes flanked by terminal repeats (Fig. 1). The utility of this type of lineage labeling is in being able to express one transgene in only the birthdated progeny (first member of a lineage near the time of transfection) but not in the subsequent progeny of the lineage. We also demonstrated that the *piggyBac* system can be readily adapted to gain-of-function applications. The modular plasmid toolkit can be used to create RNA*i*, bicistronic expression, and/or selected transgene integration into defined progenitors and progeny. The relative ease of implementation, and inherent flexibility of a plasmid-based system, should make this method and toolkit valuable to many interested in marking and manipulating neural lineages in the CNS.

Any method taking advantage of multiple random genomic integration events raises the risk of insertional mutagenesis altering results. In fact, insertional mutagenesis by transposases has been used for identification of cancer related genes in engineered mouse lines (Collier et al., 2005; Starr et al., 2009). These systems of mutagenesis however require constant expression of the transposase to allow for multiple transposition events, and the system we used results in *piggyBac* transposase expression that is limited to immediate progeny and not propagated into dividing members of the lineage. Moreover, we did not observe evidence of mutagenesis based on inspection of morphologies of thousands of neurons and even more astrocytes labeled with the *piggyBac* IUE method.

In conclusion, *piggyBac* mediated transgenesis approach will complement existing methods for the study of neural lineages and glial cells in brain development. The *piggyBac* toolkit shall be proven powerful in radial glia lineage labeling and manipulation.

Methods

Plasmids

Both the 3' and 5' *piggyBac* terminal repeats (3'TR and 5'TR) were amplified from pZGs (Wu et al., 2007). To make pPBCAG-eGFP, the 3'TR was cloned into pCAG-eGFP (Matsuda and Cepko, 2007) using *SalI* and *SpeI* sites and the 5'TR was cloned into the same vector using *PstI* and *HindIII* sites. For construction of pPBCAG-mRFP, the eGFP cassette in pPBCAG-eGFP was replaced by mRFP cassette from pCAGGS-mRFP (Manent et al., 2009) using *XbaI* and *BglII*. pCAG-PBase was constructed by replacing eGFP with PBase sequence (Wu et al., 2007) in pCAG-eGFP using *EcoRI* and *NotI* sites. pGLAST-PBase was made by inserting PBase downstream of GLAST promoter provided by Dr. DJ Volsky (Kim et al., 2003). To make

pPBCAG-EGFR, human wild type EGFR was PCR amplified from EGFR WT (Greulich et al., 2005) (Addgene plasmid 11011), and inserted into *KpnI* and *NotI* sites of pPBCAG-eGFP.

Construction of a *piggyBac* Toolkit

To make pPBCAG-CFP, CFP sequence was amplified from CMV-Brainbow-1.0 (Livet et al., 2007), (Addgene plasmid 18721) and replaced the eGFP cassette in pPBCAG -eGFP using *EcoRI* and *NotI* sites. For construction of pNestin-PBase, pGFAP-PBase and pTalpha1-PBase, PBase coding sequence was directly inserted downstream of the rat Nestin promoter, a gift from Dr. Steven Goldman (Roy et al., 2000), mouse GFAP promoter, a gift from Dr. Vijay Sarthy (Kuzmanovic et al., 2003) and Talpha1 promoter, a gift from Dr. Albert Ayoub and Dr. Pasko Rakic (Gal et al., 2006), respectively. For construction of pPBGFAP-eGFP, pPBDCX-eGFP, pPBCamKII-eGFP and pPBMBP-eGFP, CAG promoter in pPBCAG-eGFP was replaced with mouse GFAP promoter provided by Dr. Vijay Sarthy (Kuzmanovic et al., 2003), mouse DCX promoter, a gift from Dr. Qiang Lu (Wang et al., 2007), rat MBP promoter, a gift from Dr. Robin Miskimins (Wei et al., 2003), and CamKII promoter (Chow et al.), (Addgene plasmid 22217), respectively. For construction of bicistronic donor plasmid pPBCAG-eGFPt2amRFP, T2A sequence *gagggcaggg gaagtctact aacatgcggg gacgtggagg aaaatcccgg ccca* was added to the 3' end of eGFP coding sequence using standard PCR method and then eGFP T2A was inserted into the *XbaI/EcoRI* sites of pPBCAG-mRFP. For future cloning into the T2A plasmid, *EcoRI/ BglII* sites can be used to replace mRFP with gene of interest. Construction of pPB-mU6pro was achieved by inserting *piggyBac* terminal repeats into the mU6pro vector (Yu et al., 2002). 3'TR

was inserted into the *Not1* site and 5'TR was inserted into the *PstI/HindIII* sites of mU6pro. *shRNA* sequence can be cloned into the *XbaI/BbsI* sites.

Animals

Pregnant Wistar rats were obtained from Charles River Laboratories, Inc. (Wilmington, MA) and maintained at the University of Connecticut vivarium. Animal gestational ages were determined and confirmed during surgery. Both male and female embryos were used. All procedures and experimental approaches were approved by the University of Connecticut IACUC.

In utero electroporation

In utero electroporation was performed as previously described (Bai et al., 2003; Ramos et al., 2006). Briefly, rats were anesthetized with a mixture of ketamine/xylazine (100 / 10 mg/kg i.p.). Metacam analgesic was administered daily at dosage of 1 mg/kg s.c. for 2 days following surgery. To visualize the plasmid during electroporation, plasmids were mixed with 2mg/ml Fast Green (Sigma). In all conditions, pPBCAG-eGFP, pPBCAG-mRFP, pPBCAG-EGFR, pCAG-eGFP and pCAG-mRFP were used at the final concentration of 1.0 μg/μl, while pCAG-PBase and pGLAST-PBase were used at the final concentration of 2.0 μg/μl. Electroporation was performed at embryonic day 13 or 15 (E13 or E15). During surgery, the uterine horns were exposed and one lateral ventricle of each embryo was pressure injected with 1-2 μl of plasmid DNA. Injections were made through the uterine wall and embryonic membranes by inserting a pulled glass microelectrodes (Drummond Scientific) into the lateral ventricle and injecting by pressure pulses delivered with a Picospritzer II (General Valve). Electroporation was accomplished with a BTX 8300 pulse generator (BTX Harvard Apparatus) and BTX

tweezertrodes. A voltage of 65-75v was used for electroporation. Hippocampal electroporation was performed as previously described (Navarro-Quiroga et al., 2007).

Immunohistochemistry

Animals were deeply anesthetized with isoflurane and perfused transcardially with 4% paraformaldehyde/PBS (4% PFA). Brain samples were post fixed overnight in 4% PFA and sectioned at 65 μm thickness on vibratome (Leica VT 1000S). Sections were processed as free-floating sections. After blocking in PBS containing 5% of normal goat serum (Sigma,) and 0.3% Triton X-100 (Sigma) for 1h at room temperature, tissue sections were incubated with primary antibodies overnight at 4℃ in the blocking solution. The following primary antibodies were used: mouse anti-GFP (1:1000, Molecular Probes), rat anti-DsRed (1:1000, Molecular Probes), rabbit anti-Ki67 (1:1000, Novus Biologicals),mouse anti-GFAP (1:200, Chemicon) , mouse anti NG2 (1:500, Chemicon), mouse anti-CC1(1:200, Santa Cruz).Tissue sections were washed in PBS, incubated with the appropriate secondary antibodies (all Alexa Fluor in 1: 200, Invitrogen,) for 2hs at room temperature (Alexa Fluor 488 anti-mouse IgG, Alexa Fluor 488 anti-rabbit IgG, Alexa Fluor 568 anti-mouse IgG, Alexa Fluor 568 anti-rabbit IgG, Alexa Fluor 647 anti-rabbit IgG, Invitrogen) and washed in PBS. In some tissues, nuclei were labeled with TOPRO-3 (Molecular Probes) and 4-6-diaminodino-2-phenylindole (DAPI, Invitrogen). Images were acquired on either a Leica TCS SP2 confocal system or Stereo Investigator (Microbright Field) with the HAMAMATSU digital camera C10600. Montage images were taken using the virtual slice function of Stereo Investigator (Microbright Field).

Neighbor analysis and statistics

For neighbor analysis virtual slices were taken using Stereo Investigator (Microbright Field). The virtual slices were divided into 250 × 250 μm grids. Distances between cells with the same

color were measured within the grid and was analyzed by Neurolucida Explorer (Microbright Field). Neighbor analysis was performed both in control conditions and EGFR over expression conditions. To statistically compare changes in the distance distributions in control condition and EGFR over expression condition determined by neighbor analysis, the Kolmogorov-Smirnov test was performed (http://www.physics. csbsju.edu/stats/ KS-test.n.plot_form.html). To compare ratios of labeled cells that were astrocytes or neurons, a one-way analysis of variance (ANOVA) was performed by KaleidaGraph version 4.0 (Synergy Software 2006). A confidence interval of 95% ($p < 0.05$) was required for values to be considered statistically significant. All data are presented as standard error of the mean (SEM).

Reference

Ayuso-Sacido A, Moliterno JA, Kratovac S, Kapoor GS, O'Rourke DM, Holland EC, Garcia-Verdugo JM, Roy NS, Boockvar JA. Activated EGFR signaling increases proliferation, survival, and migration and blocks neuronal differentiation in post-natal neural stem cells. J Neurooncol; 97: 323-37.

Bai J, Ramos RL, Ackman JB, Thomas AM, Lee RV, LoTurco JJ. RNAi reveals doublecortin is required for radial migration in rat neocortex. Nat Neurosci, 2003; 6: 1277-83.

Burrows RC, Wancio D, Levitt P, Lillien L. Response diversity and the timing of progenitor cell maturation are regulated by developmental changes in EGFR expression in the cortex. Neuron, 1997; 19: 251-67.

Cadinanos J, Bradley A. Generation of an inducible and optimized piggyBac transposon system. Nucleic Acids Res, 2007; 35: e87.

Cary LC, Goebel M, Corsaro BG, Wang HG, Rosen E, Fraser MJ. Transposon mutagenesis of baculoviruses: analysis of Trichoplusia ni transposon IFP2 insertions within the FP-locus of nuclear polyhedrosis viruses. Virology, 1989; 172: 156-69.

Chow BY, Han X, Dobry AS, Qian X, Chuong AS, Li M, Henninger MA, Belfort GM, Lin Y, Monahan PE, Boyden ES. High-performance genetically targetable optical neural silencing by light-driven proton pumps. Nature; 463: 98-102.

Collier LS, Carlson CM, Ravimohan S, Dupuy AJ, Largaespada DA. Cancer gene discovery in solid tumours using transposon-based somatic mutagenesis in the mouse. Nature, 2005; 436: 272-6.

Ding S, Wu X, Li G, Han M, Zhuang Y, Xu T. Efficient transposition of the piggyBac (PB) transposon in mammalian cells and mice. Cell, 2005; 122: 473-83.

Elick TA, Bauser CA, Fraser MJ. Excision of the piggyBac transposable element in vitro is a precise event that is enhanced by the expression of its encoded transposase. Genetica, 1996; 98: 33-41.

Fraser MJ, Cary L, Boonvisudhi K, Wang HG. Assay for movement of Lepidopteran transposon IFP2 in insect cells using a baculovirus genome as a target DNA. Virology, 1995; 211: 397-407.

Fraser MJ, Ciszczon T, Elick T, Bauser C. Precise excision of TTAA-specific lepidopteran transposons piggyBac (IFP2) and tagalong (TFP3) from the baculovirus genome in cell lines from two species of Lepidoptera. Insect Mol Biol, 1996; 5.

Gal JS, Morozov YM, Ayoub AE, Chatterjee M, Rakic P, Haydar TF. Molecular and morphological heterogeneity of neural precursors in the mouse neocortical proliferative zones. J Neurosci, 2006; 26: 1045-56.

Greulich H, Chen TH, Feng W, Janne PA, Alvarez JV, Zappaterra M, Bulmer SE, Frank DA, Hahn WC, Sellers WR, Meyerson M. Oncogenic transformation by inhibitor-sensitive and -resistant EGFR mutants. PLoS Med, 2005; 2: e313.

Kim SY, Choi SY, Chao W, Volsky DJ. Transcriptional regulation of human excitatory amino acid transporter 1 (EAAT1): cloning of the EAAT1 promoter and characterization of its basal and inducible activity in human astrocytes. J Neurochem, 2003; 87: 1485-98.

Kriegstein A, Alvarez-Buylla A. The glial nature of embryonic and adult neural stem cells. Annu Rev Neurosci, 2009; 32: 149-84.

Kuzmanovic M, Dudley VJ, Sarthy VP. GFAP promoter drives Muller cell-specific expression in transgenic mice. Invest Ophthalmol Vis Sci, 2003; 44: 3606-13.

Lacoste A, Berenshteyn F, Brivanlou AH. An efficient and reversible transposable system for gene delivery and lineage-specific differentiation in human embryonic stem cells. Cell Stem Cell, 2009; 5: 332-42.

Langevin LM, Mattar P, Scardigli R, Roussigne M, Logan C, Blader P, Schuurmans C. Validating in utero electroporation for the rapid analysis of gene regulatory elements in the murine telencephalon. Dev Dyn, 2007; 236: 1273-86.

Livet J, Weissman TA, Kang H, Draft RW, Lu J, Bennis RA, Sanes JR, Lichtman JW. Transgenic strategies for combinatorial expression of fluorescent proteins in the nervous system. Nature, 2007; 450: 56-62.

LoTurco J, Manent JB, Sidiqi F. New and improved tools for in utero electroporation studies of developing cerebral cortex. Cereb Cortex, 2009; 19 Suppl 1: i120-5.

Lu Y, Lin C, Wang X. PiggyBac transgenic strategies in the developing chicken spinal cord. Nucleic Acids Res, 2009; 37: e141.

Malatesta P, Hack MA, Hartfuss E, Kettenmann H, Klinkert W, Kirchhoff F, Gotz M. Neuronal or glial progeny: regional differences in radial glia fate. Neuron, 2003; 37: 751-64.

Manent JB, Wang Y, Chang Y, Paramasivam M, LoTurco JJ. Dcx reexpression reduces subcortical band heterotopia and seizure threshold in an animal model of neuronal migration disorder. Nat Med, 2009; 15: 84-90.

Matsuda T, Cepko CL. Controlled expression of transgenes introduced by in vivo electroporation. Proc Natl Acad Sci U S A, 2007; 104: 1027-32.

Navarro-Quiroga I, Chittajallu R, Gallo V, Haydar TF. Long-term, selective gene expression in developing and adult hippocampal pyramidal neurons using focal in utero electroporation. J Neurosci, 2007; 27: 5007-11.

Ramos RL, Bai J, LoTurco JJ. Heterotopia formation in rat but not mouse neocortex after RNA interference knockdown of DCX. Cereb Cortex, 2006; 16: 1323-31.

Roy NS, Benraiss A, Wang S, Fraser RA, Goodman R, Couldwell WT, Nedergaard M, Kawaguchi A, Okano H, Goldman SA. Promoter-targeted selection and isolation of neural progenitor cells from the adult human ventricular zone. J Neurosci Res, 2000; 59: 321-31.

Saito T, Nakatsuji N. Efficient gene transfer into the embryonic mouse brain using in vivo electroporation. Dev Biol, 2001; 240: 237-46.

Schuldiner O, Berdnik D, Levy JM, Wu JS, Luginbuhl D, Gontang AC, Luo L. piggyBac-based mosaic screen identifies a postmitotic function for cohesin in regulating developmental axon pruning. Dev Cell, 2008; 14: 227-38.

Starr TK, Allaei R, Silverstein KA, Staggs RA, Sarver AL, Bergemann TL, Gupta M, O'Sullivan MG, Matise I, Dupuy AJ, Collier LS, Powers S, Oberg AL, Asmann YW, Thibodeau SN,

Tessarollo L, Copeland NG, Jenkins NA, Cormier RT, Largaespada DA. A transposon-based genetic screen in mice identifies genes altered in colorectal cancer. Science, 2009; 323: 1747-50.

Sun Y, Goderie SK, Temple S. Asymmetric distribution of EGFR receptor during mitosis generates diverse CNS progenitor cells. Neuron, 2005; 45: 873-86.

Tabata H, Nakajima K. Efficient in utero gene transfer system to the developing mouse brain using electroporation: visualization of neuronal migration in the developing cortex. Neuroscience, 2001; 103: 865-72.

Trotter J, Karram K, Nishiyama A. NG2 cells: Properties, progeny and origin. Brain Res Rev; 63: 72-82.

VandenDriessche T, Ivics Z, Izsvak Z, Chuah MK. Emerging potential of transposons for gene therapy and generation of induced pluripotent stem cells. Blood, 2009; 114: 1461-8.

Ventura RE, Goldman JE. Dorsal radial glia generate olfactory bulb interneurons in the postnatal murine brain. J Neurosci, 2007; 27: 4297-302.

Wang X, Qiu R, Tsark W, Lu Q. Rapid promoter analysis in developing mouse brain and genetic labeling of young neurons by doublecortin-DsRed-express. J Neurosci Res, 2007; 85: 3567-73.

Wei Q, Miskimins WK, Miskimins R. Cloning and characterization of the rat myelin basic protein gene promoter. Gene, 2003; 313: 161-7.

Wilson MH, Coates CJ, George AL, Jr. PiggyBac transposon-mediated gene transfer in human cells. Mol Ther, 2007; 15: 139-45.

Woltjen K, Michael IP, Mohseni P, Desai R, Mileikovsky M, Hamalainen R, Cowling R, Wang W, Liu P, Gertsenstein M, Kaji K, Sung HK, Nagy A. piggyBac transposition reprograms fibroblasts to induced pluripotent stem cells. Nature, 2009; 458: 766-70.

Wu S, Ying G, Wu Q, Capecchi MR. Toward simpler and faster genome-wide mutagenesis in mice. Nat Genet, 2007; 39: 922-30.

Wu SC, Meir YJ, Coates CJ, Handler AM, Pelczar P, Moisyadi S, Kaminski JM. piggyBac is a flexible and highly active transposon as compared to sleeping beauty, Tol2, and Mos1 in mammalian cells. Proc Natl Acad Sci U S A, 2006; 103: 15008-13.

Yoshida A, Yamaguchi Y, Nonomura K, Kawakami K, Takahashi Y, Miura M. Simultaneous expression of different transgenes in neurons and glia by combining in utero electroporation with the Tol2 transposon-mediated gene transfer system. Genes Cells; 15: 501-12.

Yu JY, DeRuiter SL, Turner DL. RNA interference by expression of short-interfering RNAs and hairpin RNAs in mammalian cells. Proc Natl Acad Sci U S A, 2002; 99: 6047-52.

Yusa K, Rad R, Takeda J, Bradley A. Generation of transgene-free induced pluripotent mouse stem cells by the piggyBac transposon. Nat Methods, 2009; 6: 363-9.

Chapter 3 Contribution of Tumor Heterogeneity in a New Animal Model of CNS Tumors

(This chapter is published in Molecular Cancer Research as: Fuyi Chen, Albert Becker and Joseph J. LoTurco (2014): Contribution of Tumor Heterogeneity in a New Animal Model of CNS Tumors. Molecular Cancer Research; doi:10.1158/1541-7786.MCR-13-0531)

Abstract

The etiology of central nervous system (CNS) tumor heterogeneity is unclear. To clarify this issue, a novel animal model was developed of glioma and atypical teratoid/rhabdoid-like tumor (ATRT) produced in rats by non-viral cellular transgenesis initiated in utero. This model system affords the opportunity for directed oncogene expression, clonal labeling, and addition of tumor-modifying transgenes. By directing HRasV12 and AKT transgene expression in different cell populations with promoters that are active ubiquitously (CAG promoter), astrocyte-selective (GFAP promoter), or oligodendrocyte-selective (MBP promoter); thus, generating glioblastoma multiforme (GBM) and anaplastic oligoastrocytoma (AO), respectively. Importantly, the GBM and AO tumors were distinguishable at both the cellular and molecular level. Furthermore, proneural basic-helix-loop-helix (bHLH) transcription factors, Ngn2 (NEUROG2) or NeuroD1, were expressed along with HRasV12 and AKT in neocortical radial glia, leading to the formation of highly lethal atypical teratoid/rhabdoid-like tumors (ATRT). This study establishes a unique model in which determinants of CNS tumor diversity can be parsed out and reveals that both mutation and expression of neurogenic bHLH transcription factors contributes to CNS tumor diversity.

Introduction

Tumors of the central nervous system (CNS) have significant intra- and inter-tumor heterogeneity in terms of cellular composition, cellular proliferation, invasiveness and epigenetic status (Sturm et al., 2012; Verhaak et al., 2010). Integrative large scale gene expression analysis of 200 GBM tumors revealed 4 subtypes: proneural, neural, classical and mesenchymal (Verhaak et al.). A more recent GBM classification based on a combination of epigenetics, copy number variation, gene expression and genetic mutations has lead to identification of as many as six GBM subgroups (Sturm et al., 2012). In addition, there are at least two prognostic subgroups of pediatric GBM based on association with or without aberrantly active Ras/AKT pathway (Faury et al., 2007; Haque et al., 2007). Heterogeneity in GBM tumors may be responsible for differential response to therapeutic interventions (Verhaak et al., 2010), and understanding the etiology of tumor heterogeneity in animal models may become increasingly important to design therapeutic strategies effective at targeting molecularly defined tumor subtypes.

Several animal models of brain tumor, including xenograft models, genetically engineered mouse models (GEMs) and models utilizing virus-mediated somatic cell transgenesis have been used to address important aspects of CNS tumor biology. For example, GEMs harboring mutations found in human gliomas have been used to assess tumorigenic effects of individual genes and mutations and to reveal the tumor cell-of-origin in some models (Liu et al., 2011; Persson et al., 2010). Endogenous cell populations have been induced to form gliomas by both viral and non-viral somatic transgenesis of oncogenes or deletion of tumor suppressor genes in specific target cell populations (Alcantara Llaguno et al., 2009; Friedmann-Morvinski et al.; Hambardzumyan et al., 2009; Holland et al., 2000; Holland et al., 1998; Holmen and Williams, 2005; Lindberg et al., 2009; Marumoto et al., 2009; Uhrbom et al., 2002; Uhrbom et al., 1998;

Wiesner et al., 2009). For example, oligodendrocyte precursor cells (OPCs) can be the cell-of-origin for adult glioma (Lindberg et al., 2009; Liu et al., 2011; Persson et al., 2010) with OPC originated glioma matching the human proneural subgroup of GBM (Lei et al., 2011; Liu et al., 2011). Friedmann-Morvinski et al. found that RNAi knock-down of NF1 and p53 expression in either astrocytes (GFAP+) or neurons (SynI+) induced formation of mesenchymal GBM subtypes, while the same RNAi in Nestin positive neural progenitors induced neural GBM subtypes (Friedmann-Morvinski et al., 2012). To more fully explore causes of tumor diversity in cerebral cortex we have developed an animal model in which multiple transgenes can be expressed in selected cell populations at different times in forebrain development.

DNA transposon systems have been previously adapted to non-viral somatic transgenesis in studies of neocortical development (Chen and LoTurco, 2012; Siddiqi et al., 2014), cellular reprogramming (Yusa et al., 2009), and to generate animal models of glioma (Wiesner et al., 2009). In utero electroporation is a relatively efficient method to deliver multiple combinations of transgenes into neuronal and glial progenitors in the developing forebrain in utero (LoTurco et al., 2009). When combined with a DNA transposon system including cell-type specific promoters, it becomes possible to introduce multiple transgenes, including oncogenes, in different populations of cells (Chen and LoTurco, 2012; Lu et al., 2009; Siddiqi et al., 2014; Yoshida et al., 2010). Active Ras pathway(Guha et al., 1997) and PI3K-AKT pathway(Holland et al., 2000; Ramaswamy et al., 1999) have been frequently found in human glioma patients and used in various glioma animal models (Holland et al., 2000; Holmen and Williams, 2005; Marumoto et al., 2009; Uhrbom et al., 2002). In the model described here, we introduced HRasV12 and AKT in cell populations in the radial glia lineage to ask whether diversity in glioma is linked to the population of cells induced to express oncogenic transgenes. We also

tested whether addition of neurogenic transcription factors to the starting progenitor population modifies tumor type. We show by several measures including morbidity, histology, developmental time course, tumor clonal pattern and molecular signature, that diverse tumors are generated when oncogene expression is directed into different cell populations. Moreover, expression of the basic helix-loop-helix transcription factors Ngn2 or NeuroD1 along with HRasV12 and AKT results in atypical teratoid rhabdoid tumor like tumors (ATRT-like), a pediatric tumor type rarely produced in existing tumor models.

Results

A model of GBM by *piggyBac*-mediated somatic transgenesis

We developed a non-viral somatic cell transgenesis approach to produce tumors from endogenous rat neural progenitors *in vivo*. HRasV12 and AKT transgenes were introduced into embryonic neocortical neural progenitors, also known as radial glial progenitors, by *in utero* electroporation of the lateral ventricles of embryonic rats. For non-viral cellular transgenesis we produced a system of plasmids consisting of a helper plasmid that expresses the *piggyBac* transposase in radial glial progenitors *via* the GLAST promoter (GLAST-PBase) and thereby drives transposon integration into the genomes of radial glia progenitors, and a set of donor plasmids containing transgenes flanked by transposon inverted terminal repeats (ITRs) to be integrated into the genome by *piggyBac* transposase activity. The donor plasmids included HRasV12 and AKT under the control of one of three different promoters (CAG, MBP or GFAP), (Figure 3-1A) and a multicolor system of donor plasmids (Siddiqi et al.) with the CAG promoter

driving expression of eGFP, mRFP or CFP to create multicolor clonal labeling (Fig 3-1A) (Siddiqi et al.; Weber et al.). Electroporation of this system of plasmids unilaterally into the lateral cerebral ventricles of E14-E15 rat embryos (Fig 3-1A) invariably resulted by twenty one days after birth in the formation of large unilateral tumors (Figure 3-2F). Tumors were composed of both regions of uniformly colored cells indicating significant regionalized clonal expansion (Fig. 3-1 C and D), and regions containing a mixture of differently colored cells indicating clonal mixing (Fig. 3-1F). In addition to tumors, streams of cells typically of one or 2 different colors were found distal to the tumor core. These streams were frequently in directionally oriented chains suggesting migration and invasion into surrounding neural tissue (Fig. 3-1E). Survival experiments showed that tumor bearing animals began dying at 3 weeks of age and the rate of death appeared stable by 31 weeks after birth for the CAG donor plasmid treated animals (Fig. 3-2E). Tumors were confirmed in all electroporated animals (30/30).

Histologically, tumors induced by HRasV12 and AKT driven by the CAG donor plasmids were composed of fibrillary and gemistocytic elements (Supplementary Figure 1A). The tumors diffusely infiltrated neighboring tissues (Supplementary Figure 1B) and had cells with highly pleomorphic cytological appearance, and increased mitotic activity indicative of malignancy (Supplementary Figures 1C). Tumor cells frequently invaded the subarachnoidal space (Fig.3-2G), and tumors had areas of necrosis indicative of high malignancy (Fig 3-2H arrow). Tumors appeared by P7 and necrotic areas were found as early as at P4. Immunohistochemical analysis revealed that tumor cells showed strong positivity for GFAP (Figure 3-2I), Vimentin (Figure 3-2 J) and MAP2 (Figure 3-2K). Some neurons entrapped within tumors were positive for synaptophysin, while the bulk of the tumors did not show synaptophysin positivity. Interestingly, we did not observe vascular proliferation in the rat tumors produced by the CAG donor plasmids

but observed vascular proliferation in tumors induced by all other plasmid combinations used in this study. Moreover when cultured in neurosphere suspension medium, tumor cells can form tumor spheres (Supplementary Figure 2). In sum, the *piggyBac* transposon system effectively produces a tumor model resembling human GBM (WHO Grade IV).

Figure 3-1 Multicolor rat glioma

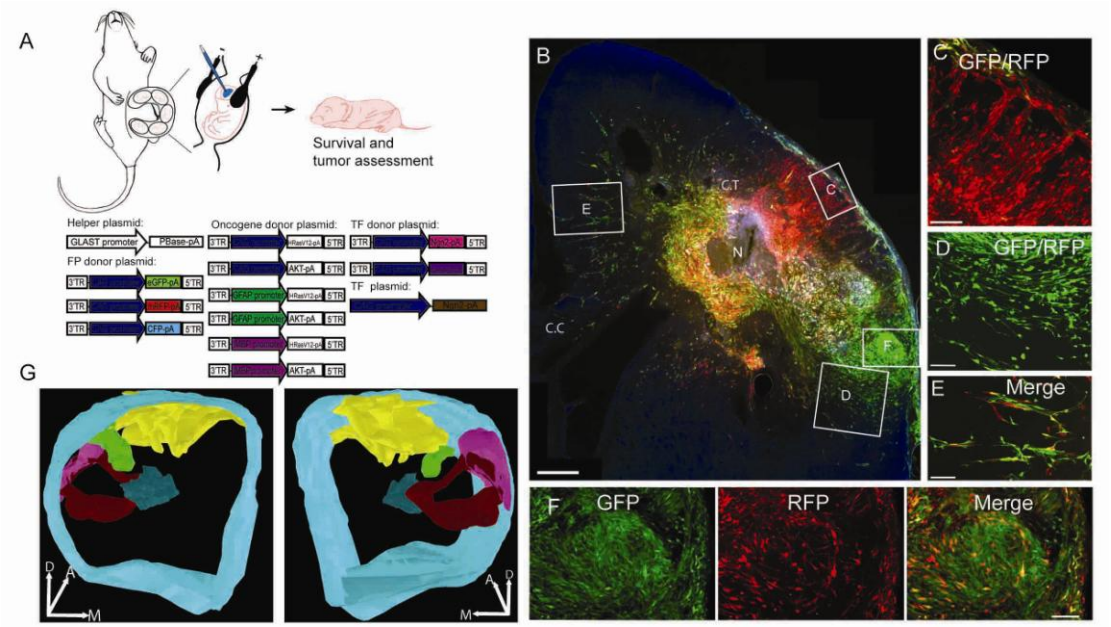

(A) Schematic representation of *piggyBac* IUE approach and plasmids used. *In utero* electroporation was performed between E14-E15 with plasmids listed. We used the multicolor *piggyBac* system to clonally label cells, oncogene donor plasmids to induce tumors and both donor and conventional epsiomal plasmids encoding transcription factors to evaluate their role in gliomagenesis. After the animals were born, tumor assessment was performed at different postnatal ages. (B) Representative images of a P22 rat brain hemisphere transfected with multicolor *piggyBac* plasmids and PBCAG-HRasV12/ATK donor plasmids. Necrosis is labeled with N. (C) Overlay image showing large regions of tumor cells were uniformly labeled with mRFP. (D) Overlay image showing other regions of tumor were uniformly labeled with eGFP.

(E) Streams of tumor cells invading tissue adjacent to tumors. (F) Region of the tumor containing a mixture of red and green labeled tansformed cells indicating regions of clonal mixing. (G) 3D reconstruction of 5 tumor clones in a P27 rat transfected with PBGFAP-HRasV12/AKT. CT, cortex. CC, corpus callosum. Scale bar: 500 μm in B and 100 μm in C, D, E and F.

MBP and GFAP promoter directed oncogene expression produces distinct tumor types

The binary *piggyBac* system allows for directing insertion of transgenes in one population of cells (i.e. radial glia neural progenitors), but then delayed expression of oncogene expression in later generated cell types in the lineage. This feature allowed us to introduce oncogenes into neural progenitors at the embryonic lateral ventricle surfaces, but then have their expression turned on later, primarily in either astrocytes, or oligodendrocytes. For this experiment, we constructed donor plasmids in which HRasV12 and AKT expression was controlled by either a mouse GFAP promoter fragment (Chen and LoTurco, 2012) (PBGFAP-HRasV12/AKT) or a rat MBP promoter fragment (Wei et al., 2003) (PBMBP-HRasV12/AKT). We first assessed the activity of the mouse GFAP and rat MBP promoters using GFP as a reporter. We found that the GFAP promoter resulted in 69.3±3% astrocytes, 19.4±2% neurons, 7.1±2% oligodendrocytes and 4.3±0.7% oligodendrocyte precursor cells. In contrast, the MPB promoter construct (PBMBP-eGFP/mRFP) labeled 57.0±2% oligodendrocytes, 16.2±0.7% astrocytes, 19.3±2% neurons, and 7.5±0.7% oligodendrocyte precursor cells (Figure 3-2C and D). One way ANOVA showed a significant difference between GFAP and MBP promoter labeled astrocytes (p= 6.91E-05) and oliogodendrocytes (p=2.69E-05). A significant difference was also found between NG2 cells labeled by GFAP and MBP promoters (One-way ANOVA, p=0.021172), but no significant

difference was found between the fraction of labeled neurons (One-way ANOVA, p=0.989884). The differences in the cell populations labeled by the MBP and GFAP promoter fragments is consistent with enriched targeting of oligodendrocytes and astrocytes respectively; however, each promoter was also capable of labeling some fraction of each cell type.

We next compared and contrasted tumors produced by the donor plasmids containing either the GFAP or MBP promoters driving oncogene expression. For both donor plasmids, tumors resulted in all animals and death resulted in 65.2% (15/23) of animals by 40 weeks (Figure 3-2 E and F). A log rank test showed no significant difference in survival among animals bearing tumors induced by GFAP, MBP or CAG donor plasmids (Log rank test, p=0.194 between CAG and GFAPP, p=0.554 between GFAP and MBP donor plasmids transfected animals. For comparison between CAG and MBP donor plasmids transfected animals, Log rank test p=0.093, Breslow test p=0.121, Tarone-Ware test p=0.106). A histopathological analysis of tumors in both GFAP and MBP promoter conditions indicated frequent mitotic figures (Supplementary Figure 1D, Fig. 3-2R, black arrow), similar to the CAG promoter condition described above, but also showed vascular proliferates consistent with highly malignant tumor types. Tumors were observed in 23 out of 23 animals assessed for tumors 14 days to 280 days after birth. In addition, GFAP donor plasmid induced tumors, unlike the MBP plasmids, resulted in tumors with prominent necrotic foci frequently surrounded by "pseudopalisading" tumor cells (Figure 3-2M arrow). Immunohistological assessment of tumors induced by GFAP donor plasmids indicated process rich astroglial cells with delicate processes positive for GFAP, Vimentin and MAP2 (Figure 3-2N-P). We conclude based on the histopathological findings that the GFAP donor plasmid induced tumors are malignant astroglial tumors resembling human GBM (WHO Grade IV). While similar in many ways to tumors induced by the CAG donor plasmid the multicolor

clonal analysis indicated that the GFAP donor plasmids resulted in tumors with larger clonal territories than the CAG donor plasmids. Similarly, the tumors in the GFAP donor plasmid condition showed more clonally associated invasion and expansion into striatum than did tumors in the CAG donor plasmid condition.

In contrast to the GFAP and CAG donor plasmid induced tumors, the MBP donor plasmids induced tumors contained a mixture of astroglial and oligogdendroglial components, and lacked prominent necrotic foci and pseudopalisading cell arrangements typical of the GFAP donor plasmids induced tumors (Figure 3-2M). In some areas of MBP donor plasmid induced tumors there were processes with GFAP and Vimentin positivity (Figure. 3-2S and T), but these areas were less frequently observed than in the GFAP donor plasmid induced tumors. In addition to the small astroglial cell fraction, the MBP donor plasmid induced tumors contained prominent 'honeycomb'-like cell clusters (Figure 3-2Q) with round isomorphic nuclei located centrally to perinuclear halos (Figure 3-2R inset): a feature resembling cytological characteristics of human oligodendroglioma. Cells were largely negative for Vimentin (Fig. 3-2T), but positive for MAP2, an immunostaining pattern consistent with mixed oligodendroglial and astroglial components. MAP2 immunopositivity showed strong perinuclear cytoplasmic staining without significant process labeling (Figure 3-2U black arrow, inset) typical of oligodendroglioma. Some MAP2 stained cells in MBP donor plasmid induced tumors displayed bi- or multi-polar processes typical of astroglial cells (Figure 3-2U grey arrow). In sum, the histological and immunohistochemical patterns observed in the tumors induced by MBP donor plasmids were distinct from those observed with the GFAP and CAG donor plasmids, and are most similar to human anaplastic oligoastrocytoma (WHO Grade III).

Figure 3-2 Distinct tumor types are induced by different donor plasmids

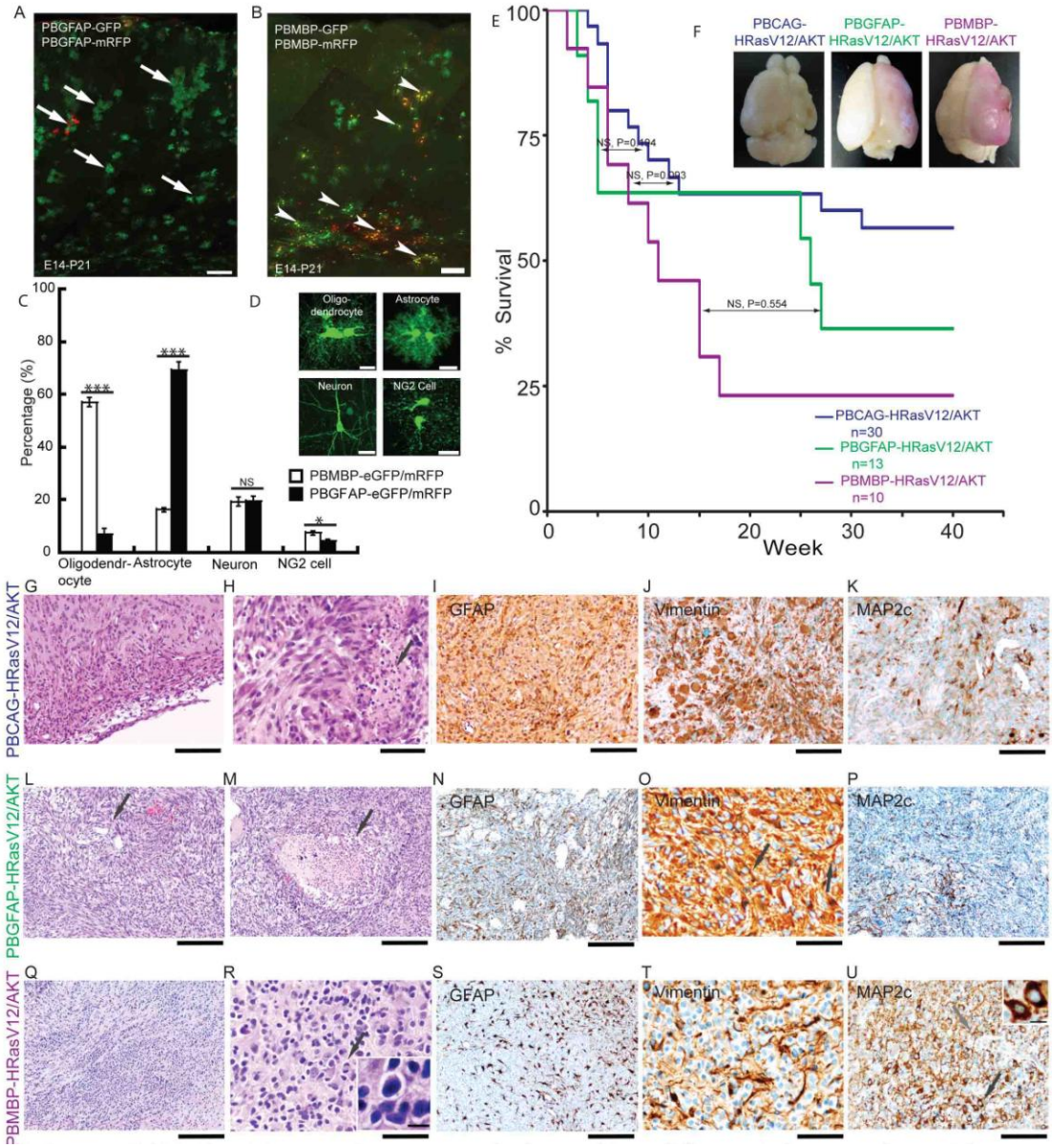

(A)Mouse GFAP promoter fragment labeled astrocytes. (B) Rat MBP promoter fragment labeled oligodendrocytes.

(C) Quantification of proportions of labeled cells by GFAP and MBP promoter fragments (One way ANOVA * indicates P<0.05 and *** indicates P<0.01. NS indicates no significance difference). (D) Representative images of neuron, astrocyte, oligodendrocyte and NG2 cell. (E-F)

Kaplan-Meier survival curves and representative appearance of tumor bearing brains. Log rank test showed no difference in survival across all groups. (G-K) Characterization of tumors induced by PBCAG-HRasV12/AKT. (G) Subarachnoidal spread of tumor cells (H&E). (H) Necrosis (black arrow, H&E). (I-K) Tumor cells with fibrillary processes were positive for GFAP, vimentin and MAP2. (L-P) Characterization of tumors induced by PBGFAP-HRasV12/AKT. (L) Overview of H&E staining. Black arrow indicates vessels. (M) Necrosis (black arrow). (N-P) GFAP, Vimentin and MAP2 positive processes. (Q-U) Characterization of tumors induced by PBMBP-HRasV12/AKT. (Q) Prominent oligodendroglial components (H&E). (R) Round cell appearance of tumor cell (inset) and mitosis (black arrow, H&E). (S) GFAP positive astroglial process. (T) Oligodendroglial cells were vimentin negative while astroglial elements were vimentin positive. (U) MAP2 positive oligodendroglial component (black arrow, inset) and MAP2 positive astrocytes component (gray arrow).

Scale bar: 200 μm in A,B, L-N, P, Q, S; 100 μm in G, I-K and ; 50 μm in H, O, R, T; 20 μm in D and 10 μm in inset in R and U.

Expression of basic helix-loop-helix transcription factors modifies tumor type

Next we addressed whether addition of neurogenic transcription factors, Neurogenin2 (Ngn2) and Neuronal Differentiation1 (NeuroD1) known to alter the fates of neural progenitors (Cai et al., 2000) would change tumor phenotype. We chose Ngn2 and NeuroD1 because they have been previously shown to block the differentiation of neural progenitors into astrocytes and to promote differentiation into neurons (Cai et al., 2000). We hypothesized that transcription

factors with neuron promoting effects would either inhibit tumor formation, or result in the formation of tumors distinct from CAG donor plasmid induced tumors. Indeed, expression of either Ngn2 or NeuroD1 along with the CAG donor plasmids resulted in a distinct tumor type that we never observed with any of the three other tumor inducing plasmid combinations. Furthermore, animals transfected with the Ngn2 or NeuroD1 modifying plasmids showed earlier death and higher rates of death than the other tumorigenic plasmid conditions (Figure 3-3A) Log-rank tests showed animals transfected with Ngn2 or NeuroD1 modifying plasmids had significantly shorter survivals ($P<0.0001$) than animals transfected with CAG, GFAP or MBP donor plasmids (Figure 3-3A).

Upon postmortem analysis of cerebral tumors in Ngn2 and NeuroD1 donor plasmid conditions we encountered large cerebral tumors with highly irregular surfaces by 14 days of age (Figure 3-3B). Histologically these large tumors contained cells that were poorly differentiated and showed regions of extensive necrosis and proliferative features. The tumors contained prominent rhabdoid cellular elements demonstrated in H&E sections (black arrow in Figure 3-3H and L). The overall immunhistochemical profile indicated teratoid characteristics. Cells had characteristic,"capping"-type expression patterns of Vimentin (black arrow in Figure 3-3I), and some cells were strongly positive for Actin (Figure 3-3J). There was also focal expression of epithelial membrane antigen (Figure 3-3K). We also did not observe significant expression of cytokeratin (Lu-5 epitope). Nuclear expression of INI (hSNF5/SMARCB1) was preserved in cells in these tumors. While poorly differentiated, the tumors showed regions of focal expression of astroglial GFAP (Supplementary Figure 4B, Supplementary Figure 5C) and Vimentin positive processes (Figure 3-3I,M) as well as scattered positivity for the neuronal markers MAP2 (Supplementary Figure 3-4D, Supplementary Figure 5B) and synaptophysin (Supplementary

Figure 3-4C). Intriguingly, synaptophysin positivity marked areas and clusters of tumor cells with cytologically neuronal features. The non-organoid distribution of respective elements argues against entrapped neurons. MAP2c expression appeared to reflect dendritic neuronal structures. In sum, the tumors induced by combining Ngn2 or NeuroD1 donor plasmids with the CAG donor plasmid histologlically most resembled atypical teratoid rhabdoid tumor (ATRT) like tumors.

Hertwig et al (Hertwig et al.) has reported that a panel of 7 signature genes can be used in error freely classification of three CNS tumors: glioma, PNET and ATRT. We therefore assessed the expression of this panel of 7 genes in the tumors induced by HRasV12/AKT in combination with Ngn2. We found significant up-regulation in the expression of 6 out of 7 genes in the tumors induced by HRasV12/AKT in and Ngn2 (Supplementary Figure 6). Among the 6 up-regulated genes, SPP1, which has been suggested as a diagnostic marker to distinguish ATRT from PNET and medulloblastoma (Kao et al., 2005) and as grade indicator of glioma(Toy et al., 2009), showed the greatest up-regulation (6.6 fold). The pattern of gene up-regulation combined with the histological features suggest that the tumors induced by HRasV12/AKT in combination with Ngn2 or NeuroD1 are ATRT-like tumors.

As the bHLH transfection conditions resulted in a unique and highly lethal tumor we next addressed whether this apparent phenotypic transformation from GBM to ATRT like tumors was due to a transient expression of bHLH factors in radial glia progenitors or to expression in tumor cells. The *piggyBac* transposon system allows for gating whether a transgene is integrated into a transfected cells or whether it remains episomal and is thus lost in cells that undergo subsequent proliferation (Chen and LoTurco, 2012). We substituted the Ngn2 donor plasmids used above with a plasmid, CAG-Ngn2, in which the CAG-Ngn2 transgene is not flanked by ITR sequences

and so is not subject to transposase-mediated genomic integration (Chen and LoTurco, 2012). As a result, transgene expression from these episomal plasmids is lost in 1-2 cell divisions (Chen and LoTurco, 2012; Siddiqi et al., 2014). Addition of episomal CAG-Ngn2 was sufficient to produce tumors (Supplementary Figure 3, Figure 3-3C-E) with clusters of tumor cells expressing epithelia membrane antigen (Figure 3-3F) and isolated cells expressing cytokeratin (Lu-5 epitope, Figure 3-3G). Nuclear INI1 was also preserved (data not shown). Thus, transient expression of Ngn2 in radial glial progenitors and their immediate progeny is sufficient to produce ATRT-like tumors.

Figure 3-3 ATRT like tumor was induced by addition of Ngn2 or NeuroD1 to PBCAG-HRasV12/AKT

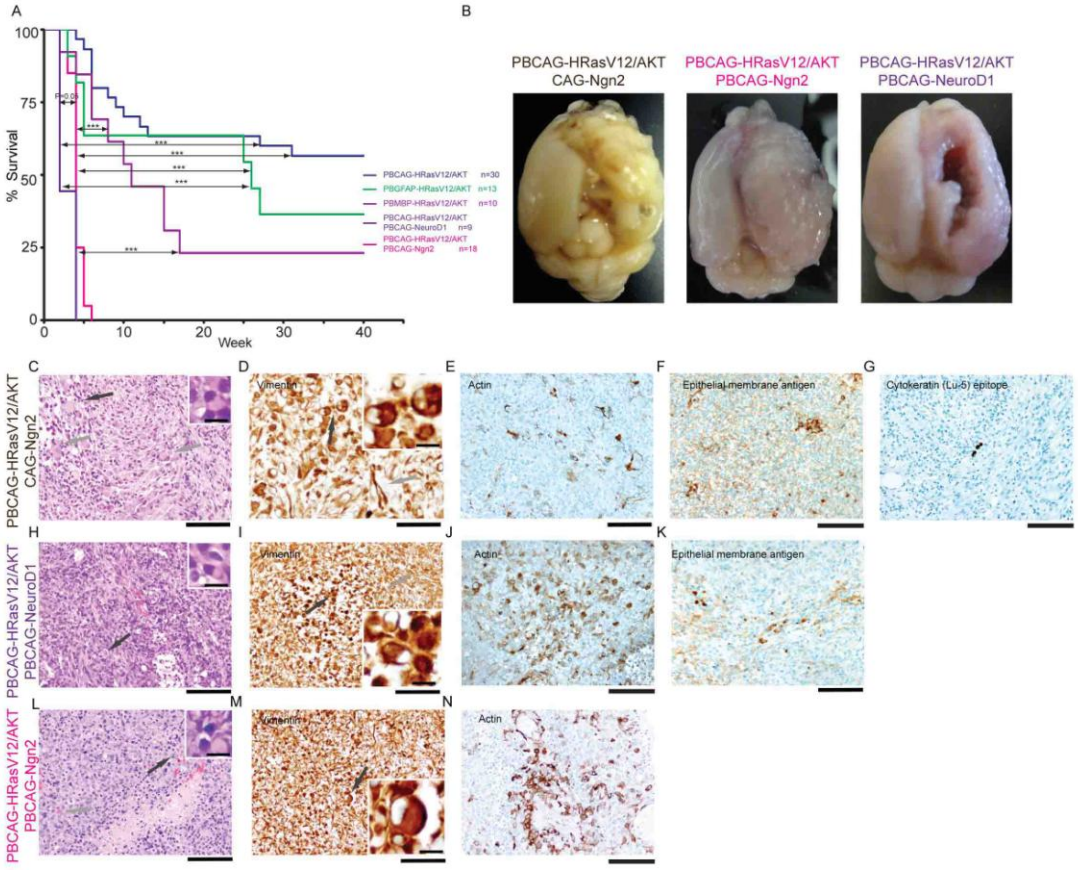

(A, B) Kaplan-Meier survival curves and representative images of ATRT like tumor bearing brains.

ATRT like tumor bearing animals had significantly short survival compared to GBM and anaplastic oligoastrocytoma bearing animals (log-rank test ,* indicates P< 0.05, *** indicates P<0.01). (C-G) ATRT like tumor is induced by addition of CAG-Ngn2 to PBCAG-HRasV12/AKT mixture. (C) Rhabdoid components (black arrow, inset), neuronal differentiation (grey arrows, H&E). (D) Vimentin rhabdoid cellular elements (black arrow, inset), and processes/glial differentiation (grey arrows). (E) Individual cells were actin positive. (F) Clusters of cells express epithelial membrane antigen. (G) Few cells were positive for cytokeratin (Lu-5 epitope). (H-K) ATRT like tumor is induced by addition of PBCAG-NeuroD1 to PBCAG-HRasV12/AKT mixture. (H) Necrotizing tumor with mitoses, rhabdoid cellular differentiation (black arrow, inset), process rich and epitheloid portions (H&E). (I)Vimentin positive rhabdoid components (black arrow, inset) as well as Vimentin positive processes (grey arrow). (J) Actin positive cells. (K) Epithelial membrane antigen – clusters of positive cells. (L-N) ATRT like tumor is induced by addition of PBCAG-Ngn2 to PBCAG-HRasV12/AKT mixture. (L) H&E – tumor with high cellularity and undifferentiated appearance (mitotic figure – grey arrow; rhabdoid cell - black arrow, inset). (M) Vimentin staining, individual rhabdoid components (black arrow, inset) in an environment of a glial process rich meshwork. (N) Clusters of actin positive cells.

Scale bar: 100 μm in C and E-N and 50 μm in D and 10 μm in all insets.

Distinct developmental patterns of tumors

The four tumor inducing conditions we describe above (CAG donor plasmid, GFAP donor plasmid, MBP donor plasmid, and CAG donor plasmid with a bHLH transcription factor

modifying donor plasmid) each produced histologically distinct tumors when assessed at similar postnatal developmental time points. We next sought to address whether these differences might be reflected in differences in the developmental time course of each tumor type. As shown in figure 3-4 A-E, we found that the CAG donor plasmid condition resulted in very early signs of abnormal cell proliferation with large aggregates of fluorescently labeled cells invading striatum and the ventricular and subventricular zones of neocortex by the day of birth (P0) in all animals examined (3/3) . In contrast, aggregates of proliferative cells were not apparent in either the GFAP (0/3) or MBP donor plasmid (0/3) condition in the first few days after birth (P2-P3; Figure 3-4 F,K), but instead normally differentiating neurons were apparent a few days after birth with only scattered cells outside of the neuronal cortical plate. By the end of the first postnatal week, masses of aberrantly proliferating cells appeared in both the MBP and GFAP donor plasmid conditions (Figure 3-4G, L) (3 out of 3 animals in MBP, GFAP donor transfected animals respectively). These masses were often of a single clonally labeled color and were present in areas centered within white matter and the sub-pial zone (Figure 3-4 G,L). The time course of tumor growth was similar in the MBP and GFAP donor plasmid conditions, however as indicated in the histopathological analysis the morphology of cells in the two conditions differed in morphology by P21 (Figure 3-4 H, I, J, and M, N, O). In spite of the delayed appearance of large tumors in the GFAP and MBP donor plasmid conditions relative to the CAG donor plasmid, the size of tumors in the MBP and GFAP donor plasmid conditions by P21 reached sizes larger than those in the CAG donor plasmid condition (Figure 3-4C, H, M). Finally, consistent with the early lethality and highly aggressive nature of the tumors induced by CAG donor plasmids with addition of Ngn2 modifying plasmid, the tumors in this condition (Figure 3-4, P-U) were obvious by the day of birth (4/4) and expanded rapidly into very large tumors with street-like necroses

invading the entire cerebral hemisphere by three weeks after birth (7/7). The developmental patterns observed are consistent with when the promoters expressing the oncogenes are most active, the ubiquitous CAG promoter is strongly active early in progenitors while the GFAP and MBP promoters are most active latter in the lineage when glial cells begin differentiating.

Figure 3-4 Induced tumors show distinct developmental time course

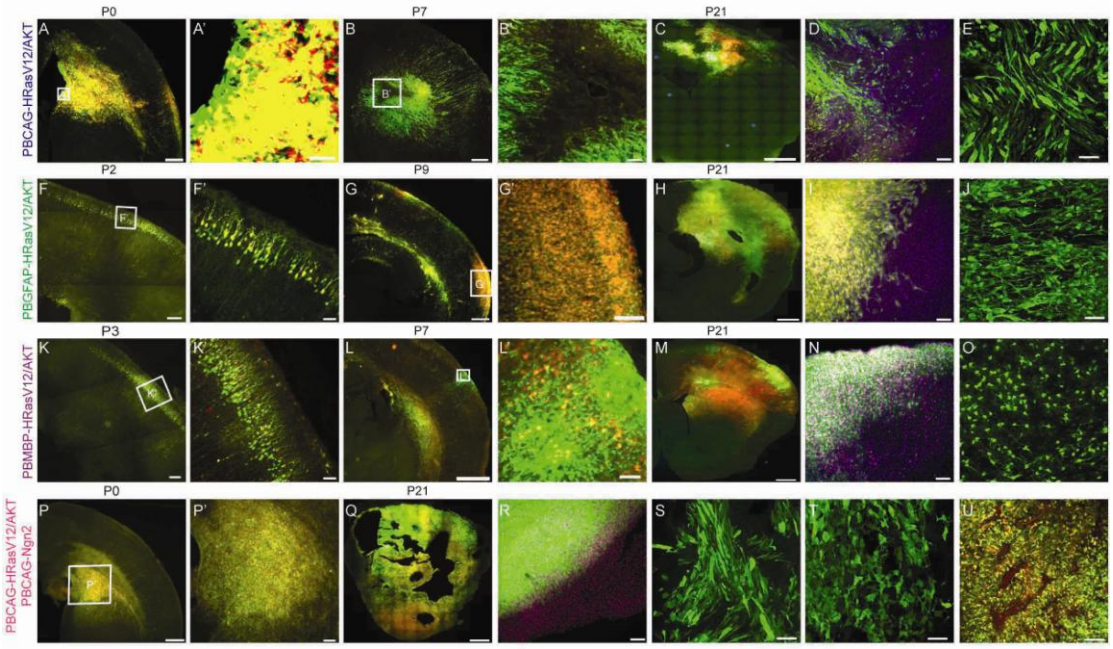

(A-E) Developmental time course for PBCAG-HRasV12/AKT induced tumor. (A) Densely packed cells were found in VZ/SVZ, striatum, neocortex and pia at P0. Magnified view of boxed area is shown in A'. (B) Necrosis at P7. Magnified view of boxed area is shown in B'. (C) Representative image of PBCAG-HRasV12/AKT transfected brain at P21. (D) Edge of PBCAG-HRasV12/AKT induced tumor. DAPI is shown in magenta. (E) Bipolar long spindle cells in PBCAG-HRasV12/AKT induced tumors. (F-J) Developmental time course for PBGFAP-HRasV12/AKT induced tumor. (F) A representative section from a P2 brain transfected with PBGFAP-HRasV12/AKT. Magnified view of boxed area is shown in F'. (G) P9 section from PBGFAP-HRasV12/AKT transfected brain. Magnified view of boxed area is shown in G'. (H)

Representative image of PBGFAP-HRasV12/AKT transfected brain at P21. (I) Edge of PBGFAP-HRasV12/AKT induced tumor. DAPI is shown in magenta. (J) Bipolar pyramidal cells with long processes in tumors induced by PBGFAP-HRasV12/AKT (K-O) Developmental time course for PBMBP-HRasV12/AKT induced tumor. (K) A representative section from a P3 brain transfected with PBMBP-HRasV12/AKT. Magnified view of boxed area is shown in K'. (L) P7 section from PBMBP-HRasV12/AKT transfected brain. Magnified view of boxed area is shown in L'. (M) Representative image of PBMBP-HRasV12/AKT transfected brain at P21. (N) Edge of PBMBP-HRasV12/AKT induced tumor. DAPI is shown in magenta. (O) Small round cells with short processes in tumors induced by PBMBP-HRasV12/AKT. (P) A representative image section from a brain transfected with PBCAG-Ngn2, PBCAG-HRasV12/AKT at P0. Magnified view of boxed area is shown in P'. (Q) A section from P21 animal showed tumor cells spreading whole cerebral hemisphere. (R) Edge of tumor induced by PBCAG-Ngn2, PBCAG-HRasV12/AKT. DAPI is shown in magenta. (S-T), Tumor cells frequently found in PBCAG-Ngn2, PBCAG-HRasV12/AKT induced tumors. (U) Extensive street like necrosis.

Scale bar: 1000 μm in C, H, M and Q; 500 μm in B, G, L and P; 200 μm in A, F and K; 100 μm in B', D, G' I, L', N, P', T, U; 50μm in A' E, F', K'J, O, S and T.

Gene expression differences in tumor types

The Cancer Genome Atlas research network (TCGA) identified 4 subtypes of glioblastoma multiforme subtypes by gene expression profiles and gene mutation (Verhaak et al., 2010). Through this analysis a group of 24 signature genes was identified that could be used to

categorize the 4 subtypes (Verhaak et al., 2010). We therefore used expression levels of these 24 signature genes to further assess whether the four tumor patterns produced in our study could be distinguished based on the expression of this set of genes. To do this, we used q-PCR and unsupervised hierarchical clustering analysis to compare and categorize the tumors produced by the four conditions. We found, consistent with the agreement in histopathological analysis, that the tumors produced by the CAG and GFAP donor plasmids clustered together in terms of expression of the 24 genes (Figure 3-5). The tumors that were most distinct in histopathology, those produced by the MBP donor plasmids and modified by the Ngn2 donor plasmids, differed in gene expression patterns relative both to each other and to the CAG and GFAP donor plasmid conditions (Figure 3-5). EGFR is frequently amplified and overexpressed in human GBMs; however, EGFR transcript was not prominent in all tumor types. This might be because Ras/AKT are downstream factors of EGFR pathway (Marumoto et al., 2009). We also found p53 was neither mutated nor deleted (data not shown) and p53 transcript showed about 2 fold of up regulation. Thus, the heterogeneity we find in tumors produced by differing promoter conditions and modifying transcription factor expression are also reflected in different gene expression patterns.

Figure 5 Induced tumors show different molecular signature

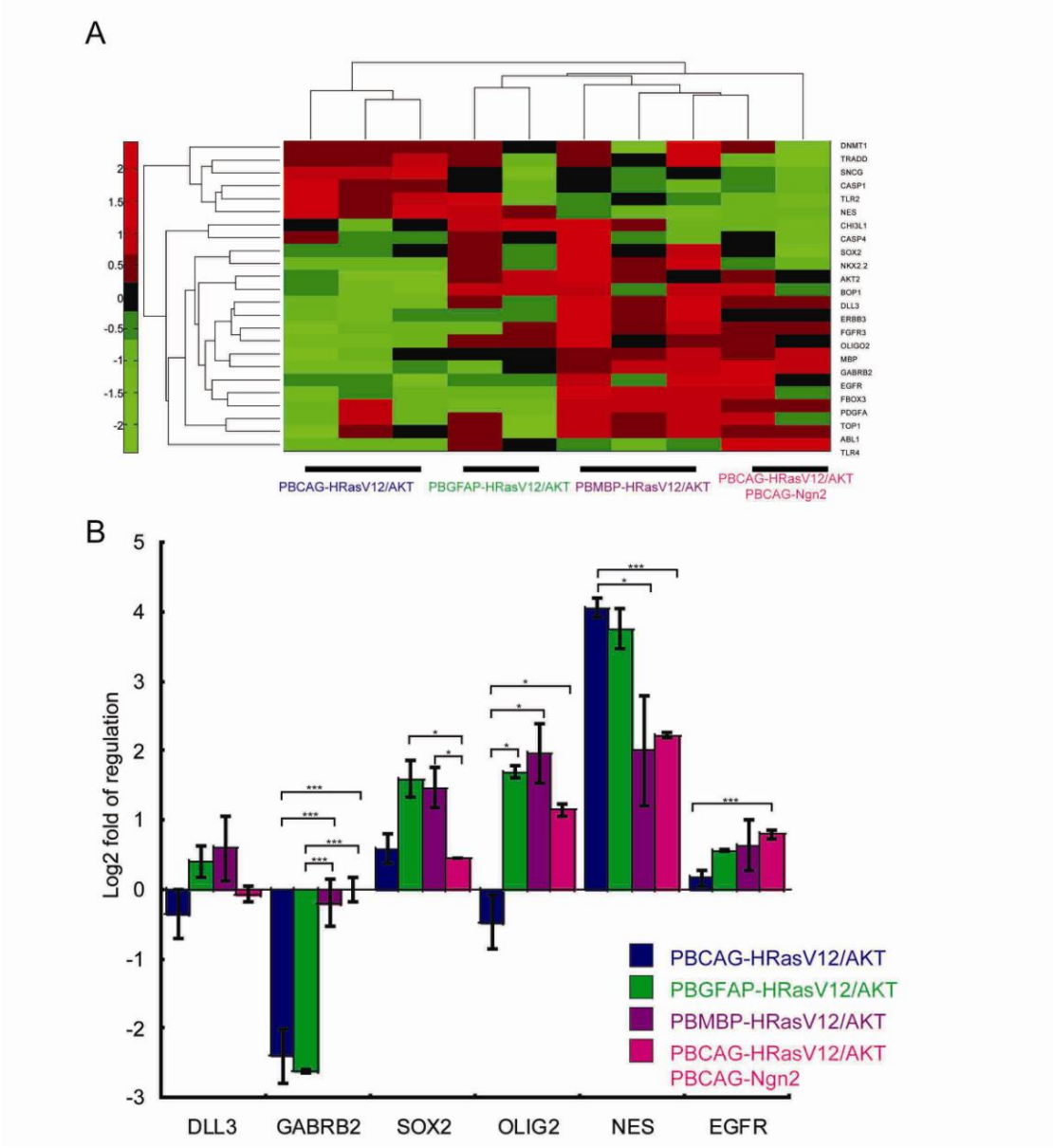

(A)

Unsupervised cluster analysis of qRT-PCR based gene expression data for 24 genes selected from Verhaak *et al* (Verhaak et al.) across different donor plasmids induced tumors. Heat map shows fold change in gene expression in induced tumors relative to tumor free brain tissues. The 24 genes screened are listed on the left. Color scale represents fold changes of expression with red indicating up regulation and green indicating down regulation of gene expression. Gene

expression across 4 conditions was shown in rows and expression of the whole set of 24 gene in each tumor sample was shown in columns. (B) Averaged fold of regulation for 6 representative genes selected from (A). Error bar indicates standard error of mean (SEM). (One way ANOVA, * indicates $P<0.05$, *** indicates $P<0.01$).

Discussion

Two, not mutually exclusive, explanations of tumor heterogeneity have been proposed (Visvader, 2011). Overwhelming experimental and clinical evidence show that different genetic mutations result in different tumor types including different CNS tumor types (Sieber et al., 2005). For example, Hertwig *et al* (Hertwig et al., 2012) showed that infection of postnatal mouse neural stem cells with viruses containing V12HRAS or c-MYC could result in formation of 3 different tumor types depending upon the combination and sequence in which oncogenes were introduced. Similarly, Jacques *et al* (Jacques et al., 2010) showsed that different combinations of conditional genetic deletions in p53, Rb and PTEN in mouse subventricular zone neural stem cells could induce formation of either PNET or glioma. Evidence for differing cell types being a source of CNS tumor heterogeneity has also been found (Brown et al., 1998; Gibson et al., 2010; Ince et al., 2007; Swartling et al., 2012). For example, transduction of mutationally stabilized N-Myc into neural stem cells from perinatal murine cerebellum and brain stem resulted in formation of medulloblastoma/primitive neuroectodermal tumors, while N-Myc transduced into NSCs isolated from forebrain resulted in diffuse glioma tumors (Swartling et al., 2012). As different neural progenitor types have different gene expression profiles that may modify tumor cell differentiation it seems likely that both cell of origin and differences in gene mutation contribute to tumor type diversity in the CNS (Visvader, 2011). Our study indicates

that in the developing neocortex cell populations of origin can contribute to tumor diversity, and moreover, that expression of non-oncogenic transcription factors expressed in the same population can also modify tumor type.

Although pediatric GBM shares histological similarities with adult GBM, they are now thought to be different entities with different molecular characteristics (Paugh et al., 2010; Sturm et al., 2012). It has been shown, for example, that pediatric GBM display a spectrum of copy number variations distinct from adult GBM (Bax et al., 2010). Integrated molecular profiling experiments also reveal differences between pediatric and adult GBM. For example, IDH hotspot mutations are frequently found in adult high grade glioma but not in pediatric tumors (Paugh et al., 2010; Sturm et al., 2012). In addition, whereas PDGFRA is the predominant target of focal amplification in pediatric high grade glioma, in adult glioblastoma EGFR is the most common target (Paugh et al., 2010). Moreover, histone H3.3 mutations are frequently found in pediatric GBM while they are absent in adult GBM (Schwartzentruber et al., 2012; Sturm et al., 2012). The cell of origin of pediatric GBM is unknown and might be different from adult GBM as well. We have used the CAG donor plasmids to induce GBM which appeared as early as P7 in the rat and shows necrotic areas as early as at P4 a developmental time period in the precocial rat that corresponds to the neonatal period in human. Future experiments will be needed to determine whether the early arising tumors modeled in this system are more similar to pediatric or adult GBM in their molecular identity and cell of origin.

Our study indicates that the cell of mutation for both ATRT like and GBM can be radial glial cells of embryonic neocortex. The *in utero* electroporation method we used targets radial glia and radial neural progenitor cells that line the lateral ventricles of the lateral forebrain. This population of progenitors at the ventricular surface of E14/15 rat forebrain contains sub-

populations of progenitors capable of generating neurons of different types, and primarily glia or primarily neurons (Siddiqi et al., 2014). We used the ubiquitous CAG donor plasmid to induce expression of HRasV12 and AKT immediately in the radial progenitor population. Ngn2 or NeuroD1 expressed by the same immediately active promoter was sufficient to change the tumor type generated. The tumor difference was apparent as early as the day of birth, approximately one week after induced gene expression. We also found that transient expression of Ngn2 (by a non-donor episomal plasmid) in radial glia was sufficient to produce ATRT like tumors. The effectiveness of transient Ngn2 expression, in combination with previous findings that Ngn2 or NeuroD1 expressed in glioma cells induces cell death and neuronal differentiation without changing tumor type (Guichet et al., 2013; Zhao et al., 2012) supports the idea that Ngn2 and NeuroD1 acts in early stage radial progenitors to change the type of tumor generated. We have co-expressed Ngn2 with GFAP donor plasmids and found the resulted tumors were similar to tumors induced by GFAP donor plasmids alone. But we did found rhabdoidal cells in the resulted tumors (data not shown). However, the results have to be interpreted with caution since the mouse GFAP promoter fragment is also active in radial glia. In the future, combining Ngn2 with MBP donor plasmids may distinguish the time of action of Ngn2.

Loss of function in the INI1 gene is believed to be a significant cause of ATRT in humans (Biegel, 2006). INI1 knockout mice develop tumors but these do not appear to be ATRT (Klochendler-Yeivin et al., 2000). Hertwig *et al* (Hertwig et al., 2012) showed that transplantation of NSC/NPCs serially infected with c-MYC and V12HRAS could generate ARTR like tumors with gene expression profiles similar to human ATRT suggesting that in rodent models additional mutation types can lead to ATRT. Similarly, we demonstrated in this study that ATRT like tumors are generated by HRasV12 and AKT transfection of neocortical

radial glia, but only when co-expressed with the bHLH transcription factors Ngn2 or NeuroD1, two genes that on their own are non-oncogenic. This underscores the strong possibility that tumor type diversity may be influenced not only by the cell of mutation but also by the specific molecular context present in that cell.

Our current results also show that the GFAP and MBP promoter-active populations in the radial glia lineage generate tumors with different molecular and histological features. Interestingly, all cell types are labeled by the GFAP and MBP donor plasmids, but yet the tumor types generated were consistently different in histology and molecular signature. This may suggest that tumor diversity is determined by the predominant cell type in a population that undergoes transformation. By mixing the GFAP and MBP donor plasmids in future experiments and tracking their clonal expansion we may be able to distinguish whether one tumor cell population is dominant over the other.

Several attributes of *piggyBac* transposon system demonstrated here make this model potentially useful for a variety of novel applications in tumor biology. The main advantage of the *piggyBac* IUE method is that it allows for introduction of multiple transgenes. In this study, for example, we simultaneously introduced a transposase helper plasmid to target stable transgenesis in GLAST positive cells, two oncogene expressing donor plasmids with their own promoters, 3 fluorescent reporter genes (Figure 1, 2 and 3), and a transcription factor. The high coexpression efficiency allowed us to direct expression in different subpopulations in sequence, introduce a clonal labeling method, and a modifying transcription factor. This functionality should make this approach a useful platform for screening potential modifiers of tumor development and for determining further how genetic modifiers alter tumor development.

Methods

Plasmids

A system of *piggyBac* transposon donor and helper plasmids were produced and used in this study. To make the donor plasmid PBCAG-HRasV12 and PBCAG-AKT, HRasV12 was PCR amplified from pTomo (Marumoto et al., 2009) (Addgene plasmid 26292), human AKT was amplified from 1036 pcDNA3 Myr HA Akt1, (Ramaswamy et al., 1999) (Addgene plasmid 9008) respectively and inserted into the EcoRI/NotI sites of pPBCAG-eGFP (Chen and LoTurco, 2012). For construction of PBGFAP-HRasV12/AKT, PBMBP- HRasV12/AKT, HRas-V12 and AKT were inserted into EcoRI/NotI sites of PBGFAP-GFP and PBMBP-GFP respectively (Chen and LoTurco, 2012). For the bHLH donor plasmids PBCAG-Ngn2 and PBCAG-NeuroD1, human Neurogenin2 cDNA clone (IMAGE ID 5247719), human Neuronal differentiation1 cDNA (IMAGE ID 3873419) were purchased from Open Biosystem, PCR amplified and inserted into PBCAG-eGFP EcoRI/NotI sites. CAG-Ngn2 was made by inserting Ngn2 coding sequence into EcoRI/NotI sites of pCAG-eGFP.

Animals

Pregnant Wistar rats were obtained from Charles River Laboratories, Inc. (Wilmington, MA) and maintained at the University of Connecticut vivarium on a 12 h light cycle and fed *ad libitum*. Animal gestational ages were determined and confirmed during surgery. Both male and female subjects were used for tumor induction. For the purpose of constructing survival curves (Figures 2A, 3A) rats were removed from the experiment for humane purposes when they became unable to eat or drink. At the end of the 40 week survival experiment, percentage of

survival for each preceding week was calculated and % survival curves were generated. For tumors induced by PBCAG-Ngn2/PBCAG-HRasV12/AKT and PBCAG-NeuroD1/PBCAG-HRasV12/AKT, survival rates were also calculated for each day. To statistically compare survival rates a log rank test, Breslow test and Tarone-Ware test were performed using SPSS (IBM SPSS statistics 21). All procedures and experimental approaches were approved by the University of Connecticut IACUC.

In utero electroporation

In utero electroporation was performed as previously described (Chen and LoTurco, 2012). Electroporation was performed at embryonic day 14 or 15 (E14 or E15) and gestation age was confirmed during surgery. All plasmids were used at the final concentration of 1.0 μg/μl except PBCAG-CFP and GLAST-PBase were used at the final concentration of 2.0 μg/μl.

Image acquisition and 3D reconstruction

Multi color imaging was performed as described using Zeiss Axio imager M2 microscope with Apotome with 488/546/350 nm filter cubes and the X-Cite series 120Q light source (Siddiqi et al., 2014). All the images were further processed in Adobe Photoshop CS3 software (San Jose, CA). For 3D reconstruction, P27 Wistar rats were deeply anesthetized with Isoflurane and perfused transcardially with 4% paraformaldehyde/PBS (4% PFA). Samples were post fixed overnight in 4% PFA and sectioned at 65 μm thickness on vibratome (Leica VT 1000S). Sections were mounted onto microscope slides in sequential order, all aligned in the same dorsal-ventral and left-right arrangement. Images were acquired with Stereo Investigator (Microbright

Field, VT). After imaging acquisition, outlines of the cerebral hemisphere and tumor clones were traced using color-coded contours for the hemisphere and each clone. Then traced images were transferred to Neurolucida Explorer (Microbright Field, VT), in which several contours from sequential sections were appended to one another, and organized and stacked in order. 3D model was created using Neurolucida Explorer software 3D visualization option to visualize the clonality of selected clones of tumor cells.

Immunohistochemistry

Animals were deeply anesthetized with Isoflurane and perfused transcardially with 4% paraformaldehyde/PBS (4% PFA). Samples were post fixed overnight in 4% PFA. For immunofluorescence, brains were sectioned at 65 μm thickness on a vibratome (Leica VT 1000S). Sections were processed as free-floating sections and stained with GFAP (Cell Signaling, 3670X), CC1 (Calbiochem, OP80) and NG2 (Chemicon, AB5320) antibody. Images were acquired and processed as previous described (Chen and LoTurco; Siddiqi et al.).

For histological analysis, immnunohistochemsitry and H&E staining were carried out on paraffin embedded 4 μm sections as described in (Schick et al., 2007a; Schick et al., 2007b) using GFAP (DAKO, Z0334), MAP2c (Sigma, M4403), Vimentin (DAKO, M0725), Synaptophysin (DAKO, M0776), Cytokeratin (BMA Medicals, T-1302), Actin (DAKO, M0851), epithelial membrane antigen (DAKO, M0613) antibody.

Tumor cell culture

Tumors were dissected from PBCAG-HRasV12/AKT transfected animals at the age P21. After dissection, tumor tissues were chopped and trypsinized into single cell suspension. Then cells were cultured in a serum-free medium consisting of DMEM with L-glutamine, sodium pyruvate, B-27, N-2, bFGF and EGF (Invitrogen, CA). 2 days later, tumor cell adherent cultures were passaged into neurosphere suspension cultures at a density of 10cells/μl and allowed to grow for 3 days to form tumor spheres.

RNA extraction, cDNA synthesis and qRT-PCR

Animals aged P21 to P27 were deeply anesthetized with isoflurane. Brains were quickly removed on ice. Tumors were identified on the brain surface, removed and then chopped into cubes. Tissue from the opposite hemisphere that was tumor free was used as control. RNA extraction was performed using Ambion® RNAqueous® Kit (Invitrogen, CA) according to manufacturer's instructions. cDNA synthesis was performed using Transcriptor First Strand cDNA synthesis kit (Roche) following manufacture's protocol. qRT-PCR was performed using Fast SYBR® Green master mix (Applied Biosystem, CA). Primer sequences are listed in Supplementary Table 1. Triplicates were included from each sample. Fold of regulation of gene expression was calculated using ΔΔCt method. More specifically, the Ct values obtained from tumor and control brain RNA samples are directly normalized to a housekeeping gene (GAPDH). ΔΔCt is the difference in the ΔCt values between the tumor and control samples. The fold-change in expression of the gene of interest between the tumor and control brain is then equal to 2^ (-ΔΔCt). Unsupervised hierarchical clustering was performed on fold of regulation for each of the 24 genes profiled and a heat map was generated using the clustergram command in the

MATLAB bioinformatics toolbox (Math Works, MA). Other statistical analyses were performed using KaleidaGraph version 4.0 (SynergySoftware 2006). A confidence interval of 95% ($p < 0.05$) was required for values to be considered statistically significant. All data are presented as means and standard error of the mean (SEM).

References

Alcantara Llaguno, S., Chen, J., Kwon, C.H., Jackson, E.L., Li, Y., Burns, D.K., Alvarez-Buylla, A., and Parada, L.F. (2009). Malignant astrocytomas originate from neural stem/progenitor cells in a somatic tumor suppressor mouse model. Cancer Cell *15*, 45-56.

Bax, D.A., Mackay, A., Little, S.E., Carvalho, D., Viana-Pereira, M., Tamber, N., Grigoriadis, A.E., Ashworth, A., Reis, R.M., Ellison, D.W., *et al.* (2010). A distinct spectrum of copy number aberrations in pediatric high-grade gliomas. Clin Cancer Res *16*, 3368-3377.

Biegel, J.A. (2006). Molecular genetics of atypical teratoid/rhabdoid tumor. Neurosurg Focus *20*, E11.

Brown, K., Strathdee, D., Bryson, S., Lambie, W., and Balmain, A. (1998). The malignant capacity of skin tumours induced by expression of a mutant H-ras transgene depends on the cell type targeted. Curr Biol *8*, 516-524.

Cai, L., Morrow, E.M., and Cepko, C.L. (2000). Misexpression of basic helix-loop-helix genes in the murine cerebral cortex affects cell fate choices and neuronal survival. Development *127*, 3021-3030.

Chen, F., and LoTurco, J. (2012). A method for stable transgenesis of radial glia lineage in rat neocortex by piggyBac mediated transposition. J Neurosci Methods *207*, 172-180.

Faury, D., Nantel, A., Dunn, S.E., Guiot, M.C., Haque, T., Hauser, P., Garami, M., Bognar, L., Hanzely, Z., Liberski, P.P., *et al.* (2007). Molecular profiling identifies prognostic subgroups of pediatric glioblastoma and shows increased YB-1 expression in tumors. J Clin Oncol *25*, 1196-1208.

Friedmann-Morvinski, D., Bushong, E.A., Ke, E., Soda, Y., Marumoto, T., Singer, O., Ellisman, M.H., and Verma, I.M. (2012). Dedifferentiation of neurons and astrocytes by oncogenes can induce gliomas in mice. Science *338*, 1080-1084.

Gibson, P., Tong, Y., Robinson, G., Thompson, M.C., Currle, D.S., Eden, C., Kranenburg, T.A., Hogg, T., Poppleton, H., Martin, J., *et al.* (2010). Subtypes of medulloblastoma have distinct developmental origins. Nature *468*, 1095-1099.

Guha, A., Feldkamp, M.M., Lau, N., Boss, G., and Pawson, A. (1997). Proliferation of human malignant astrocytomas is dependent on Ras activation. Oncogene *15*, 2755-2765.

Guichet, P.O., Bieche, I., Teigell, M., Serguera, C., Rothhut, B., Rigau, V., Scamps, F., Ripoll, C., Vacher, S., Taviaux, S., *et al.* (2013). Cell death and neuronal differentiation of glioblastoma stem-like cells induced by neurogenic transcription factors. Glia *61*, 225-239.

Hambardzumyan, D., Amankulor, N.M., Helmy, K.Y., Becher, O.J., and Holland, E.C. (2009). Modeling Adult Gliomas Using RCAS/t-va Technology. Transl Oncol *2*, 89-95.

Haque, T., Faury, D., Albrecht, S., Lopez-Aguilar, E., Hauser, P., Garami, M., Hanzely, Z., Bognar, L., Del Maestro, R.F., Atkinson, J., *et al.* (2007). Gene expression profiling from formalin-fixed paraffin-embedded tumors of pediatric glioblastoma. Clin Cancer Res *13*, 6284-6292.

Hertwig, F., Meyer, K., Braun, S., Ek, S., Spang, R., Pfenninger, C.V., Artner, I., Prost, G., Chen, X., Biegel, J.A., *et al.* (2012). Definition of genetic events directing the development of distinct types of brain tumors from postnatal neural stem/progenitor cells. Cancer Res *72*, 3381-3392.

Holland, E.C., Celestino, J., Dai, C., Schaefer, L., Sawaya, R.E., and Fuller, G.N. (2000). Combined activation of Ras and Akt in neural progenitors induces glioblastoma formation in mice. Nat Genet *25*, 55-57.

Holland, E.C., Hively, W.P., DePinho, R.A., and Varmus, H.E. (1998). A constitutively active epidermal growth factor receptor cooperates with disruption of G1 cell-cycle arrest pathways to induce glioma-like lesions in mice. Genes Dev *12*, 3675-3685.

Holmen, S.L., and Williams, B.O. (2005). Essential role for Ras signaling in glioblastoma maintenance. Cancer Res *65*, 8250-8255.

Ince, T.A., Richardson, A.L., Bell, G.W., Saitoh, M., Godar, S., Karnoub, A.E., Iglehart, J.D., and Weinberg, R.A. (2007). Transformation of different human breast epithelial cell types leads to distinct tumor phenotypes. Cancer Cell *12*, 160-170.

Jacques, T.S., Swales, A., Brzozowski, M.J., Henriquez, N.V., Linehan, J.M., Mirzadeh, Z., C, O.M., Naumann, H., Alvarez-Buylla, A., and Brandner, S. (2010). Combinations of genetic mutations in the adult neural stem cell compartment determine brain tumour phenotypes. Embo J *29*, 222-235.

Kao, C.L., Chiou, S.H., Ho, D.M., Chen, Y.J., Liu, R.S., Lo, C.W., Tsai, F.T., Lin, C.H., Ku, H.H., Yu, S.M., *et al.* (2005). Elevation of plasma and cerebrospinal fluid osteopontin levels in patients with atypical teratoid/rhabdoid tumor. Am J Clin Pathol *123*, 297-304.

Klochendler-Yeivin, A., Fiette, L., Barra, J., Muchardt, C., Babinet, C., and Yaniv, M. (2000). The murine SNF5/INI1 chromatin remodeling factor is essential for embryonic development and tumor suppression. EMBO Rep *1*, 500-506.

Lei, L., Sonabend, A.M., Guarnieri, P., Soderquist, C., Ludwig, T., Rosenfeld, S., Bruce, J.N., and Canoll, P. (2011). Glioblastoma models reveal the connection between adult glial progenitors and the proneural phenotype. PLoS One *6*, e20041.

Lindberg, N., Kastemar, M., Olofsson, T., Smits, A., and Uhrbom, L. (2009). Oligodendrocyte progenitor cells can act as cell of origin for experimental glioma. Oncogene *28*, 2266-2275.

Liu, C., Sage, J.C., Miller, M.R., Verhaak, R.G., Hippenmeyer, S., Vogel, H., Foreman, O., Bronson, R.T., Nishiyama, A., Luo, L., *et al.* (2011). Mosaic analysis with double markers reveals tumor cell of origin in glioma. Cell *146*, 209-221.

LoTurco, J., Manent, J.B., and Sidiqi, F. (2009). New and improved tools for in utero electroporation studies of developing cerebral cortex. Cereb Cortex *19 Suppl 1*, i120-125.

Lu, Y., Lin, C., and Wang, X. (2009). PiggyBac transgenic strategies in the developing chicken spinal cord. Nucleic Acids Res *37*, e141.

Marumoto, T., Tashiro, A., Friedmann-Morvinski, D., Scadeng, M., Soda, Y., Gage, F.H., and Verma, I.M. (2009). Development of a novel mouse glioma model using lentiviral vectors. Nat Med *15*, 110-116.

Paugh, B.S., Qu, C., Jones, C., Liu, Z., Adamowicz-Brice, M., Zhang, J., Bax, D.A., Coyle, B., Barrow, J., Hargrave, D., *et al.* (2010). Integrated molecular genetic profiling of pediatric high-grade gliomas reveals key differences with the adult disease. J Clin Oncol *28*, 3061-3068.

Persson, A.I., Petritsch, C., Swartling, F.J., Itsara, M., Sim, F.J., Auvergne, R., Goldenberg, D.D., Vandenberg, S.R., Nguyen, K.N., Yakovenko, S., *et al.* (2010). Non-stem cell origin for oligodendroglioma. Cancer Cell *18*, 669-682.

Ramaswamy, S., Nakamura, N., Vazquez, F., Batt, D.B., Perera, S., Roberts, T.M., and Sellers, W.R. (1999). Regulation of G1 progression by the PTEN tumor suppressor protein is linked to inhibition of the phosphatidylinositol 3-kinase/Akt pathway. Proc Natl Acad Sci U S A *96*, 2110-2115.

Schick, V., Majores, M., Engels, G., Hartmann, W., Elger, C.E., Schramm, J., Schoch, S., and Becker, A.J. (2007a). Differential Pi3K-pathway activation in cortical tubers and focal cortical dysplasias with balloon cells. Brain Pathol *17*, 165-173.

Schick, V., Majores, M., Koch, A., Elger, C.E., Schramm, J., Urbach, H., and Becker, A.J. (2007b). Alterations of phosphatidylinositol 3-kinase pathway components in epilepsy-associated glioneuronal lesions. Epilepsia *48 Suppl 5*, 65-73.

Schwartzentruber, J., Korshunov, A., Liu, X.Y., Jones, D.T., Pfaff, E., Jacob, K., Sturm, D., Fontebasso, A.M., Quang, D.A., Tonjes, M., *et al.* (2012). Driver mutations in histone H3.3 and chromatin remodelling genes in paediatric glioblastoma. Nature *482*, 226-231.

Siddiqi, F., Chen, F., Aron, A.W., Fiondella, C.G., Patel, K., and Loturco, J.J. (2014). Fate Mapping by PiggyBac Transposase Reveals That Neocortical GLAST+ Progenitors Generate More Astrocytes Than Nestin+ Progenitors in Rat Neocortex. Cereb Cortex.

Sieber, O.M., Tomlinson, S.R., and Tomlinson, I.P. (2005). Tissue, cell and stage specificity of (epi)mutations in cancers. Nat Rev Cancer *5*, 649-655.

Sturm, D., Witt, H., Hovestadt, V., Khuong-Quang, D.A., Jones, D.T., Konermann, C., Pfaff, E., Tonjes, M., Sill, M., Bender, S., *et al.* (2012). Hotspot mutations in H3F3A and IDH1 define distinct epigenetic and biological subgroups of glioblastoma. Cancer Cell *22*, 425-437.

Swartling, F.J., Savov, V., Persson, A.I., Chen, J., Hackett, C.S., Northcott, P.A., Grimmer, M.R., Lau, J., Chesler, L., Perry, A., *et al.* (2012). Distinct neural stem cell populations give rise to disparate brain tumors in response to N-MYC. Cancer Cell *21*, 601-613.

Toy, H., Yavas, O., Eren, O., Genc, M., and Yavas, C. (2009). Correlation between osteopontin protein expression and histological grade of astrocytomas. Pathol Oncol Res *15*, 203-207.

Uhrbom, L., Dai, C., Celestino, J.C., Rosenblum, M.K., Fuller, G.N., and Holland, E.C. (2002). Ink4a-Arf loss cooperates with KRas activation in astrocytes and neural progenitors to generate glioblastomas of various morphologies depending on activated Akt. Cancer Res *62*, 5551-5558.

Uhrbom, L., Hesselager, G., Nister, M., and Westermark, B. (1998). Induction of brain tumors in mice using a recombinant platelet-derived growth factor B-chain retrovirus. Cancer Res *58*, 5275-5279.

Verhaak, R.G., Hoadley, K.A., Purdom, E., Wang, V., Qi, Y., Wilkerson, M.D., Miller, C.R., Ding, L., Golub, T., Mesirov, J.P., *et al.* (2010). Integrated genomic analysis identifies clinically relevant subtypes of glioblastoma characterized by abnormalities in PDGFRA, IDH1, EGFR, and NF1. Cancer Cell *17*, 98-110.

Visvader, J.E. (2011). Cells of origin in cancer. Nature *469*, 314-322.

Weber, K., Thomaschewski, M., Warlich, M., Volz, T., Cornils, K., Niebuhr, B., Tager, M., Lutgehetmann, M., Pollok, J.M., Stocking, C., *et al.* RGB marking facilitates multicolor clonal cell tracking. Nat Med *17*, 504-509.

Wei, Q., Miskimins, W.K., and Miskimins, R. (2003). Cloning and characterization of the rat myelin basic protein gene promoter. Gene *313*, 161-167.

Wiesner, S.M., Decker, S.A., Larson, J.D., Ericson, K., Forster, C., Gallardo, J.L., Long, C., Demorest, Z.L., Zamora, E.A., Low, W.C., *et al.* (2009). De novo induction of genetically engineered brain tumors in mice using plasmid DNA. Cancer Res *69*, 431-439.

Yoshida, A., Yamaguchi, Y., Nonomura, K., Kawakami, K., Takahashi, Y., and Miura, M. (2010). Simultaneous expression of different transgenes in neurons and glia by combining in utero electroporation with the Tol2 transposon-mediated gene transfer system. Genes Cells *15*, 501-512.

Yusa, K., Rad, R., Takeda, J., and Bradley, A. (2009). Generation of transgene-free induced pluripotent mouse stem cells by the piggyBac transposon. Nat Methods *6*, 363-369.

Zhao, J., He, H., Zhou, K., Ren, Y., Shi, Z., Wu, Z., Wang, Y., Lu, Y., and Jiao, J. (2012). Neuronal transcription factors induce conversion of human glioma cells to neurons and inhibit tumorigenesis. PLoS One *7*, e41506.

Chapter 4 Modeling Neurodevelopmental Disorder and Glioblastoma multiforme Using CRISPR/Cas9 System

Abstract

Tools for somatic cell transgenesis are important for modeling human somatic mutation diseases. In this report, we developed a CRISPR-IUE approach combining the CRISPR/Ca9 system and *in utero* electroporation approach to induce somatic mutations in cells in neural progenitor lineage and to model neurodevelopmental disorder as well as glioblastoma multiforme. We first designed guide sequences targeting rat PTEN. The PTEN CRISPR constructs successfully abolished PTEN expression in neuron. Moreover, PTEN null neurons demonstrated phenotypes that were similar to PTEN knockout or knockdown neuron, including hypertrophy and altered membrane properties. At last, tumors resembling human glioblastoma multiforme were induced by combinations of three CRISPR constructs targeting rat PTEN, NF1 and P53. These results demonstrated the utility of CRSIPR/Cas9 system in studying neocortical development as well as in modeling human genetic disease caused by somatic mutations.

Introduction

Most of human genetic diseases including cancers and neurological disorders are caused by somatic mutations {Bamford, 2004 #16;Futreal, 2004 #18;Hua, 2003 #17;Poduri, 2013 #15}. For example, loss of function of tumor suppressor phosphotase and tensin homolog (PTEN) caused by somatic mutations have been found in various cancers including glioblastoma multiforme (Wang et al., 1997), breast cancer (Minobe et al., 1999), metastatic melanoma (Celebi et al.,

2000). To fully understand pathology and effects of those somatic mutations, animal models bearing those somatic mutations are needed.

Recent breakthrough in genome engineering techniques such as zinc finger nuclease (ZFN), transcription activator like effector nuclease (TALEN) and clustered regularly interspaced short panlindromic repeats (CRISPR) (Cong et al., 2013; Mali et al., 2013), especially the CRISPR system, have enabled precise genome engineering with unprecedented speed. The type II CRSIPR/Cas9 system is the most frequently used genome engineering tool and has been used to generate transgenic animals in multiple species (Cho et al., 2013; Gratz et al., 2013; Hai et al., 2014; Yang et al., 2013), to induce or correct genetic mutations *in vivo* (Ding et al., 2014), to screen for genes involved in specific biological process (Shalem et al., 2014; Wang et al., 2014), to activate or repress gene expression (Cheng et al., 2013; Gilbert et al., 2013; Qi et al., 2013) and to isolate specific genomic regions of interest (Fujita and Fujii, 2013) or visualize specific genomic regions of interest (Chen et al., 2013). The multiplex CRISPR/Cas9 system has provided the technical platform to model human genetic diseases caused by somatic genetic mutations in animals.

In utero electroporation (IUE) is an efficient approach to deliver multiple transgenes into neural progenitors in developing forebrain in rodent. It has been widely used in studies of neocortical development (LoTurco et al., 2009). When combined with DNA transposon system, for example *piggyBac* transposon system, we are able to use *in utero* electroporation to fate-map neural progenitors (Chen et al., 2014a; Chen and LoTurco, 2012; Siddiqi et al., 2014) as well as to model central nervous tumors (Chen and LoTurco, 2012). In this report, we developed a CRISPR-IUE approach combining the CRISPR/Ca9 system and *in utero* electroporation approach to induce somatic mutations in cells in neural progenitor lineage and to model

neurodevelopmental disorder as well as glioblastoma multiforme. We first designed guide sequences targeting rat PTEN. The PTEN CRISPR constructs successfully abolished PTEN expression in neuron. Moreover, PTEN null neurons demonstrated phenotypes that were similar to PTEN knockout or knockdown neuron, including hypertrophy and altered membrane properties. At last, tumors resembling human glioblastoma multiforme were induced by combinations of three CRISPR constructs targeting rat PTEN, NF1 and P53. These results demonstrated the utility of CRSIPR/Cas9 system in studying neocortical development as well as in modeling human genetic disease caused by somatic mutations.

Results

Loss of PTEN expression caused by CRISPR induced somatic mutation

To investigate the application of CRISPR system in central nervous system, we designed two guide RNAs (gRNAs) targeting rat phosphatase and tensin homolog (PTEN) exon 6 (E6) and exon 8 (E8) (Figure4-1A). We cloned these two sgRNAs in pX330 construct containing the wild type SpCas9 (Cong et al. 2013). *In vitro* SURVEYOR assay showed both sgRNAs were able to introduce mutations at PTEN genomic loci (Supplementary Figure 4-1A).

In utero electroporation is an efficient method to deliver multiple plasmids DNA into neural progenitor cells in developing forebrains thus are used to label and manipulate cells in neural progenitor lineage such as neuron, astrocyte and oligodendrocyte (Chen et al., 2014a; Chen and LoTurco, 2012; Siddiqi et al., 2014) (Figure 4-1B). To test whether gRNAs targeting PTEN were able to introduce mutation *in vivo,* we used *in utero* electroporation to deliver pX330-PTEN E6 and pX330-PTEN E8 into E14 neocortical neural progenitors in rat. Empty pX330 vector containing wild type Cas9 but no gRNA was used to as control for Cas9 activity and CAG-

mRFP was used as transfection control. All plasmids were used at the concentration of 1.5μg/μl. 1μg/μl CAG-eGFP was used to visualize transfection in all conditions. To further demonstrate gRNA targeting PTEN can induce somatic mutation, we performed *in vivo* SURVEYOR assay on a P19 pX330-PTEN E6 transfected brain. As shown in Supplementary Figure4-1B, gRNA targeting PTEN exon 6 successfully induced mutations at PTEN locus *in vivo*.

At P19, PTEN immuohistochemistry showed 86% (86/100) in pX330-PTEN E6 and 82 % (81/99) in pX330-PTEN E8 transfected neurons (GFP positive) were negative for PTEN (Figure 4-1C, D). No PTEN negative neurons were found in pX330 and pCAG-mRFP transfected animals (data not shown). These results indicate gRNAs targeting PTEN exon 6 and 8 were able to introduce mutations *in vivo* at PTEN genomic loci and these mutations were able to abolish PTEN protein expression with high efficacy. In pX330-PTEN E6 and E8 transfected brains, most of GFP labeled neurons migrated normally to proper laminar position layer II/III, whereas about 10% GFP labeled neurons were ectopically located in white matter (Figure 4-1E). This result is consistent with previous studies showing that migration defect only occurred in subset of PTEN null neurons (Backman et al., 2001; Kwon et al., 2001; Zhu et al., 2012).

Figure 4-1 CRISPR knocks out PTEN expression in vivo

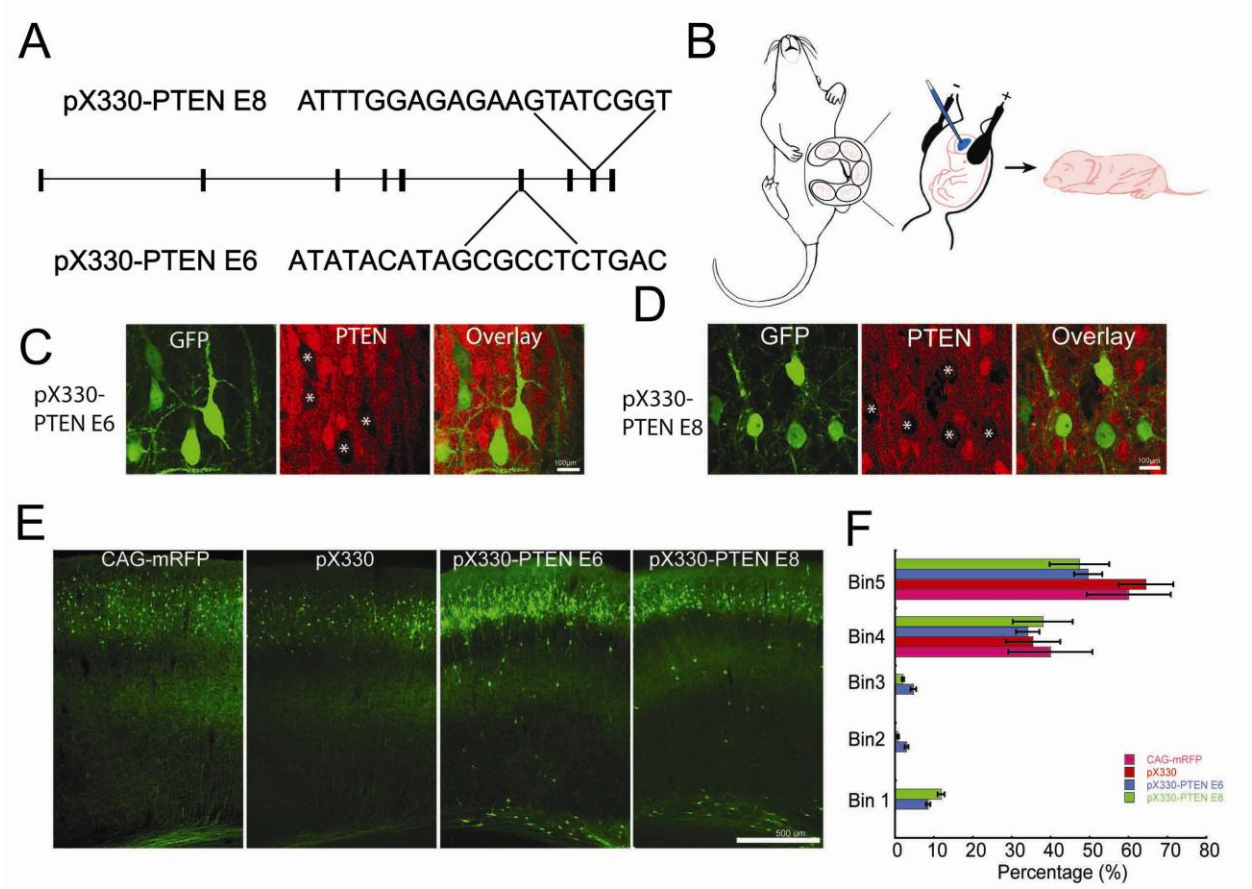

A, Schematic of gRNAs targeting PTEN exon 6 and exon 8

B, Schematic of in utero electroporation

C-D, GFP+ PTEN negative neurons in pX330-PTEN exon 6 and exon 8 transfected brains

E-F, Small population of neurons showed disrupted migration.

PTEN mutated neurons were hypertrophic and showed altered membrane properties

Consistent with previous reports of hypertrophy in PTEN deleted or knocked down neurons (Fraser et al., 2004; Kwon et al., 2001; Luikart et al.), neurons transfected with PTEN targeting gRNAs showed increased soma size (Figure 4-2A). At P19, pX330 (212.7±5.7 μm^2, n=85) and

CAG-mRFP (201.2 ± 5 μm^2, n=74) transfected neurons had similar size (One way ANONVA, p=0.08) (Figure 4-2B). Somas of pX330-PTEN E6 (453.8 ± 5.2 μm^2, n=72) transfected neurons were significantly increased compared to neurons transfected with pX330 (One way ANOVA, p= 3.16671E-48) or CAG-mRFP (One way ANOVA, 8.97499E-58). Similarly, pX330-PTEN E8 transfected neurons had average soma size of $428.5.3 \pm 12$ μm^2 (n=88) and were significantly larger than neurons transfected with pX330 (One way ANOVA, p= 1.27038E-29) or CAG-mRFP (One way ANOVA, p=1.58021E-36). However, pX330-PTEN E6 and E8 transfected neurons showed comparable sized soma (One way ANOVA, p= 0.097757973).

To quantify the primary dendritic width, we measured the width of the primary dendrites at 50μm to the center of the soma. Neurons transfected with CAG-mRFP and pX330 had similar primary dendritic width(CAG-mRFP, 2.9 ± 0.2μm, n=14; pX330,2.8 ± 0.2μm,(n=25; p=0.72 One way ANOVA) (Figure 4-2C). The primary dendritic width in pX330-PTEN E6 transfected neurons was 4.7 ± 0.2μm (n=24) and was significantly larger than CAG-mRFP (One way ANOVA, p=3.70486E-06) and pX330 (One way ANOVA, p= 9.50806E-09) transfected neurons. Similarly, pX330-PTEN E8 transfected neurons had significantly thicker primary dendrite (5.4 ± 0.2 μm n=18) than CAG-mRFP (One way ANOVA, p= 5.36052E-09) or pX330 (One way ANOVA, p= 3.99844E-12) transfected neurons.

We then looked at the electrophysiological properties of transfected neurons. Neurons transfected with CAG-mRFP, pX330 and pX330-PTEN E8 had similar resting membrane potential (Figure 4-2D; CAG-mRFP,-74.99 ± 3.5 mV, n=13; pX330,-72.98 ± 2.6mV, n=6; pX330-PTEN E8,-71.71 ± 4.1mV, n=9; ANOVA with Turkey multiple comparison, ns). We found, consistent with the increased soma size in pX330-PTEN E8 transfected cortical pyramidal neurons, significantly decreased input resistance through whole cell recording(Figure 4-2E). The

input resistance for pX330-PTEN E8 transfected neurons were 44.03±3.566M Ω (n=7) and were significantly lower than pX330 and CAG-mRFP transfected neurons (pX330: 76.66±5.941M Ω; ANOVA with Turkey multiple comparison, $p<0.01$, n=12; CAG-mRFP: 98.42 ±11.98M Ω, ANOVA with Turkey multiple comparison, $p<0.01$, n=6). No significant difference was observed between pX330 and CAG-mRFP transfected neurons (ANOVA with Turkey multiple comparison, ns).

We next looked at the spontaneous synaptic events. In control recordings, there were no differences between CAG-mRFP and pX330 transfected cortical pyramidal neurons (CAG-mRFP: 5.025±0.9015Hz, n=6; pX330: 3.754±0.5996Hz, n=12; One way ANOVA with Turkey multiple comparison, ns) (Figure 4-2F). pX330-PTEN E8 transfected pyramidal neurons showed markedly increased spontaneous EPSC (sEPSC) frequency (8.273±1.009Hz, n=7; pX330-PTEN E8 *vs* pX330, $p< 0.01$; pX330-PTEN E8 *vs* CAG-mRFP, $p<0.05$, ANOVA with Turkey multiple comparison) (Figure 4-2F). Similarly, in the presence of tetrodotoxin, no differences in miniature EPSC (mEPSC) between CAG-mRFP and pX330 transfected pyramidal neurons were observed (CAG-mRFP, 1.334±0.1996Hz, n=6; pX330, 2.951±0.5272Hz, n=12; ANOVA with Turkey multiple comparison, ns) (Figure 4-2G). pX330-PTEN E8 transfected pyramidal neurons showed markedly increased mEPSC frequency (4.787±0.4990Hz, n=7; pX330-PTEN E8 *vs* pX330, $p< 0.05$; pX330-PTEN E8 *vs* CAG-mRFP, $p<0.01$, ANOVA with Turkey multiple comparison) (Figure 4-2G). These results are consistent with previous reports on PTEN knockout or knockdown neurons using transgenic animals or shRNA and indicate that gRNAs targeting PTEN are highly specific and CRISPR/Cas9 can be used *in vivo* neuronal function studies.

Figure 4-2 PTEN null neurons showed hypertrophy and altered membrane properties

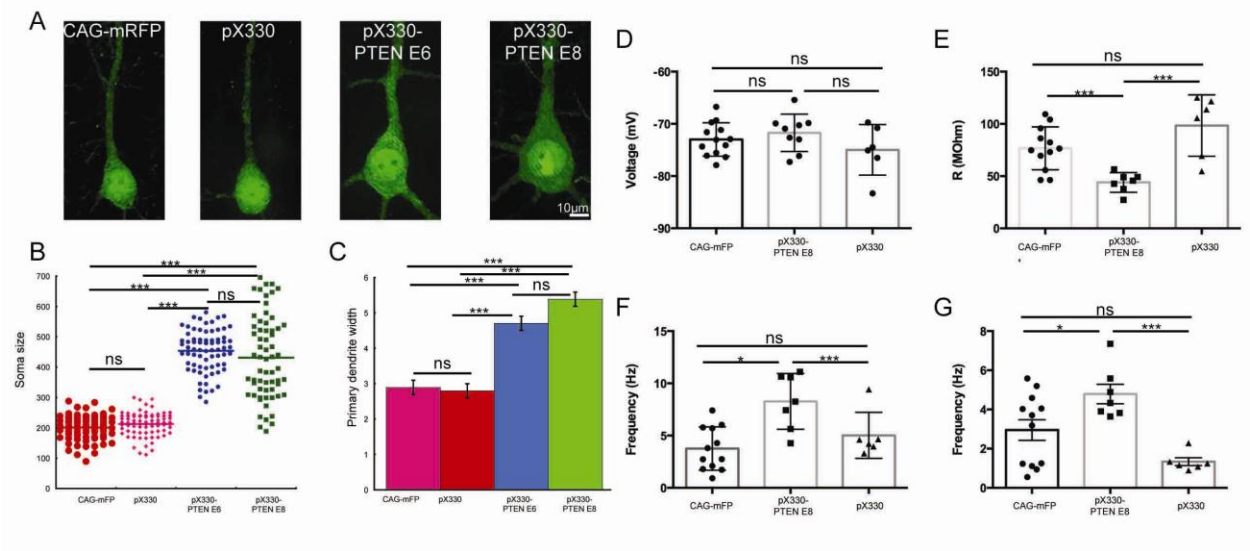

A, Morphologies of neurons transfected with CAG-mRFP, pX330, pX330-PTEN E6 and pX330-PTEN E8.

B, Neurons transfected with pX330, pX330-PTEN E6 and pX330-PTEN E8 showed increased soma size.

C, Neurons transfected with pX330, pX330-PTEN E6 and pX330-PTEN E8 showed thickened primary dendrites.

D-E, Membrane properties of neurons transfected with pX330-PTEN E8. pX330-PTEN E8 transfected neurons had similar resting membrane potential as control neurons (D), decreased input resistance (E) and increased sEPSC (F) and mEPSC (G).

(Eelectrophysiological experiments were performed by Alicia Yue Che)

Combination of CRISPR constructs targeting PTEN, NF1 and P53 induce tumor formation

Loss of function of tumor suppressors caused by somatic mutations has been implicated in various cancers. We have showed that CRISPR/Cas9 system can induce mutation in targeting genomic locus *in vivo*. We therefore hypothesized that loss of function of tumor suppressors mediated by CRSIPR/Cas9 system can lead tumor formation *in vivo*. To test this, we designed

two additional gRNAs targeting Neurofibromin 1 (NF1) exon 1 and P53 exon 6 and cloned them into pX330 vector, named pX330-NF1 E1 and pX330-p35 E6 respectively. *In vitro* SURVEYOR assays showed both gRNAs were able to introduce mutations at targeted genomic locus (Supplementary Figure 4-2) and immunohistochemistry showed both gRNAs were able to abolish endogenous gene expression in neurons (Supplementary Figure 4-2B).

We electroporated CRISPR constructs with gRNA targeting PTEN, NF1 and P53 alone or in combination with each other into E14 rat brains. *PiggyBac* plasmids (GLAST-PBase, PBCAG-eGFP, or PBCAG-mRFP) were used to track the radial glia lineage. Episomal CAG-eGFP or CAG-mRFP was also used to distinguish experimental conditions (Figure 4-3 and Supplementary Figure 4-3). When looked at P19, in brains transfected with gRNAs targeting PTEN, P53 either alone or in combinations (Figure 4-3B, C, E and F; Figure Supplementary Figure 4-3B, C E and F), fluorescently labeled glia showed similar morphology and proliferation as in pX330 (Figure 4-3 A) transfected brains. However, in brains transfected with gRNA targeting NF1 either alone or in combination with gRNAs targeting PTEN , increased glia proliferation was frequently observed. Large patches of densely packed fluorescently labeled cell were frequently found in neocortex and striatum. (Figure 4-3 D, G, H; Supplementary Figure 4-3 D, G, H). These big patches of labeled glia were largely absent in either pX330 or gRNAs targeting PTEN and /or p53 transfected brains. This increased glia proliferation in pX330-NF1 E1 transfectesd brains is consistent with previous report that deletion of NF1 induced glia prolieferation but no tumor formation (Fraser et al., 2004).

Figure 4-3 Loss of NF1 expression caused increase proliferation of glia.

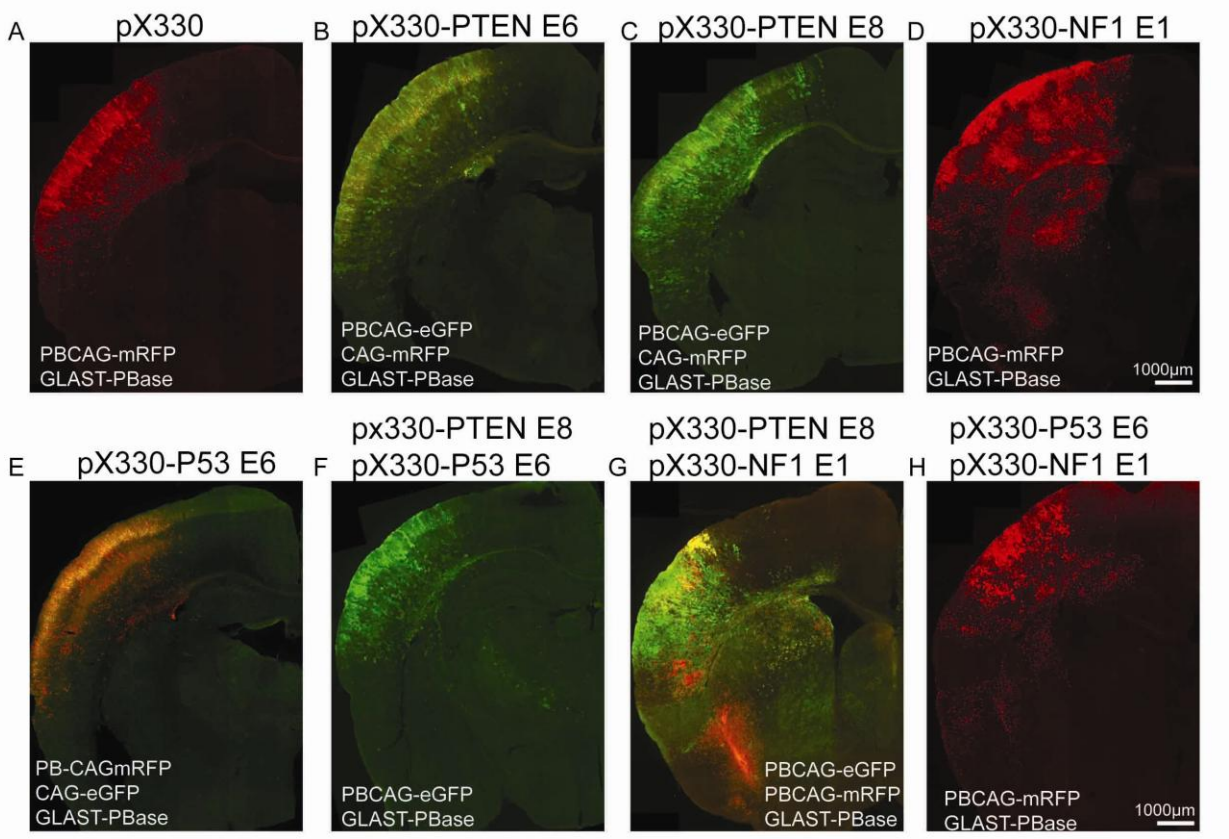

A, Representative image of P19 rat brain transfected with pX330

B, Representative image of P19 rat brain transfected with pX330-PTEN E6

C, Representative image of P19 rat brain transfected with pX330-PTEN E8

D, Representative image of P19 rat brain transfected with pX330-NF1 E1. Note the increased density of labeled cells in neocortex and striatum.

E, Representative image of P19 rat brain transfected with pX330-P53 E6.

F, Representative image of P19 rat brain transfected with pX330-PTEN E8 and pX330-P53 E6.

G, Representative image of P19 rat brain transfected with pX330-PTEN E8 and pX330-NF1 E1. Note the increased density of labeled cells in neocortex and striatum.

H, Representative image of P19 rat brain transfected with pX330-P53 E6 and pX330-NF1 E1. Note the increased density of labeled cells in neocortex and striatum.

However, in P19 brains transfected with CRISPR constructs targeting PTEN E8， P53 E6 and NF1 E1, significant cell proliferation was observed as indicated by massive fluorescently labeled cells densely populating almost whole brain hemisphere (Figure 4-4A). The massive cell proliferation suggested the presence of tumor. We have previously established the multicolor lineage labeling approach using *piggyBac* transposon system (Siddiqi et al., 2014) and successfully labeled brain tumors (Chen et al., 2014a). We next electroporated the *piggyBac* multicolor system (GLAST-PBase, PBCAG-eGFP,PBCAG-mRFP and PBCAG-CFP) with CRISPR constructs targeting PTEN, P53 and NF1 to clonally label resulted tumor cells. Transfected animals showed sign of illness and started to demise at the age of P63. All animals (n=8) had died by P75. Upon postmortem analysis of transfected brains, we immediately noticed that transfected hemisphere was significantly enlarged indicating the presence of tumor. Figure 4-4B showed the multicolor tumor from a postmortem brain of a P63 rat. Tumor clones labeled with different colors were apparent. It is also noticeable that tumor cells can also be found in cerebral hemisphere that was not transfected indicating these tumors cell were highly migratory and invasive. It is also interesting to notice that tumor cells found in non transfected hemispheres were either in single colored clusters (Figure 4-4C) indicating that these tumor cells are clonally related or in mixed color clusters (Figure 4-4D) indicating mixing of different tumor clones.

Figure4- 4 Multicolor labeling of CRISPR constructs induced tumor

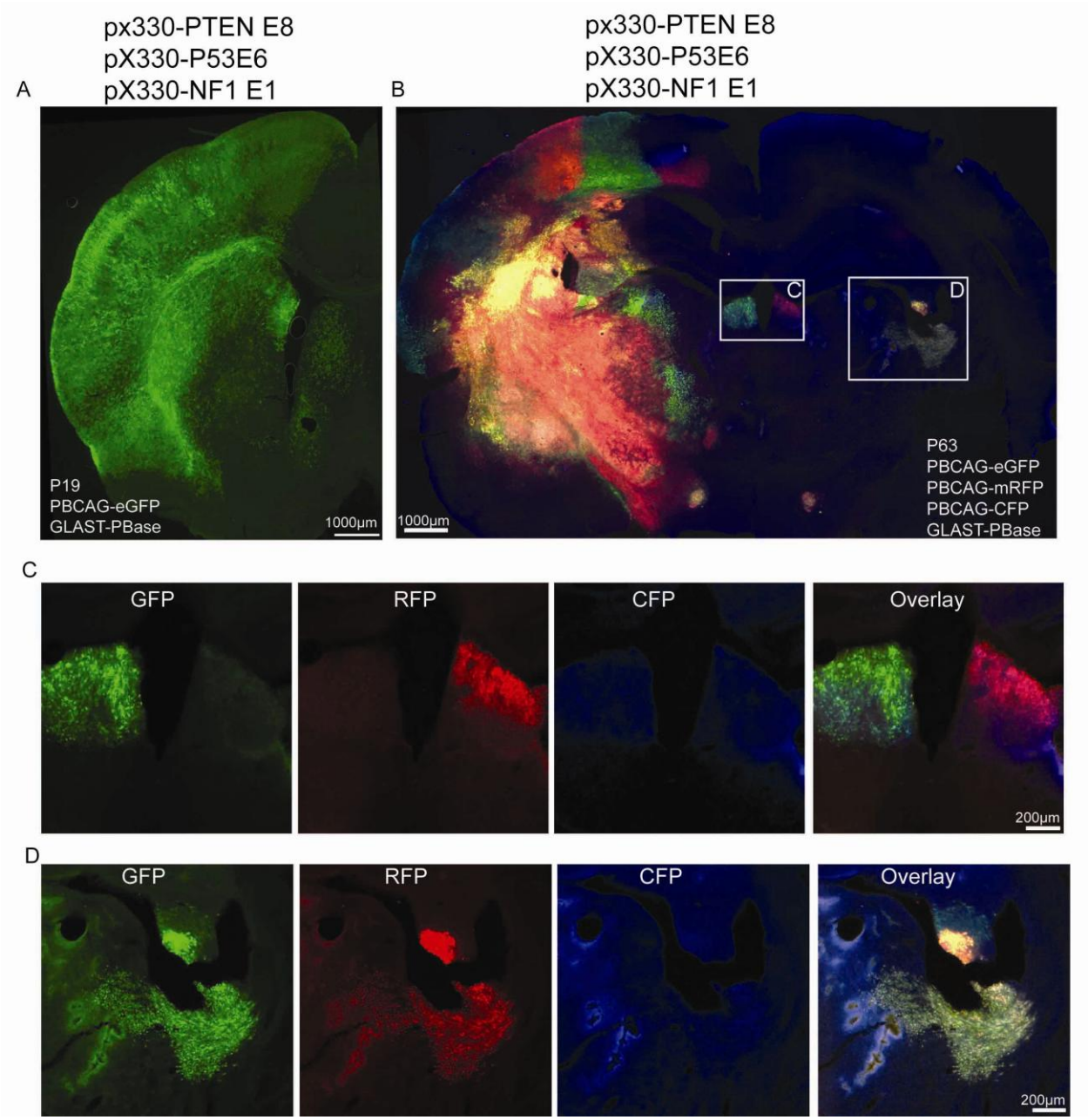

A, Representative image of CRISPR targeting PTEN, P53, NF1 from a P1 rat.

B, Multicolor labeling of tumor cells

C and D, enlarged view of boxed area in B. C showed separation of two tumor clones. D showed the mixing of different colored tumor clones.

Histopathological analysis revealed increased cell density in tumor core and tumors cells frequently were mitotic (Figure4-5 A). Tumor cells diffusely infiltrated neighboring tissue (Figure 4-5A, B) and exhibited glomeruloid vascular proliferation (Figure 4-5B) which is important histopathological features of human glioblastoma multiforme. Several multinucleated large cells are visible in the tumor, suggesting the differential diagnosis of giant cell glioblastoma (Figure 4-5C black arrow). However, this cellular pattern was only occasionally observed, arguing against this differential diagnosis. Tumors cells demonstrated features for astroglial differentiation with strong vimentin (Figure 4-5D), GFAP (Figure 4-5E) and MAP2 (Figure 4-5F) expression in a process rich pattern. In summary, the histological features of induced tumors are most similar to human glioblastoma multiforme (WHO grade IV). In summary, we have successfully induced highly malignant glioblastoma multfiorme using CRISPR/Cas9 system.

We further performed *in vivo* SURVEYOR assay using tumor genomic DNA. All three gRNAs introduced mutations at high efficacy at targeted geonic loci (Supplementary Figure4-4A). Sequencing of the the mutated PTEN allele showed that both insertions and deletions were induced and indels significantly altered the protein amino acids sequence downstream the double strand break sites (Supplementary Figure 4-4B).

Figure 4-5, Histological features of CRISPR constructs induced tumors

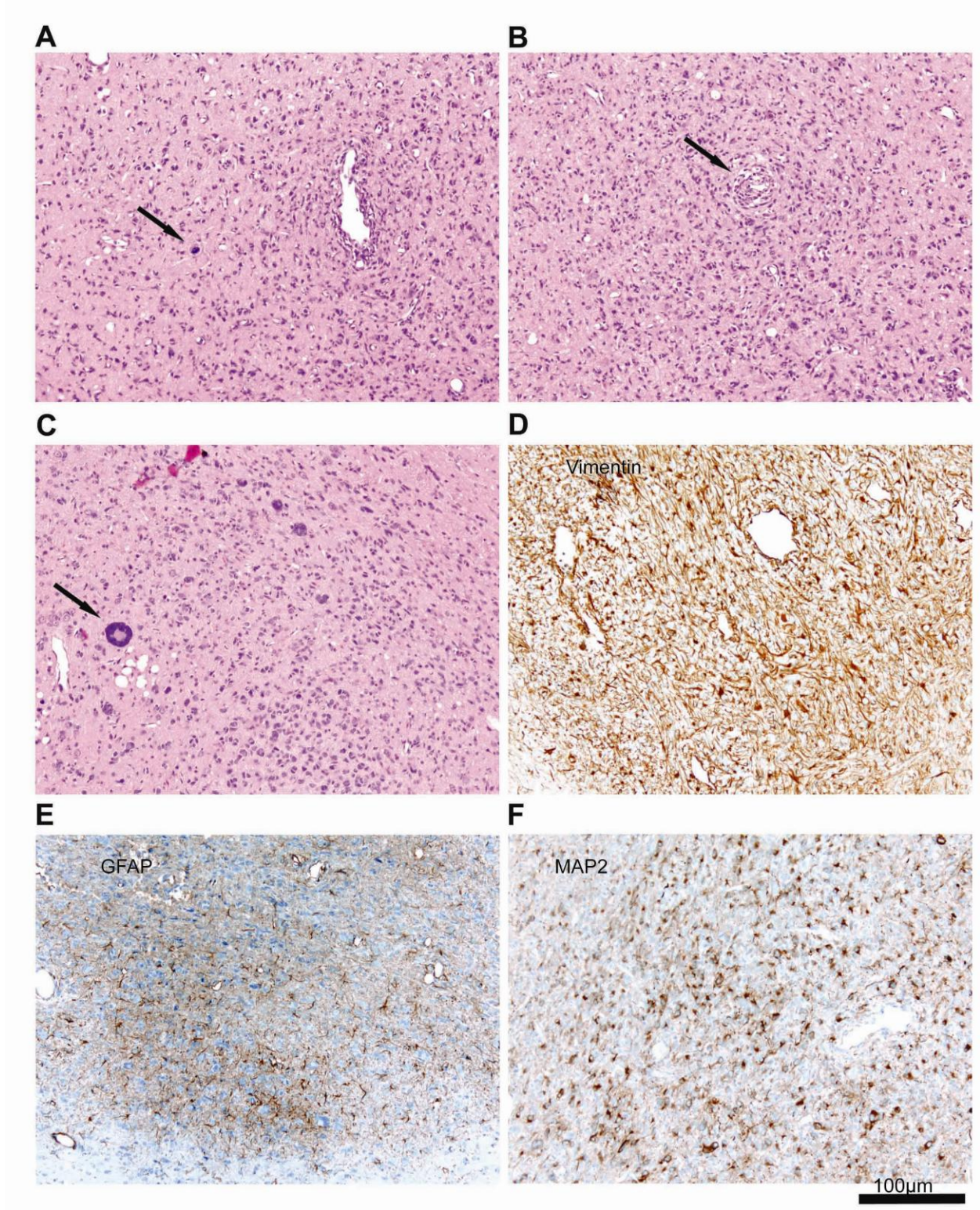

A) Diffusely infiltrating glial tumor with changing cellular densities and mitotic figure as sign of frank malignancy (black arrow).

B) Pleomorphic diffusely infiltrating tumor with a process rich matrix and glomeruloid vascular proliferate (black arrow).

C) Several multinucleated large cells are visible in the tumor, suggesting the differential diagnosis of giant cell glioblastoma (black arrow). However, this cellular pattern was only occasionally observed, arguing against this differential diagnosis.

D) Tumor cells are strongly expressing vimentin in a process rich pattern.

E) Tumor cells with characteristic expression of glial fibrillary acidic protein (GFAP) in a process-oriented pattern.

F) Tumor cells in parallel show a similar expression pattern for MAP2.

Discussion

In this report, we have demonstrated the applications of CRSIPR/Cas9 system to abolish gene expression in developing neocortex and to model human neurodevelopmental disorder as well glioblastoma multiforme. To our knowledge, this is the first report of using CRSIPR/Cas9 system to model human tumors and neurodevelopmental disorders. This study revealed several features of CRISPR/Cas9 system which make it a powerful biological tool.

CRISPR/Cas9 system introduces mutations in *vivo* at targeting genomic locus and abolishes gene expression with high efficacy. gRNAs targeting two different exons of PTEN (exon 6 and 8) abolished PTEN expression in 86% and 82% of transfected neurons at P19 respectively. This high loss of expression efficiency of CRISPR/Cas9 system makes it an ideal tool to study gene function *in vivo*.

Genome wide binding assay of Cas9 in mammalian cells showed that dCas9 (mutant Cas9) is able to bind to genomic DNA even without the presence of gRNA (Wu et al., 2014).It is unclear that whether wild type Cas9 will cleave the genome without gRNA. It is critical to know whether wild type Cas9 can cause experimental artifact through random cleavage of genome without gRNA. We have compared membrane properties of neurons transfected with plasmid only contains wild type Cas9 but not gRNA (pX330) with neurons transfected with commonly used plasmid only encoding mRFP (CAG-mRFP) and found that neurons transfected with pX330 had similar membrane properties including resting membrane potential, sEPSC and mEPSC. Additionally, no migration defect was observed in neurons transfected with pX330. This suggests that at least wild type Cas9 doesn't cause functional genomic changes that can affect resting membrane potential, eEPSCs, mEPSC and neuronal migration.

Compared to *sh*RNA, CRISPR/Cas9 is much more effective to knockout gene expression (Shalem et al., 2014). Like *sh*RNA, CRISPR/Cas9 also suffers from off target effect. However, it is impossible to predict off target sites for *sh*RNA, off target sites for CRISPR/Cas9 is predictable thus it is possible to assess whether mutations are introduced at off target sites. Functional off target can be avoided by choosing gRNAs don't have off target sites in functional genes. The gRNAs used here all have no predicted off target in gene coding regions (data not shown). We also showed neurons transfected with two gRNAs targeting exon 6 and exon 8 of PTEN showed same phenotype, indicating the resulted phenotype is due to on target effect other than off target effect of gRNAs. We also showed that PTEN null neurons exhibited phenotypes similar to PTEN knockout or knock down neurons. These results indicate gRNA targeting PTEN is highly specific and the results generated from CRISPR system are comparable to results

obtained from *sh*RNA or knockout studies. Of course CRISPR might also have off target effect in non-predictable sites; special attention is needed when assessing experiment results.

We have successfully induced glioblastoma multiforme using CRISPR/Cas9 system by targeting 3 tumor suppressor genes, PTEN, NF1 and p53. This tumor model is highly malignant and invasive. In combination of multicolor labeling, this multi color GBM animal model will be ideal to study tumor cell migration. Above all, we have demonstrated the application of multiplex CRISPR/Cas9 in modeling human somatic diseases. The ease of production, high efficacy will make CRISPR/Cas9 system in studying brain development in both normal and dseased state.

Methods:

Plasmids and gRNA sequence

Guide RNA sequences were designed using on-line program (crispr.mit.edu) as described in (Hsu et al., 2013). Guide sequences were cloned into pX330 vector (Addgene plasmid 42230) {Cong, 2013 #4} following normal cloning procedure. The guide sequences are: PTEN exon 6 forward: 5'- GATATACATAGCGCCTCTGAC-3'; PTEN exon 6 reverse: 5'-GTCAGAGGCGCTATGTATATC-3';PTEN exon 8 forward: 5'-ATTTGGAGAGAAGTATCGGT-3'; PTEN exon8 reverse: 5'-ACCGATACTTCT CTCCAA AT -3'; NF1 exon 1 forward: 5'-GGTCAGCCGCTTCGACGAGC-3';NF1 exon 1 reverse 5'-GCTCGTCGAAGCGGCTGACC -3'; P53 exon 6 forward: 5'-

CTTCCACCCGGATAAGATGT-3'; P53 exon 6 reverse: 5'-ACATCTTATCCGGGT GGA AGC -3'.

Animals

Pregnant Wistar rats were obtained from Charles River Laboratories, Inc. (Wilmington, MA) and maintained at the University of Connecticut vivarium on a 12 h light cycle and fed *ad libitum*. Animal gestational ages were determined and confirmed during surgery. Both male and female subjects were used for tumor induction. All procedures and experimental approaches were approved by the University of Connecticut IACUC.

In utero electroporation

In utero electroporation was performed as previously described {Centanni, 2012 #41;Centanni, 2014 #40;Chen, 2014 #5;Chen, 2012 #88;Chen, 2014 #37}. Electroporation was performed at embryonic day 14 or 15 (E14 or E15) and gestation age was confirmed during surgery. All plasmids were used at the final concentration of 1.0 μg/μl GLAST-PBase was used at the final concentration of 2.0 μg/μl.

Image acquisition

Multi color imaging was performed as previously described (Chen and LoTurco, 2012) using Zeiss Axio imager M2 microscope with Apotome with 488/546/350 nm filter cubes and the X-

Cite series 120Q light source (Chen et al., 2014a)All the images were further processed in Adobe Photoshop CS3 software (San Jose, CA).

Immunohistochemistry

Animals were deeply anesthetized with Isoflurane and perfused transcardially with 4% paraformaldehyde/PBS (4% PFA). Samples were post fixed overnight in 4% PFA. For immunofluorescence, brains were sectioned at 65 µm thickness on a vibratome (Leica VT 1000S). Sections were processed as free-floating sections and stained with PTEN (Cell Signaling, 9559), NF1 (Santa Cruz, 9559) and p53 (Cell Signaling, 2524), antibody. Images were acquired and processed as previous described {Siddiqi, 2014 #150}.

For histological analysis, immnunohistochemsitry and H&E staining were carried out on paraffin embedded 4µm sections as described in (Schick et al., 2007a; Schick et al., 2007b)using GFAP (DAKO, Z0334), MAP2c (Sigma, M4403), Vimentin (DAKO, M0725), antibody.

SURVEYOR assay

For *in vitro* SURVEYOR assay, rat neuroblastoma cells were transfected with CRISPR constructs using lippfectomine 2000 (Invitrogen) according to manufacturer's instruction. Two days post transfection, cells were harvested and genomic DNA was extracted using Blood and Tissue DNA easy kit (Qiagen). Genomic region flanking targeting sites were PCR amplified and SUVEYOR assay was performed using SURVEYOR assay kit (Transgenomics) according to manufacturer's instruction. For *in vivo* SURVEYOR assay, we freshly removed the brain and carefully dissected out transfected cortical region under fluorescent dissection microscope. Brain

tissues were chopped into small pieces and genomic DNA was extracted using Blood and Tissue DNA easy kit (Qiagen). Primers for SURVEYOR assays are: PTEN exon 6 Forward: CATCCATGTGAGGAACCCTGGGTG; PTEN exon 6 Reverse: CACTTACTG CAAGTTCCGCC; PTEN exon 8 Forward: CCACAAGGTGTTTGCCTTCA; PTEN exon 8 Reverse: CTCGAGATCCAAAGGCATTG; NF1 exon 1 Forward: GACGTCACCTCCAGGAGGAC; NF1 exon 1 Reverse: TGGGATAAAGGGGATGGAGGG; P53 exon 6 Forward: CCCACTTTGACCCTTGATCC; P53 exon 6 Reverse: CAGGCACAAACACGAACCTC.

References

Backman, S.A., Stambolic, V., Suzuki, A., Haight, J., Elia, A., Pretorius, J., Tsao, M.S., Shannon, P., Bolon, B., Ivy, G.O., *et al.* (2001). Deletion of Pten in mouse brain causes seizures, ataxia and defects in soma size resembling Lhermitte-Duclos disease. Nat Genet *29*, 396-403.

Bamford, S., Dawson, E., Forbes, S., Clements, J., Pettett, R., Dogan, A., Flanagan, A., Teague, J., Futreal, P.A., Stratton, M.R., *et al.* (2004). The COSMIC (Catalogue of Somatic Mutations in Cancer) database and website. Br J Cancer *91*, 355-358.

Celebi, J.T., Shendrik, I., Silvers, D.N., and Peacocke, M. (2000). Identification of PTEN mutations in metastatic melanoma specimens. J Med Genet *37*, 653-657.

Centanni, T.M., Booker, A.B., Sloan, A.M., Chen, F., Maher, B.J., Carraway, R.S., Khodaparast, N., Rennaker, R., LoTurco, J.J., and Kilgard, M.P. (2012). Knockdown of the dyslexia-associated gene kiaa0319 impairs temporal responses to speech stimuli in rat primary auditory cortex. Cereb Cortex *24*, 1753-1766.

Centanni, T.M., Chen, F., Booker, A.M., Engineer, C.T., Sloan, A.M., Rennaker, R.L., LoTurco, J.J., and Kilgard, M.P. (2014). Speech sound processing deficits and training-induced neural plasticity in rats with dyslexia gene knockdown. PLoS One *9*, e98439.

Chen, B., Gilbert, L.A., Cimini, B.A., Schnitzbauer, J., Zhang, W., Li, G.W., Park, J., Blackburn, E.H., Weissman, J.S., Qi, L.S., *et al.* (2013). Dynamic imaging of genomic loci in living human cells by an optimized CRISPR/Cas system. Cell *155*, 1479-1491.

Chen, F., Becker, A.J., and Loturco, J.J. (2014a). Contribution of tumor heterogeneity in a new animal model of CNS tumors. Mol Cancer Res *12*, 742-753.

Chen, F., and LoTurco, J. (2012). A method for stable transgenesis of radial glia lineage in rat neocortex by piggyBac mediated transposition. J Neurosci Methods *207*, 172-180.

Chen, F., Maher, B.J., and LoTurco, J.J. (2014b). PiggyBac Transposon-Mediated Cellular Transgenesis in Mammalian Forebrain by In Utero Electroporation. Cold Spring Harb Protoc *2014*, pdb prot073650.

Cheng, A.W., Wang, H., Yang, H., Shi, L., Katz, Y., Theunissen, T.W., Rangarajan, S., Shivalila, C.S., Dadon, D.B., and Jaenisch, R. (2013). Multiplexed activation of endogenous genes by CRISPR-on, an RNA-guided transcriptional activator system. Cell Res *23*, 1163-1171.

Cho, S.W., Lee, J., Carroll, D., and Kim, J.S. (2013). Heritable gene knockout in Caenorhabditis elegans by direct injection of Cas9-sgRNA ribonucleoproteins. Genetics *195*, 1177-1180.
Cong, L., Ran, F.A., Cox, D., Lin, S., Barretto, R., Habib, N., Hsu, P.D., Wu, X., Jiang, W., Marraffini, L.A., *et al.* (2013). Multiplex genome engineering using CRISPR/Cas systems. Science *339*, 819-823.
Ding, Q., Strong, A., Patel, K.M., Ng, S.L., Gosis, B.S., Regan, S.N., Rader, D.J., and Musunuru, K. (2014). Permanent Alteration of PCSK9 With In Vivo CRISPR-Cas9 Genome Editing. Circ Res.
Fraser, M.M., Zhu, X., Kwon, C.H., Uhlmann, E.J., Gutmann, D.H., and Baker, S.J. (2004). Pten loss causes hypertrophy and increased proliferation of astrocytes in vivo. Cancer Res *64*, 7773-7779.
Fujita, T., and Fujii, H. (2013). Efficient isolation of specific genomic regions and identification of associated proteins by engineered DNA-binding molecule-mediated chromatin immunoprecipitation (enChIP) using CRISPR. Biochem Biophys Res Commun *439*, 132-136.
Futreal, P.A., Coin, L., Marshall, M., Down, T., Hubbard, T., Wooster, R., Rahman, N., and Stratton, M.R. (2004). A census of human cancer genes. Nat Rev Cancer *4*, 177-183.
Gilbert, L.A., Larson, M.H., Morsut, L., Liu, Z., Brar, G.A., Torres, S.E., Stern-Ginossar, N., Brandman, O., Whitehead, E.H., Doudna, J.A., *et al.* (2013). CRISPR-mediated modular RNA-guided regulation of transcription in eukaryotes. Cell *154*, 442-451.
Gratz, S.J., Cummings, A.M., Nguyen, J.N., Hamm, D.C., Donohue, L.K., Harrison, M.M., Wildonger, J., and O'Connor-Giles, K.M. (2013). Genome engineering of Drosophila with the CRISPR RNA-guided Cas9 nuclease. Genetics *194*, 1029-1035.
Hai, T., Teng, F., Guo, R., Li, W., and Zhou, Q. (2014). One-step generation of knockout pigs by zygote injection of CRISPR/Cas system. Cell Res *24*, 372-375.
Hsu, P.D., Scott, D.A., Weinstein, J.A., Ran, F.A., Konermann, S., Agarwala, V., Li, Y., Fine, E.J., Wu, X., Shalem, O., *et al.* (2013). DNA targeting specificity of RNA-guided Cas9 nucleases. Nat Biotechnol *31*, 827-832.
Hua, Y., and Crino, P.B. (2003). Single cell lineage analysis in human focal cortical dysplasia. Cereb Cortex *13*, 693-699.
Kwon, C.H., Zhu, X., Zhang, J., Knoop, L.L., Tharp, R., Smeyne, R.J., Eberhart, C.G., Burger, P.C., and Baker, S.J. (2001). Pten regulates neuronal soma size: a mouse model of Lhermitte-Duclos disease. Nat Genet *29*, 404-411.
LoTurco, J., Manent, J.B., and Sidiqi, F. (2009). New and improved tools for in utero electroporation studies of developing cerebral cortex. Cereb Cortex *19 Suppl 1*, i120-125.
Luikart, B.W., Schnell, E., Washburn, E.K., Bensen, A.L., Tovar, K.R., and Westbrook, G.L. (2011). Pten knockdown in vivo increases excitatory drive onto dentate granule cells. J Neurosci *31*, 4345-4354.
Mali, P., Yang, L., Esvelt, K.M., Aach, J., Guell, M., DiCarlo, J.E., Norville, J.E., and Church, G.M. (2013). RNA-guided human genome engineering via Cas9. Science *339*, 823-826.
Minobe, K., Bando, K., Fukino, K., Soma, S., Kasumi, F., Sakamoto, G., Furukawa, K., Higuchi, K., Onda, M., Nakamura, Y., *et al.* (1999). Somatic mutation of the PTEN/MMAC1 gene in breast cancers with microsatellite instability. Cancer Lett *144*, 9-16.
Poduri, A., Evrony, G.D., Cai, X., and Walsh, C.A. Somatic mutation, genomic variation, and neurological disease. Science *341*, 1237758.

Qi, L.S., Larson, M.H., Gilbert, L.A., Doudna, J.A., Weissman, J.S., Arkin, A.P., and Lim, W.A. (2013). Repurposing CRISPR as an RNA-guided platform for sequence-specific control of gene expression. Cell *152*, 1173-1183.
Schick, V., Majores, M., Engels, G., Hartmann, W., Elger, C.E., Schramm, J., Schoch, S., and Becker, A.J. (2007a). Differential Pi3K-pathway activation in cortical tubers and focal cortical dysplasias with balloon cells. Brain Pathol *17*, 165-173.
Schick, V., Majores, M., Koch, A., Elger, C.E., Schramm, J., Urbach, H., and Becker, A.J. (2007b). Alterations of phosphatidylinositol 3-kinase pathway components in epilepsy-associated glioneuronal lesions. Epilepsia *48 Suppl 5*, 65-73.
Shalem, O., Sanjana, N.E., Hartenian, E., Shi, X., Scott, D.A., Mikkelsen, T.S., Heckl, D., Ebert, B.L., Root, D.E., Doench, J.G., *et al.* (2014). Genome-scale CRISPR-Cas9 knockout screening in human cells. Science *343*, 84-87.
Siddiqi, F., Chen, F., Aron, A.W., Fiondella, C.G., Patel, K., and Loturco, J.J. (2014). Fate Mapping by PiggyBac Transposase Reveals That Neocortical GLAST+ Progenitors Generate More Astrocytes Than Nestin+ Progenitors in Rat Neocortex. Cereb Cortex.
Wang, S.I., Puc, J., Li, J., Bruce, J.N., Cairns, P., Sidransky, D., and Parsons, R. (1997). Somatic mutations of PTEN in glioblastoma multiforme. Cancer Res *57*, 4183-4186.
Wang, T., Wei, J.J., Sabatini, D.M., and Lander, E.S. (2014). Genetic screens in human cells using the CRISPR-Cas9 system. Science *343*, 80-84.
Wu, X., Scott, D.A., Kriz, A.J., Chiu, A.C., Hsu, P.D., Dadon, D.B., Cheng, A.W., Trevino, A.E., Konermann, S., Chen, S., *et al.* (2014). Genome-wide binding of the CRISPR endonuclease Cas9 in mammalian cells. Nat Biotechnol *32*, 670-676.
Yang, H., Wang, H., Shivalila, C.S., Cheng, A.W., Shi, L., and Jaenisch, R. (2013). One-step generation of mice carrying reporter and conditional alleles by CRISPR/Cas-mediated genome engineering. Cell *154*, 1370-1379.
Zhu, G., Chow, L.M., Bayazitov, I.T., Tong, Y., Gilbertson, R.J., Zakharenko, S.S., Solecki, D.J., and Baker, S.J. (2012). Pten deletion causes mTorc1-dependent ectopic neuroblast differentiation without causing uniform migration defects. Development *139*, 3422-3431.

Chapter 5 Summary and further discussion

Summary

This dissertation is aimed to develop new tools for radial glia lineage tracing and modeling central nervous system tumors. To this end, I first established the *piggyBac in utero* electroporation approach to label and manipulate the lineage of neural progenitors. I then used this *piggyBac*-IUE approach to establish new central nervous system tumor model. I further explored the sources of CNS tumor heterogeneity using this animal model. At last, I applied the newly developed RNA guided genome engineering tool CRISPR/Cas9 system to study neocortical development. Using CRISPR/Cas9 *in utero* electroporation approach, I have successfully modeled neural development disorder as well as glioblastoma multiforme. In sum, I have established three novel methods which have been proven to be useful to study normal and diseased brain development.

In Chapter 2, I took advantage of the features of *in utero* electroporation and *piggyBac* transposon system and established *piggyBac*-IUE approach to trace neural progenitor lineage. The *piggyBac*-IUE approach successfully labeled cells in the neural progenitor lineage including neurons, astrocytes, oligodendrocytes, oligodendrocytes precursors as well as olfactory bulb interneurons. I also constructed a modular *piggyBac* toolkit that can be used to label and manipulate neural progenitor lineage. As proof of principle, I also demonstrated of the utility of *piggyBac* IUE approach in gain of function experiment by over expressing EGFR.

In Chapter 3, I first utilized the *piggyBac* IUE approach to induce brain tumors by over expressing two well studied oncogenes HRasV12 and AKT. Expression of HRasV12/AKT controlled by ubiquitous CAG promoter *in piggyBac* donor plasmids, induced glioblastoma multiforme in rat. To assess contributions of astrocytes and oligodendrocytes in brain

tumorigenesis, I expressed HRasV12/AKT in mainly astrocytes and oligodendrocytes using *piggyBac* GFAP and MBP donor plasmids respectively. Expression of HRasV12/AKT in astrocytes induced glioblastoma multiforme, whereas expression of HRasV12/AKT in oligodendrocytes induced anaplastic oligoastrocytoma. This result indicates that cellular context contributes to tumor heterogeneity. Next, I co-transfected the tumor inducing *piggyBac* CAG donor plasmids together with neurogenic bHLH family transcription factor Ngn2 or NeuroD1 and found that malignant pediatric atypical teratoid rhabdoid tumor like tumor was induced. This result indicates that molecular context also contributes to tumor heterogeneity. I further showed that tumors induced by *piggyBac* CAG donor plasmids, GFAP donor plasmids, MBP donor plasmids as well as CAG donor plasmids with modifying transcription factors showed distinct developmental time course and molecular signature. Taken together, oncogenic events occurring in disparate cell types and/or molecular context leads to different tumor formation.

In Chapter 4, I explored the feasibility of using CRISPR/Cas9 system to study brain development. I used *in utero* electroporation approach to deliver Cas9 together with gRNAs targeting PTEN exon 6 and 8 into developing rat forebrain. Both gRNAs were able to introduce mutations into PTEN genomic loci and as a result, abolished PTEN expression with high efficiency in cells of the neural progenitor lineage. Moreover, PTEN null neurons showed similar phenotypes as neurons with knocked out or knocked down PTEN expression. I next demonstrated application of CRISPR/Cas9 system to model human brain tumor. *In utero* electroporation of plasmids mixture of Cas9 and gRNAs targeting three tumor suppressors PTEN, NF1 and P53 induced glioblastoma multiforme.

Features of *piggyBac* IUE

Key attributes of *piggyBac* transposon system and *in utero* electroporation method make this approach innovative and potentially useful for a variety of applications. First, *in utero* electroporation with *piggyBac* plasmids overcome the loss of conventional episomal plasmids in IUE, thus making neural progenitor lineage labeling possible (Chen et al., 2014a; Chen and LoTurco, 2012; Chen et al., 2014b; Siddiqi et al., 2014). Second, *piggyBac* has larger cargo capacity. Ding and colleagues (Ding et al., 2005) have reported *piggyBac* can carry up to 14.3Kb insert without affecting the transposition efficiency. Lacoste and colleagues (Lacoste et al., 2009)reported that the engineered *piggyBac* called "*ePiggyBac*" could deliver up to 18Kb inserts. Rostovskaya et al used *piggyBac* system to insert bacterial artificial chromosome into host genome (Rostovskaya et al., 2012). The large capacity makes it possible to deliver several transgenes into the genome (Yusa et al., 2009).Since 80% of human cDNA is less than 7kb (Lander et al., 2001), *piggyBac* is able to deliver more than 80% of all human cDNAs. Compared to *piggyBac*, the cargo capacity for retroviral and lentiviral vectors is limited (Thomas et al., 2003).

Third, in combination of *piggyBac* transposon system with episomal plasmid, immediate progenies in the lineage can be distinguished from the following progeny (Chen and LoTurco, 2012; Chen et al., 2014b). This allows to express one transgene in only the birthdated progeny (first member of a lineage near the time of transfection) but not in the subsequent progeny of the lineage (Figure 2-1).

Fourth, *piggyBac* IUE inherits features of spatial and temporal control of gene expression as well as multiple plasmids co-delivery conferred by *in utero* electroporation. Spatial control is achieved through spatially targeting cells within different areas (Chen and LoTurco, 2012; Chen

et al., 2014b)or cell type specific promoter driving gene expression(Chen et al., 2014a; Chen and LoTurco, 2012; Chen et al., 2014b; Siddiqi et al., 2014). *PiggyBac* IUE method allows for introduction of multiple transgenes controlled by independent promoters. The high co-expression rates allowed us to direct expression in different subpopulations in sequence (Figure 3-3).Temporal control can be attained by transfection time and using inducible gene expression system. Precise temporal control of gene expression can now be achieved through *piggyBac* based inducible gene expression systems (Li et al., 2013; Saridey et al., 2009) gated by tetracycline. Therefore transgenes can be introduced embryonically but will not express until treated by tetracycline at desirable time depending on experimental need.

Last, because *piggyBac* transposon system is binary, it is possible to direct genomic integration in a subset of progenitors by the choice of promoter driving the expression of PBase, and to drive expression of the integrated transgenes in selected progeny by the promoter in the donor plasmid.

Limitations of *piggyBac* IUE approach comes from inherent limitation of IUE approach. IUE has been used to target cerebral cortex (Bai et al., 2003; Chen and LoTurco, 2012; Chen et al., 2014b; Maher and LoTurco) , hippocampus (Chen and LoTurco, 2012), as well as cerebellum (Kita et al., 2013)Other brain areas such as hypothalamus, brain stem are inaccessible using IUE.

Applications of *piggyBac* IUE approach

Using promoter fragments that are active in neural progenitors driving expression of PBase, it is possible to label lineage of neural progenitor subpopulations. Neural progenitor is highly heterogeneous (Kriegstein and Alvarez-Buylla, 2009). Lineage labeling of neural progenitor

subpopulation makes it possible to study functions and properties of neural progenitor subpopulations. For example, we have used GLAST and Nestin promoter fragments driving PBase expression (GLAST-PBase and Nestin-PBase) to label the lineage of GLAST+ and Nestin+ neural progenitors. Our results showed that GLAST+ neural progenitor generates not only more astrocytes, but also bigger astrocytes clonal clusters than Nestin+ neural progenitors do(Siddiqi et al., 2014).

By mixing and matching *piggyBac* donor and helper plasmids with different promoters, it is also possible to label the lineage of subset of neural progenitors but only express transgenes in specific cell types within the lineage. For example, by using GLAST-PBase and PBGFAP-eGFP, I was able to label GFAP+ cells within the GLAST+ progenitor lineage (Figure 3-2A).

PiggyBac IUE approach offers an effective way to manipulate cells within the neural progenitor lineage, i.e. neurons, astrocytes, oligodendrocytes, OPCs and olfactory bulb interneurons. By using promoter of interest, we can direct transgene of interest expression in cells of interest. For example, using CAG promoter driving EGFR expression in *piggyBac* donor plasmid (PBCAG-EGFR), I was able to express EGFR in all cells in the progenitor lineage. Further, I directed oncogene HRasV12/AKT expression in astrocytes and oligodendrocytes using *piggyBac* GFAP and MBP promoter in *piggyBac* donor plasmids and induced different tumor types.

Neuron - glia interaction has been long appreciated in regulating CNS homeostasis. *PiggyBac* IUE allows for independent labeling and manipulation of neurons and glia therefore it is an ideal tool to study neuron glia interaction *in vivo*. Use *piggyBac* IUE, astrocytes can be manipulated as desired and evaluate its effect on neurons and vice versa.

Applications of *piggyBac* IUE CNS tumor model

Using *piggyBac* IUE, I established novel somatic engineered CNS tumor model in rat in which determinants of CNS tumor diversity can be parsed out. In this animal model, I used the *piggyBac* multicolor system (Siddiqi et al., 2014) to clonally label tumor clones. The multicolor clonal labeling makes this animal model a useful tool for *in vivo* tumor imaging. *In vivo* tumor imaging can be used to study many fundamental questions in tumor biology such as primary tumor growth, tumor cell motility and invasion, metastatic seeding and colonization, angiogenesis, and the interaction between the tumor and its microenvironment (Hoffman, 2005). Previous *in vivo* imaging studies, from whole body or direct view imaging using epifluorescent microscope (Yamamoto et al., 2011; Yang et al., 2000; Yang et al., 2002) to two photon microscopy imaging (Barretto et al., 2011; Madden et al., 2013), fluorescently labeled tumor cells lines were used to generate tumor. However those orthotopic xenograft mouse models are not regarded to entirely resemble human tumors (Dai and Holland, 2001). This multicolor tumor model described here resembled human tumor histology thus can recapitulate human tumor cells behavior. It can be used not only in *in vivo* imaging but also in experiments that require visualization of tumor clonality. The establishment of the somatic engineered rat multicolor brain tumor model (Figure 3-1) will greatly facilitate and play an important role in *in vivo* tumor imaging.

In utero electroporation shows high multiple plasmids co-transfection efficiency(Chen and LoTurco; Siddiqi et al.), and I have shown here as many as 7 plasmids cotransfection had been achieved (Fig 3). Addition of Ngn2 or NeuroD1 to HRasV12/AKT mix induced a substantial change in the cytological appearance and the immunhistochemical pattern of resulting tumors, i.e.

ATRT like tumor formation demonstrating that *piggyBac* IUE tumor model should be a valuable platform for screening for gene therapy target as well as validating genes selected from forward genetic studies. Certainly, the role of respective genes needs to be assessed in respective human brain tumors. By addition of luciferase expressing plasmid to tumor inducing plasmid mixture, this system can easily be adapted to monitor tumor progression *in vivo* using bioluminescence imaging (Bhang et al., 2011; Uhrbom et al., 2004) which will make this system a valuable tool for high throughput anti-cancer drug screening.

It is unclear that whether different tumor types or subtypes come from different neural progenitor population or tumors generated from different subsets of neural progenitors have different behaviors. As mentioned above, *piggyBac* IUE allows for labeling of neural progenitor subpopulations. Therefore, now it is feasible to express oncogenes in lineage of subsets of neural progenitors and evaluate their contribution to tumorigenesis. We have shown that astrocytes from the GLAST+ progenitors have larger clonal clusters than astrocytes from Nestin+ progenitors (Siddiqi et al., 2014). It is reasonable to ask are astrocytes in GLAST+ progenitor lineage more susceptible to tumor induction? Are tumors induced from astrocytes in GLAST+ progenitor lineage more malignant? These questions can be addressed by selectively expressing oncogenes in specific cell types in the lineage of neural progenitor subpopulations using *piggyBac* IUE.

One pitfall for using promoter fragment is that it sometimes cannot recapitulate endogenous promoter element activity. This is true with the mouse GFAP and rat MBP promoter fragments used in this dissertation (Figure 3-2). Even though, they showed enriched labeling of astrocytes and oligodendrocytes respectively, both promoters can label small fraction of other cell types. One solution to this is to use conditional *piggyBac* donor or helper plasmid in which transgene of

interest or PBase is flanked by loxP sites or FRT sites and transgenic mouse Cre or Flip lines. This allows genomic integration and/or transgene expression in specific cell types in radial glia subpopulations designated by transgenic mouse lines.

Sources of inter tumor heterogeneity

Cancers are highly heterogeneous. For instance, a single cancer type non small cell lung cancer, determined by cellular morphology, has over 15 subtype genomic signatures (Huang et al., 2014). There has been increasing appreciation of inter tumor heterogeneity being responsible for differential responses for cancer therapy. Understanding the sources of this heterogeneity will greatly help design effective targeted therapy and increase cancer patients' prognosis.

I have shown that in CNS oncogenic insults happening in distinct cell populations and/or molecular context can lead to different tumor types, supporting the notion that both cell of origin and genetic mutation contribute to inter tumor heterogeneity. It is more and more clear that cell of origin and genetic mutations intertwine and contribute to tumor heterogeneity. Glial cells and/or glial cell progenitors are long thought to be the cell of origin for glioma. Experimental evidences haven shown that OPCs can serve as cell of origin for proneural GBMs(Liu et al., 2011). Direct comparison of gene expression profile of different GBM subtypes with molecular profile of different CNS cells populations showed that different GBM subtypes are reminiscent of distinct neural cell types and some mutations are associated with certain GBM subtypes(Verhaak et al., 2010). For example, the Proneural class was highly enriched with the oligodendrocytic signature but not the astrocytic signature, whereas the Classical group was strongly associated with the murine astrocytic signature. NF1 mutations predominantly occurred

in Mesenchymal subtype, whereas PDGFR and IDH1 alterations are the two major features of Proneural subtype. Focal EGFR alterations define Classical GBMs (Verhaak et al., 2010). Future experiments are needed to test, for example, whether Proneural GBM can be induced by introducing EGFR mutant in oligodendrocytes.

Another example is breast cancer. Comprehensive gene expression profiling of large sets of breast cancer patients revealed 5 major subtypes: basal like, luminal A, luminal B, $Her2^{+}/ER^{-}$ and normal breast like (Polyak, 2007, 2011)It is likely that there are multiple pathways to develop each type of tumor. Different tumor subtype might be caused by tumor specific genetic and epigenetic events occurring in distinct cells serving as cell of origin (Polyak, 2007, 2011).

Lung cancer is the leading cause of cancer death worldwide. There are two main lung cancer subgroups based on histopathology classification: non small cell lung cancer (NSCLC) and small cell lung cancer (SCLC). The cell of origin for human lung cancers remains largely unknown. It is speculated that these different tumor subclasses arise from distinct cells of origin localized within a defined regional compartment/microenvironment (Sutherland and Berns, 2010). As many as 15 mutations have been observed in non small cell lung cancer patients including KRas, EGFR, PI3KCA, *etc* (Huang et al., 2014). It is reasonal to think that the variety of genetic mutaions and different cell of origins interact and contribute to lung cancer diversity. However, experimental evidences are still needed.

Applications of CRISPR/Cas9 IUE in brain development and modeling CNS tumors

CRISPR/Cas9 knocks out gene expression by inducing random mutations through the error prone NHEJ DNA repair pathway. DSB will be repaired through homology directed repair

pathway if the repair template is present. By supplying a suitable DNA repair template bearing desired mutations together with CRISPR/Cas9, point mutations can be introduced into specific genomic locus through HDR repair pathway. Many CNS disorders are caused by somatic mutations; therefore CRISPR-IUE approach provides a platform to model somatic CNS disorders. However, since HDR related enzyme mainly express at G2 phase of cell cycle, genomic engineering using HDR might not be feasible in post mitotic cells, such as neurons.

Conditional or inducbile CRISPR construct in which the Cas9 expression is gated by Cre recombinase would be very valuable in experiments that require cell type specific genetic manipulations. By combining conditional CRISPR construct and cell type specific Cre mouse lines, cell type specific genome engineering can be achieved. This combination will maxmize the utility of both approach.

DNA transposons including *piggyBac*, mediate random insertion. Many efforts have been made to direct site specific integration of transposons. Site specific integration has been achieved using DNA transposase fused to DNA binding domains of transcription factors(Wang et al., 2012), zinc finger proteins (ZFPs) (Kettlun et al., 2011; Yant et al., 2007) and TALEs(Owens et al., 2013). Since gRNA is much easier to produce than ZFPs and TALEs, CRISPR-PBase fusion will be powerful in directing site specific integration mediated by *piggyBac*. Furthermore, transposon mediated integration can also be used for genome engineering and transposition process is independent of NHEJ and HDR DNA repair pathway. CRISPR-*piggyBac* system offers an alternative and complementary approach for targeted genome engineering.

References

Bai, J., Ramos, R.L., Ackman, J.B., Thomas, A.M., Lee, R.V., and LoTurco, J.J. (2003). RNAi reveals doublecortin is required for radial migration in rat neocortex. Nat Neurosci *6*, 1277-1283.

Barretto, R.P., Ko, T.H., Jung, J.C., Wang, T.J., Capps, G., Waters, A.C., Ziv, Y., Attardo, A., Recht, L., and Schnitzer, M.J. (2011). Time-lapse imaging of disease progression in deep brain areas using fluorescence microendoscopy. Nat Med *17*, 223-228.

Bhang, H.E., Gabrielson, K.L., Laterra, J., Fisher, P.B., and Pomper, M.G. (2011). Tumor-specific imaging through progression elevated gene-3 promoter-driven gene expression. Nat Med *17*, 123-129.

Chen, F., Becker, A.J., and Loturco, J.J. (2014a). Contribution of tumor heterogeneity in a new animal model of CNS tumors. Mol Cancer Res *12*, 742-753.

Chen, F., and LoTurco, J. (2012). A method for stable transgenesis of radial glia lineage in rat neocortex by piggyBac mediated transposition. J Neurosci Methods *207*, 172-180.

Chen, F., Maher, B.J., and LoTurco, J.J. (2014b). PiggyBac Transposon-Mediated Cellular Transgenesis in Mammalian Forebrain by In Utero Electroporation. Cold Spring Harb Protoc *2014*, pdb prot073650.

Dai, C., and Holland, E.C. (2001). Glioma models. Biochim Biophys Acta *1551*, M19-27.

Ding, S., Wu, X., Li, G., Han, M., Zhuang, Y., and Xu, T. (2005). Efficient transposition of the piggyBac (PB) transposon in mammalian cells and mice. Cell *122*, 473-483.

Hoffman, R.M. (2005). The multiple uses of fluorescent proteins to visualize cancer in vivo. Nat Rev Cancer *5*, 796-806.

Huang, M., Shen, A., Ding, J., and Geng, M. (2014). Molecularly targeted cancer therapy: some lessons from the past decade. Trends in pharmacological sciences *35*, 41-50.

Kettlun, C., Galvan, D.L., George, A.L., Jr., Kaja, A., and Wilson, M.H. (2011). Manipulating piggyBac transposon chromosomal integration site selection in human cells. Mol Ther *19*, 1636-1644.

Kita, Y., Kawakami, K., Takahashi, Y., and Murakami, F. (2013). Development of cerebellar neurons and glias revealed by in utero electroporation: Golgi-like labeling of cerebellar neurons and glias. PLoS One *8*, e70091.

Kriegstein, A., and Alvarez-Buylla, A. (2009). The glial nature of embryonic and adult neural stem cells. Annu Rev Neurosci *32*, 149-184.

Lacoste, A., Berenshteyn, F., and Brivanlou, A.H. (2009). An efficient and reversible transposable system for gene delivery and lineage-specific differentiation in human embryonic stem cells. Cell Stem Cell *5*, 332-342.

Lander, E.S., Linton, L.M., Birren, B., Nusbaum, C., Zody, M.C., Baldwin, J., Devon, K., Dewar, K., Doyle, M., FitzHugh, W., *et al.* (2001). Initial sequencing and analysis of the human genome. Nature *409*, 860-921.

Li, Z., Michael, I.P., Zhou, D., Nagy, A., and Rini, J.M. (2013). Simple piggyBac transposon-based mammalian cell expression system for inducible protein production. Proc Natl Acad Sci U S A.

Liu, C., Sage, J.C., Miller, M.R., Verhaak, R.G., Hippenmeyer, S., Vogel, H., Foreman, O., Bronson, R.T., Nishiyama, A., Luo, L., *et al.* (2011). Mosaic analysis with double markers reveals tumor cell of origin in glioma. Cell *146*, 209-221.

Madden, K.S., Zettel, M.L., Majewska, A.K., and Brown, E.B. (2013). Brain tumor imaging: live imaging of glioma by two-photon microscopy. Cold Spring Harb Protoc *2013*.
Maher, B.J., and LoTurco, J.J. Disrupted-in-schizophrenia (DISC1) functions presynaptically at glutamatergic synapses. PLoS One *7*, e34053.
Owens, J.B., Mauro, D., Stoytchev, I., Bhakta, M.S., Kim, M.S., Segal, D.J., and Moisyadi, S. (2013). Transcription activator like effector (TALE)-directed piggyBac transposition in human cells. Nucleic Acids Res *41*, 9197-9207.
Polyak, K. (2007). Breast cancer: origins and evolution. J Clin Invest *117*, 3155-3163.
Polyak, K. (2011). Heterogeneity in breast cancer. J Clin Invest *121*, 3786-3788.
Rostovskaya, M., Fu, J., Obst, M., Baer, I., Weidlich, S., Wang, H., Smith, A.J., Anastassiadis, K., and Stewart, A.F. (2012). Transposon-mediated BAC transgenesis in human ES cells. Nucleic Acids Res *40*, e150.

Saridey, S.K., Liu, L., Doherty, J.E., Kaja, A., Galvan, D.L., Fletcher, B.S., and Wilson, M.H. (2009). PiggyBac transposon-based inducible gene expression in vivo after somatic cell gene transfer. Mol Ther *17*, 2115-2120.

Siddiqi, F., Chen, F., Aron, A.W., Fiondella, C.G., Patel, K., and Loturco, J.J. (2014). Fate Mapping by PiggyBac Transposase Reveals That Neocortical GLAST+ Progenitors Generate More Astrocytes Than Nestin+ Progenitors in Rat Neocortex. Cereb Cortex.
Sutherland, K.D., and Berns, A. (2010). Cell of origin of lung cancer. Molecular oncology *4*, 397-403.
Thomas, C.E., Ehrhardt, A., and Kay, M.A. (2003). Progress and problems with the use of viral vectors for gene therapy. Nat Rev Genet *4*, 346-358.
Uhrbom, L., Nerio, E., and Holland, E.C. (2004). Dissecting tumor maintenance requirements using bioluminescence imaging of cell proliferation in a mouse glioma model. Nat Med *10*, 1257-1260.
Verhaak, R.G., Hoadley, K.A., Purdom, E., Wang, V., Qi, Y., Wilkerson, M.D., Miller, C.R., Ding, L., Golub, T., Mesirov, J.P., *et al.* (2010). Integrated genomic analysis identifies clinically relevant subtypes of glioblastoma characterized by abnormalities in PDGFRA, IDH1, EGFR, and NF1. Cancer Cell *17*, 98-110.
Wang, H., Mayhew, D., Chen, X., Johnston, M., and Mitra, R.D. (2012). "Calling cards" for DNA-binding proteins in mammalian cells. Genetics *190*, 941-949.
Yamamoto, N., Tsuchiya, H., and Hoffman, R.M. (2011). Tumor imaging with multicolor fluorescent protein expression. Int J Clin Oncol *16*, 84-91.
Yang, M., Baranov, E., Jiang, P., Sun, F.X., Li, X.M., Li, L., Hasegawa, S., Bouvet, M., Al-Tuwaijri, M., Chishima, T., *et al.* (2000). Whole-body optical imaging of green fluorescent protein-expressing tumors and metastases. Proc Natl Acad Sci U S A *97*, 1206-1211.
Yang, M., Baranov, E., Wang, J.W., Jiang, P., Wang, X., Sun, F.X., Bouvet, M., Moossa, A.R., Penman, S., and Hoffman, R.M. (2002). Direct external imaging of nascent cancer, tumor progression, angiogenesis, and metastasis on internal organs in the fluorescent orthotopic model. Proc Natl Acad Sci U S A *99*, 3824-3829.
Yant, S.R., Huang, Y., Akache, B., and Kay, M.A. (2007). Site-directed transposon integration in human cells. Nucleic Acids Res *35*, e50.
Yusa, K., Rad, R., Takeda, J., and Bradley, A. (2009). Generation of transgene-free induced pluripotent mouse stem cells by the piggyBac transposon. Nat Methods *6*, 363-369.

Appendix I Supplementary Material for Chapter 3

Supplementary Figure 3-1 Additional immunohistopathological features of GBM induced by PBCAG-HRasV12/AKT or PBGFAP-HRasV12/AKT.

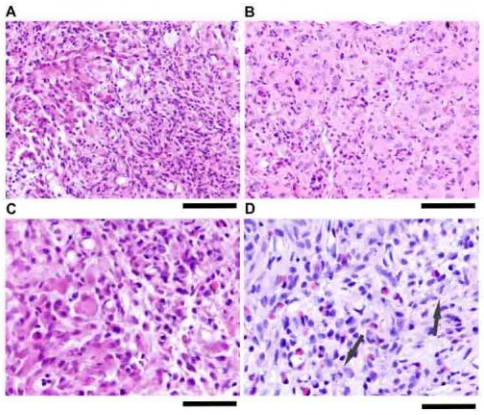

(A) Fibrillary and gemistocytic

elements (H&E) in PBCAG-HRasV12/AKT induced tumor. (B) PBCAG-HRasV12/AKT induced tumor showed diffusely infiltrating pattern (H&E). (C) Pleomorphism of tumor cells and mitotic activity (H&E) in PBCAG-HRasV12/AKT induced tumor. (D) Brisk mitotic activity in PBGFAP-HRasV12/AKT induced tumor. Black arrows indicate mitoses (H&E).

Scale bar: 100 μm in A, B and D; 50 μm in C and E.

Supplementary Figure 3-2 Tumor cells can form tumor spheres in *vitro*

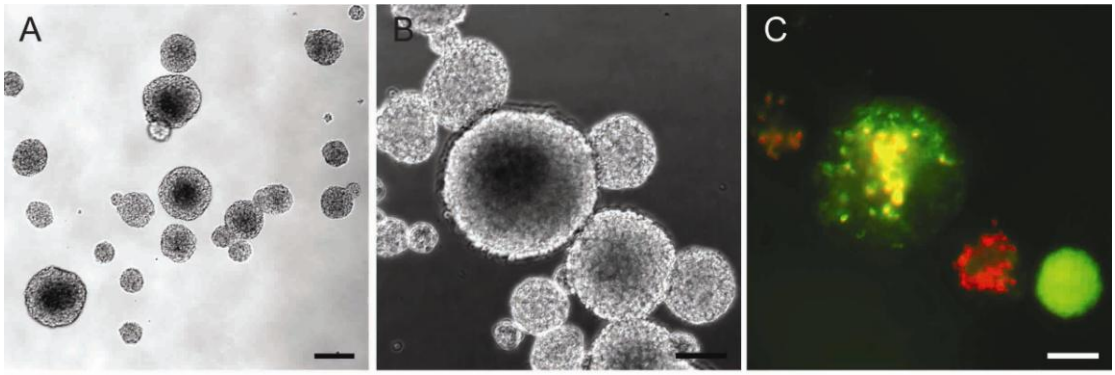

(A) 10x bright field image of tumor spheres. (B-C) Examples of tumor sphere in high magnification. B, bright filed image. C, fluorescent image. Scale bar: 300 µm in A and 200 µm in B and C.

Supplementary Figure 3-3 Additional immunohistopathological features of ATRT like tumor induced by CAG-Ngn2 and PBCAG-HRasV12/AKT.

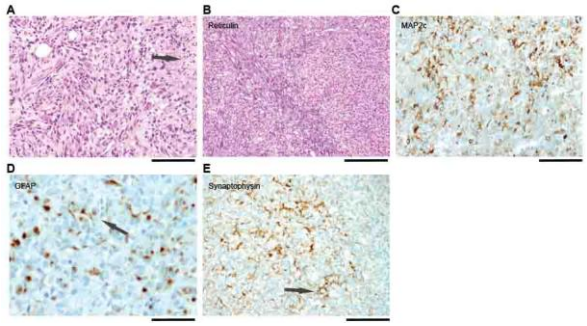

(A) Process rich and epitheloid portions of the tumor (H&E). Black arrow indicates necrotic area. (B) Reticulin fiber staining – areas of the tumors with a rather dense fiber network are intermingled with those that lack this feature. (C) Tumor cells with MAP2c positive processes. (D) Tumor cells with GFAP positive processes (black arrow). (E) Clusters of synaptophysin positive tumor cells. Black arrow indicates perisomatic expression pattern. Scale bar: 100 µm in A, C and E 50 µm in B and D.

Supplementary Figure 3-4 Additional immunohistopathological features of ATRT like tumor induced by PBCAG-NeuroD1 and PBCAG-HRasV12/AKT

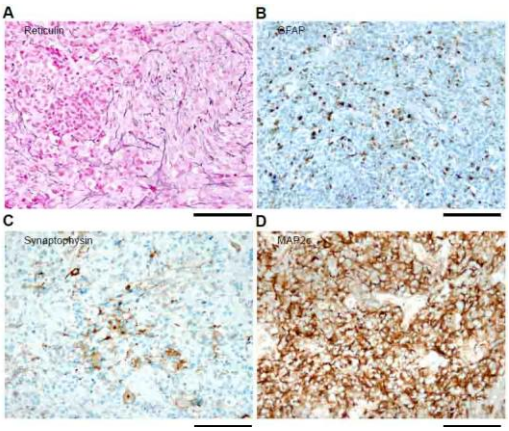

(A) Reticulin fiber staining - areas with some fiber network. (B) Tumor cells with GFAP positive processes. (C) Clusters of synaptophysin positive tumor cells. (D) MAP2c positive cells and processes. Scale bar: 100 µm in A-D.

Supplementary Figure 3-5 Additional immunohistopathological features of ATRT like tumor induced by PBCAG-NeuroD1 and PBCAG-HRasV12/AKT

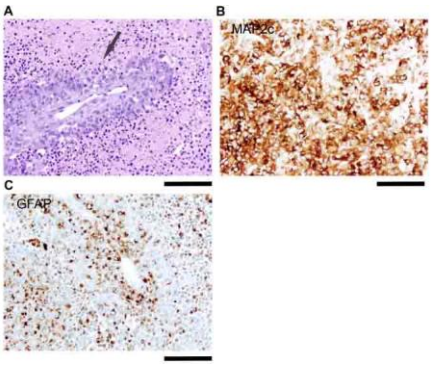

(A) Extensive necrosis in the tumor. Note the few layers of vital tumor cells around a blood vessel (black arrow) surrounded by large necrotic areas. (B)Strong and diffuse expression pattern of MAP2c. (C) Strong expression of GFAP by a subset of tumor cells, some showed process rich astroglial morphology and others showed rhabdoid morphologies. Scale bar: 100 µm in A-C.

Supplementary Figure 3-6 Gene expression profile of ATRT like tumors

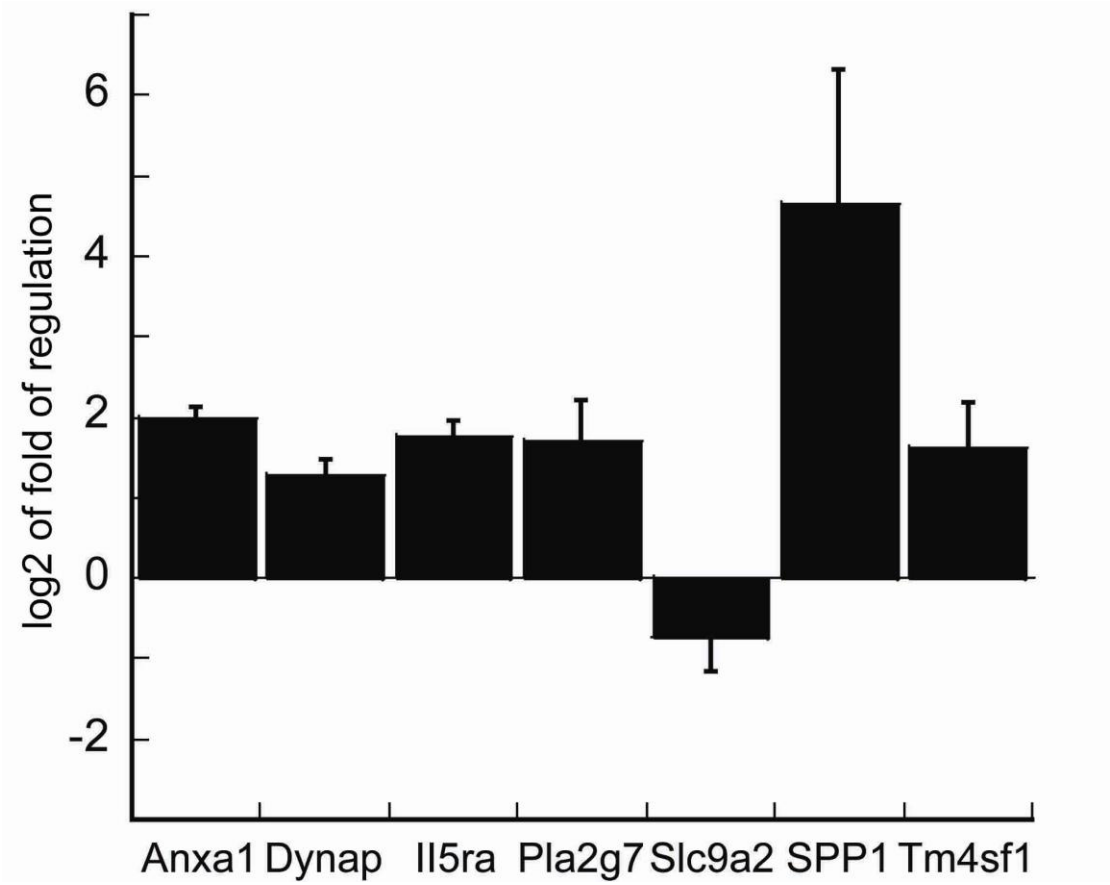

A panel of 7 genes was used to profile ATRT like tumors and qPCR results were shown here. 6 out of 7 genes profiled showed significant up regulation. Error bar indicates standard error of mean (SEM).

Supplementary Table 1 Primer sequence for qRT-PCR and SURVEYOR assay

Name	Sequence
DLL3 left	ggtgacatgcgcagatggac
DLL3 right	gaggccgccattctgacaag
NKX2-2 left	gccagcctcatccgtctcac
NKK2-2 right	aagaccggcactgccacac
SOX2 left	tccatgaccagctcgcagac
SOX2 right	ctggcctcggacttgaccac
ERBB3 left	ccacgtgacaggctctgagg
ERBB3 right	gctgcgaatggtaggcactg

OLIG2 left	agcacctcctcgtccacgtc
OLIG2 right	tccatggcgatgttgaggtc
FBXO3 left	tcctgagaaggcctgtcagttg
FBXO3 right	tgtggtgcagctggtgtattc
GABRB2 left	aagatgcgcctggatgtcaac
GABRB2 right	aggcaagcattgtgctcctg
SNCG left	ccgaggcagctgagaagacc
SNCG right	tcggtggccactgtgttgac
MBP left	ggctacggaggcagagcttc
MBP right	ccagagcggctgtctcttcc
FGFR3 left	cagtgacgctctgccgtctg
FGFR3 right	tccggacgagaggtgtgttg
PDGFA left	tacctcggagccaggtggac
PDGFA right	accttgacactgcggtggtg
EGFR left	ccacgtcacggactccactc
EGFR right	cctctgtcaggacgctggtg
AKT2 left	cttgcactcgacggatgtgg
AKT2 right	cctcaggcgccaagtactcc
NES left	agcagcgaggctctggaatg
NES right	ggctgtcagtgctgcctgtg
CASP1 left	ttcctggaccgagtggttc
CASP1 right	ggcaagacgtgtacgagtgg
CASP4 left	gcatgagccatgtggagaagg
CASP4 right	gagcaggcatgtatccggaag
CHI3L1 left	ggatctcgcctggctctacc
CHI3L1right	ctgacacggcagcactgagc
TRADD left	actggagttgcgtgctggtg
TRADD right	tccagctccgcgagttcttc
TLR2 left	cctggtccatgtcctggttg
TLR2 right	agtgcggcctggtgacactc
TLR4 left	tcgagccagaatgaggactgg
TLR4 right	ttggcagcaatggctacacc
DNMT1 left	ggcgatgtggagatgctgtg
DNMT1 right	ggaagaaccgaggccggtag
TOP1 left	acttggctggtctcctggac
TOP1 right	tcttcagtcgccgagcagtc
ABL1 left	cctgccgtctgctggtaagc
ABL1 right	gcggcctcctcagtcttcttc
BOP1 left	tcggccaagagaccttcagc
BOP1 right	cctcaatgtgccgtcgtctg
Pla2g7 left	AGCTCACCTTGCAGGATGTC
Pla2g7 right	TGTGATCCGGGAGAACTCTG
Il5ra left	ggcttgttggcaaggatg
Il5ra Right	gagtgaacagctgatccaagg
Tm4sf1 left	ATCACGGGATCTGGCTACTG

Tm4sf1 Right	AGTCACATGCCACTCCACAA
SPP1 left	TTGGCTTACGGACTGAGGTC
SPP1 right	GTTTCCACGCTTGGTTCATC
Anxa1 left	CCAGCTCAGTTTGATGCAGA
Anxa1 right	TCCAGATGTGTCCGAAGTGA
Slc9a2 left	AAGCTCACGCCAGGAGAAAT
Slc9a2 right	CTCGCGGTTTAAGCTGTTGT
Dynap left	GACACAGTGCGGCTGTAGG
Dynap right	GTCTGTGTGAACGACGATGG
P53 left	ACAGCGTGGTGGTACCGTAT
P53 right	ACAGGCACAAACACGAACCT

P53 SURVEYOR assay primer

P53 forward: ATGGAGGATTCACAGTCGGA

P53 reverse: CCC ACT TTC TTG ATC ATT GG

Appendix II Supplementary Material for Chapter 4

Supplementary Figure 4 - 1

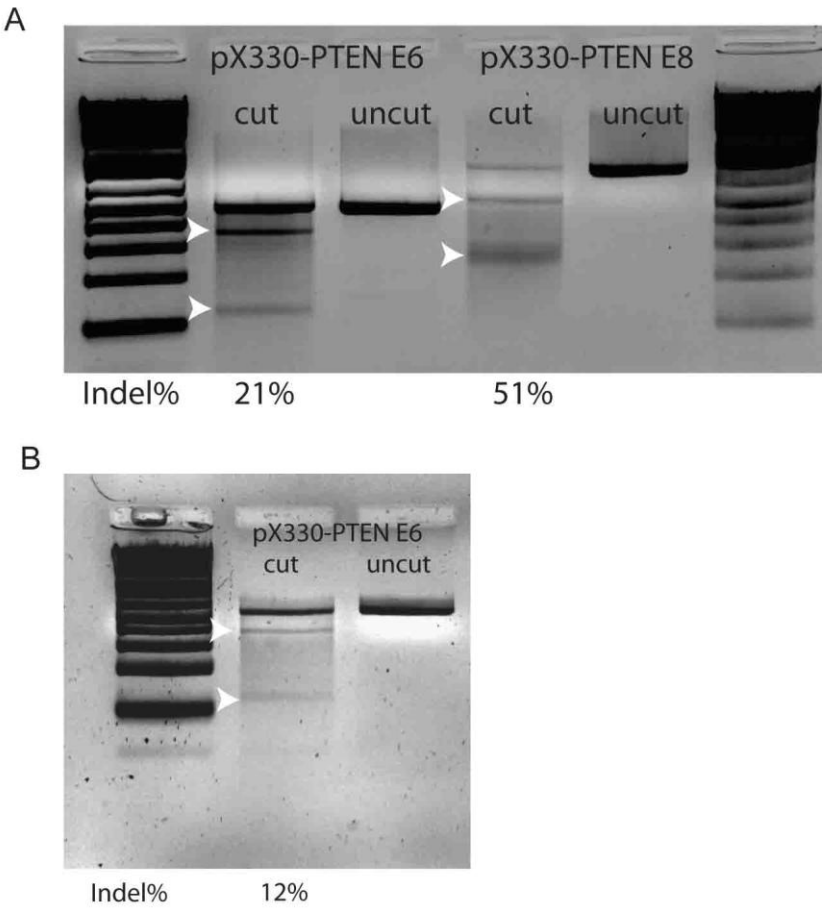

A, gRNAs targeting PTEN exon 6 and 8 introduced mutations at PTEN locus in vitro

B, gRNA targeting PTEn exon 6 introduced mutations at PTEN locus in vivo

Supplementary Figure 4-2

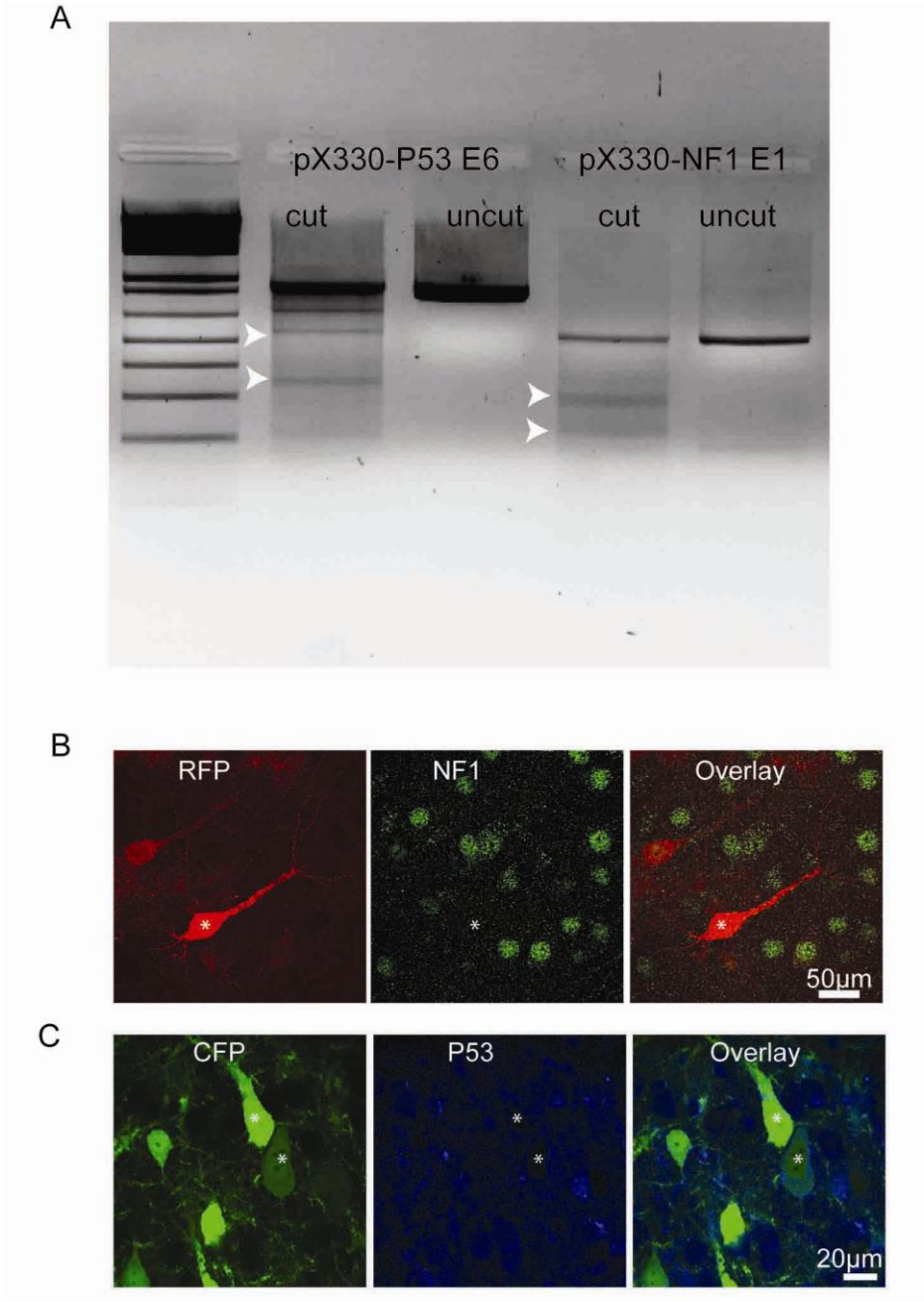

A, gRNAs targeting P53 E6 and NF1 E1 induced mutations at targeted genomic locus in neuroblastoma cells.

B, gRNA targeting NF1 E1 abolished NF1 expression in neurons.

C, gRNA targeting P53 E6 abolished P53 expression in neurons.

Supplementary Figure 4-3

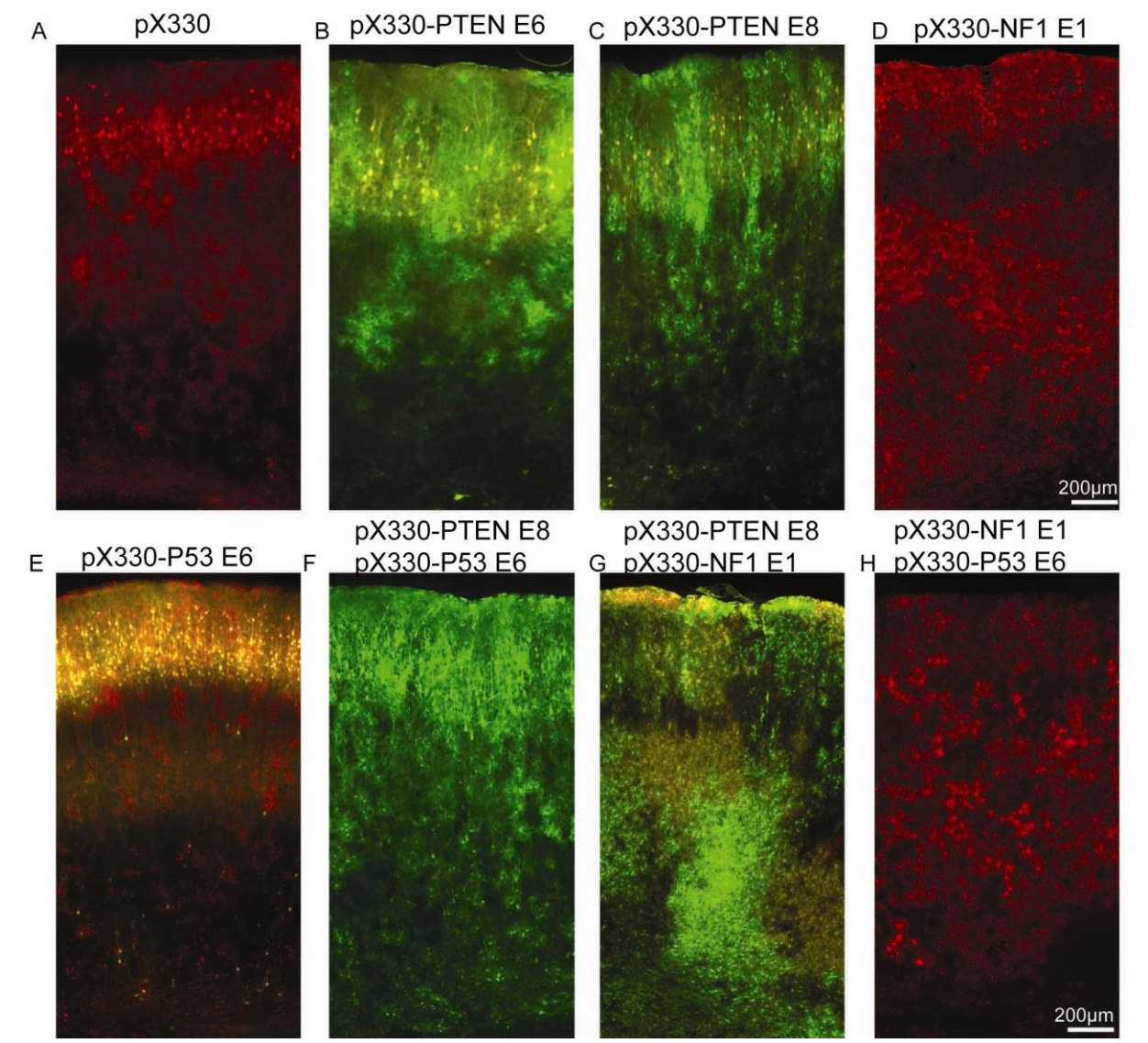

A-H, High magnification of representative images of high magnification brains transfected with CRISPR constructs. Note the increased cell density in brains transfected with pX330-NF1

Supplementary Figure4-4

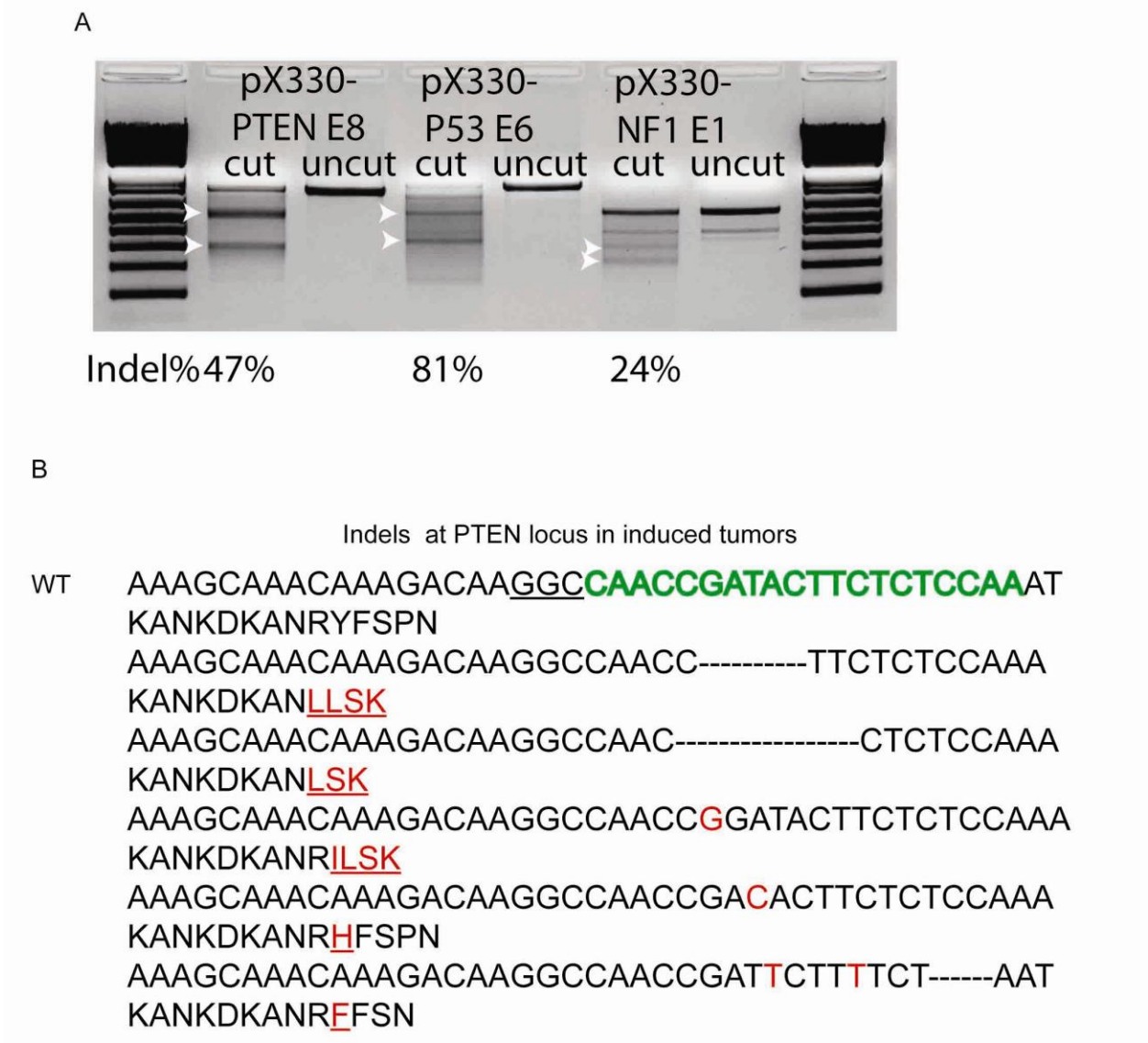

A, In vivo SURVEYOR assay using tumor genomic DNA

B, Representative sequences of mutated alleles identified at PTEN locus in induced tumors and corresponding protein sequences. Translated protein sequences were shown below the DNA sequences. Guide sequence is shown in green. PAM is underlined. Dashes, deleted bases; red bases, insertion. Mutated amino acids are shown in red and underlined.

Curriculum Vitae

EDUCATION

2008-2014 Ph.D in Physiology and Neurobiology - University of Connecticut (expected)

2004-2008 M.S in Biochemistry and Molecular Biology-Xiamen University

2000-2004 B.S in Biotechnology-Laiyang Agriculture College

HONORS AND AWARDS

2013 Doctoral Dissertation Fellowship Award, University of Connecticut

2011-2013 Neuroscience Fellowship, University of Connecticut

2000-2004 Laiyang Agreculture College scholarship

2000-2004 Excellent student award, Laiyang Agriculture College

2004 Excellent undergraduate award of Shandong province

PROFESSIONAL MEMBERSHIPS

2012-present American Association for Cancer Research

2009-present Society for Neuroscience

2006-2007 China Society for Cell Biology

TEACHING EXPERIENCE

2010-2014 Assistant instructor: Advanced Techniques in Molecular Neuroscience (ATMN) at Cold Spring Harbor Laboratory

2012-2014 Teaching assistant: Advanced Human anatomy and physiology

2008-2009 Teaching assistant: Advanced Human anatomy and physiology

PUBLICATIONS

14. Stacey Glasgow, Wenyi Zhu, C. Claus Stolt, Teng-Wei Huang , **Fuyi Chen**, Joseph J. LoTurco, Jeffrey L. Neul , Michael Wegner, Carrie Mohila, and Benjamin Deneen: Mutual Antagonism Between Sox10 and NFIA Regulates Diversification of Glial Lineages and Glioma Sub-Types. *Nature Neuroscience* (accepted).

13. **Fuyi Chen**, Albert Becker, Joseph LoTurco (2014): Sources of CNS tumor heterogeneity. *Oncoscience*: http://www.impactjournals.com/oncoscience/files/papers/1/60/60.pdf

12. TM Centanni, **F Chen**, CT Engineer, AB Booker, RL Rennaker, JJ LoTurco, MP Kilgard. Speech sound processing deficits and training-induced neural plasticity in rats with dyslexia gene knockdown (2014). *PLOS one* DOI: 10.1371/journal.pone.0098439.

11.**Fuyi Chen**, Brady J Maher, and Joseph J LoTurco: *Piggybac* Transposon-Mediated Somatic Transgenesis in Mammalian Forebrain by In Utero Electroporation. *Cold Spring Harb Protoc; doi:10.1101/pdb.prot073650. Cover image*.

10. Li-Li Liu, Li-Rong Lin, Man-Li Tong, Hui-Lin Zhang, Song-Jie Huang, Yu-Yan Chen, Xiao-Jing Guo, Ya Xi, Long Liu, **Fu-Yi Chen**, Ya-Feng Zhang, Qiao Zhang, Tian-Ci Yang (2014): Incidence and risk factors for the prozone phenomenon in serologic testing for syphilis in a large cohort. *Clin Infect Dis;* doi: 10.1093/cid/ciu325.

9. Man-Li Tong, Li-Rong Lin, Li-Li Liu, Hui-Lin Zhang, Song-Jie Huang, Yu-Yan Chen, Xiao-Jing Guo, Ya Xi, Long Liu, **Fu-Yi Chen**, Ya-Feng Zhang, Qiao Zhang, Tian-Ci Yang (2014): Analysis of 3 Algorithms for Syphilis Serodiagnosis and Implications for Clinical Management. *Clin Infect Dis*. 58 (8): 1116-1124. doi: 10.1093/cid/ciu087

8. **Fuyi Chen,** Albert Becker and Joseph J. LoTurco (2014): Contribution of Tumor Heterogeneity in a New Animal Model of CNS Tumors. *Molecular Cancer Research*; doi:10.1158/1541-7786.MCR-13-0531. *Cover image*.

7. Manli Tong, Ya Xi, Xiaojing Guo, Yuyan Chen, Yafeng Zhang, Qiao Zhang, Long Liu, **Fuyi Chen**, Songjie Huang, Huilin Zhang, Weihong Zheng, Lirong Lin, Lili Liu, Jie Jiang, Tianci Yang (2014): Association between Neurosyphilis and Diabetes Mellitus: Resurgence of an Old Problem. *Journal of Diabetes*; DOI: 10.1111/1753-0407.12119

6. T.M. Centanni, A.B. Booker, A.M. Sloan, **F. Chen**, B.J. Maher, R.S. Carraway, N. Khodaparast, J.J. LoTurco, M.P. Kilgard (2013). Knockdown of the dyslexia-associated

gene KIAA0319 impairs temporal responses to speech stimuli in rat primary auditory cortex. *Cerebral Cortex*; doi: 10.1093/cercor/bht028.

5. Faez Siddiqi*, **Fuyi Chen***, Abraham W. Aron, Christopher G. Fiondella, Komal Patel & Joseph J.LoTurco (2013): Fate Mapping by PiggyBac Transposase Reveals That Neocortical GLAST+ Progenitors Generate More Astrocytes Than Nestin+ Progenitors in Rat Neocortex. *Cerebral Cortex*, 24 (2): 508-520. * FS and FC contribute equally to this work.

4. Yan-Li Zeng, Wen-Jie Wang, Hui-Lin Zhang, **Fu-Yi Chen**, Song-Jie Huang, Gui-Li Liu, Ya Xi, Xiao-Jing Guo, Wei-Hong Zheng, Tian-Ci Yang (2013): Neuropsychiatric disorders secondary to neurosyphilis in elderly people: one theme not to be ignored. *International Psychogeriatrics*, 25(09):1513-1520.

3. Li-Li Liu, Hui-Lin Zhang, Song-Jie Huang, Long Liu, Man-Li Tong, Li-Rong Lin, Yu-Yan Chen, Ya Xi, Xiao-Jing Guo, Ya-Feng Zhang, Qiao Zhang, Wei-Hong Zheng, **Fu-Yi Chen**, Jie Jiang, Tian-Ci Yang (2013): Assessing cerebrospinal fluid abnormalities in neurosyphilis patients without human immunodeficiency virus infection. *International Immunopharmacology*, 17(4): 1120–1124.

2. Fuyi Chen, Joseph LoTurco (2012): A method for stable transgenesis of radial glia lineage in rat neocortex by piggyBac mediated transposition. Journal of Neuroscience Methods, 207 (2): 172-180.

1. **Chen Fuyi**, Peng Xuanxian (2006): Diagonal polyarcylamide gel electrophoresis in proteomics research. *Chinese Bulleting of Life Science*, 18 (1):31-34.

MANUSCRIPTS IN PREPARATION/UNDER REVIEW

1.**Fuyi Chen** Alicia Che, Albert Becker, Joesph LoTurco: Modeling Neurodevelopmental Disrutpion and Glioblastoma with CRISPR/Cas9 system (in preparation).

2. **Fuyi Chen**, Joseph LoTurco: Novel glioblastoma and oligoastrocytoma CNS models and their utility in drug discovery. Current Protocols in Pharmacology (CPPh) invited review (Manuscript in preparation).

3. Zhou Han, Lei Jin, **Fuyi Chen**, Joseph J. Loturco, Lawrence B. Cohen, Alexey Bondar, Josef Lazar and Vincent A. Pieribone. Mechanistic studies of the genetically encoded fluorescent protein voltage probe ArcLight (Under review).

ABSTRACTS

1. **Fuyi Chen**, Yu Wang, and Joseph J. LoTurco: PiggyBac mediated non-viral transgenesis in developing neocortex by in utero electroporation. Society for Neuroscience Abstract 39th Annual Meeting, Chicago, 2009

2. **Fuyi Chen**, Faez Siddiqi, Christopher G Fiondella, Abraham W Aron and Joseph J Loturco: Lineage Tracing by PiggyBac Transposition Reveals Heterogeneity Amongst Radial Glia Populations in Rat Neocortex. Society for Neuroscience Abstract 40th Annual Meeting, San Diego, 2010

3. **Fuyi Chen**, Shiva Iyer, Komal Patel and Joseph J LoTurco: A plasmid-based method for multicolor clonal labeling of neocortical astrocytes and Glioma. Society for Neuroscience Abstract 41th Annual Meeting, Washington DC, 2011

4. E. J. Markus, B. Schmidt, A. Booker, **F. Chen**, M. Argraves, E. Szkudlarek, J. LoTurco: Effects of Hippocampal Arc Knockdown on Hippocampal Dependent/Independent Learning. Society for Neuroscience Abstract 41th Annual Meeting, Washington DC, 2011

5. T.M. Rosen, A.B. Booker, **F. Chen**, N. Wasko, K. Trull, N. Khodaparast, A.M. Sloan, R. Rennaker III, J.J. LoTurco, M.P. Kilgard: Neural and behavioral speech discrimination impairment in a rat model of dyslexia. Society for Neuroscience, New Orleans, 2012

6. **Fuyi Chen**, Albert Becker, Joseph LoTurco. Systematic manipulation of brain tumor diversity using piggybac transposon mediated transgenesis approach in rat. American Association for Cancer Research Annual Meeting 2013, Washington DC

7. T. M. Centanni, A. B. Booker, **F. Chen**, C. T. Engineer, A. M. Sloan, K. Trull, N. Wasko, R. L. Rennker, J. J. LoTurco, M. P. Kilgard. Speech sound processing deficits and training-induced neural plasticity in rats with dyslexia gene knockdown. Society for Neuroscience Annual Meeting 2013, San Diego, 2013